Metal-Mediated Construction of Highly Ordered Molecular Arrays: from Synthetic Challenge to Functional Assemblies

Norifumi FUJITA

DOCTOR OF PHILOSOPHY

Department of Structural Molecular Science
School of Mathematical and Physical Science
The Graduate University for Advanced Studies

2000

Contents

Chapter 1 General Introduction

Chapter 2 Spontaneous Assembly of Ten Components into Two Interlocked Coordination Cages

Chapter 3 Reconstruction of the Three-Dimensionally Interlocked Structure from Two, Preorganized Three-Dimensional Cages

Chapter 4 A [2]Catenane Whose Rings Incorporate Two Differently Metallated Porphyrins

Chapter 5 Self-Assembly of a Porphyrin Prism: Characterization of Both Solid and Solution State Structures

Chapter 1

General Introduction

1.1 Overview of the Thesis

This thesis deals with chemical construction of functional nano-structures through spontaneous assembly of small molecular components. The author focuses his special attention to metal-directed self-assembly which has been recognized during the last decade as a promising way to the precise construction of well-defined nanometer-scale architectures. Of many target structures, the author is particularly interested in both challenging and functional architectures which had been never synthesized by conventional synthesis.

In view of synthetic challenge, the author has studied the construction of topologically complex interlocked molecules (catenanes) by self-assembly. While the efficient synthetic methodologies of simple two-ring catenanes have been established recently, the construction of their three-dimensional analog (namely, a catenane composed not of two macrocycles but of two three-dimensional cages) has been never achieved. The author furnished surprisingly efficient method for the synthesis of such a 3D-interlocked compound using the self-assembly strategy (Chapter 2 and 3). After synthesizing the 3D-catenane, the author's interest shifted from challenging to functional systems. Thus, novel porphyrin arrays were incorporated into a catenane structure. He synthesized a porphyrin catenane that showed multi-component, photo-induced electron transfer system where components were assembled and arrayed through

catenation (Chapter 4). Finally, he prepared a porphyrin-based hollow framework which is composed of three porphyrin units and six metal centers. Various organic molecules were found to be included in the large hydrophobic cavity where new photo- and electrochemistry through host-guest interaction are highly expected (Chapter 5).

1.2 Chemistry of Interlocked Molecules: Background

The author will discuss the synthesis of topologically complex molecules in the first half of this thesis. Mechanically linked ring molecules are termed as catenane, which are compounds of great attention not only due to their unique structures but also for their potential applications to molecular scale devices or composites of nano-architectures. The first synthesis of catenane was achieved by Wasserman[1] by the condensation of a long α,ω-dicarboxylic ester in the presence of a C34 macrocycle.(Figure 1) However, the yield was extremely low (<0.001%) because the catenation took place statistically. Thus, this approach has a limitation for further applications to the construction of topologically complexed molecules.

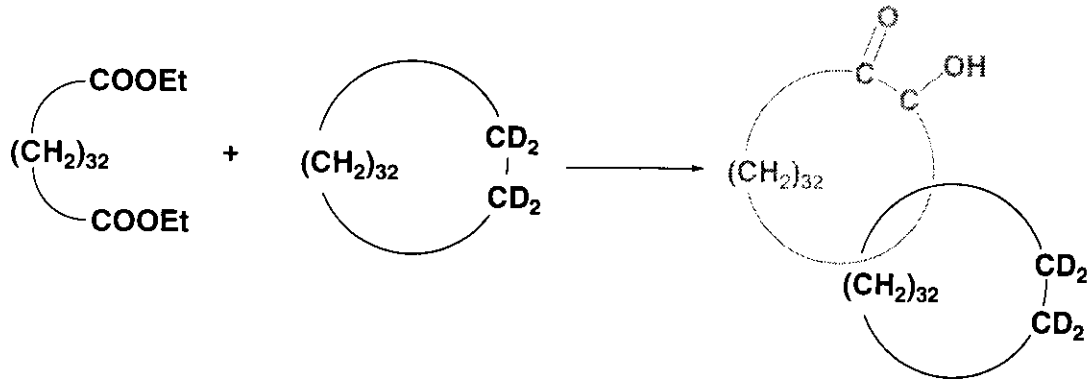

Figure 1. The first synthesis of a linked ring molecule.

A non-statistical catenane synthesis was first realized by Sauvage et al in 1983[2] where templating effect played an important role in the key step, opening the door to topological

chemistry. In their template strategy (Figure 2), phenanthroline units with hydroxyphenyl substituents at 2- and 8-positions were assembled around the tetrahedral geometry of a Cu(I) template. By linking hydroxyl groups at both ends with ethyleneglycol units, the first non-statistical synthesis of catenane was achieved.

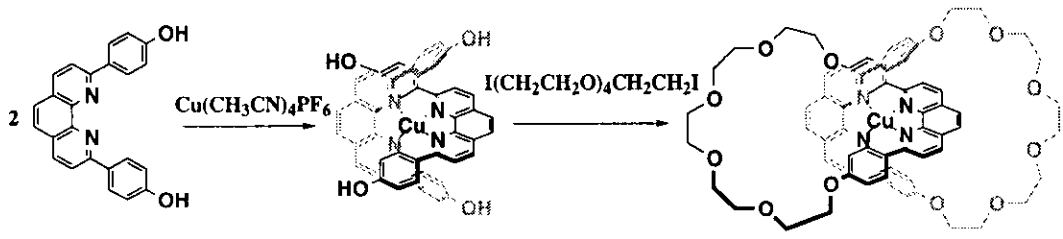

Figure 2. The first non-statistical synthesis of a linked ring molecule.

Following Sauvage's metal templated catenane synthesis, other groups employed organic templates where charge-transfer interaction[3] or hydrogen bonding[4, 5] were the driving forces for the directed catenane syntheses. In particular, Stoddart's rectangular box-shaped molecules incorporating quaternary alkylated 4,4'-bypyridine showed strong ability to bind electron-rich aromatic rings by CT complex formation. Subsequent ring closure step (Figure 3) gave the catenane in 70% yield.[3]

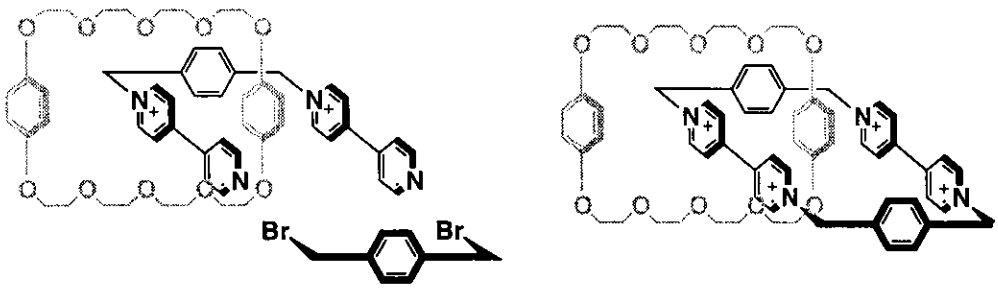

Figure 3. Non-statistical synthesis of a catenane via efficient CT-complex template.

Another approach was based on intermolecular hydrogen bonding between amide units of two macrocycles. Catenanes shown in Figure 4 were efficiently formed via a hydrogen bonding supported templating step as described below.[4, 5]

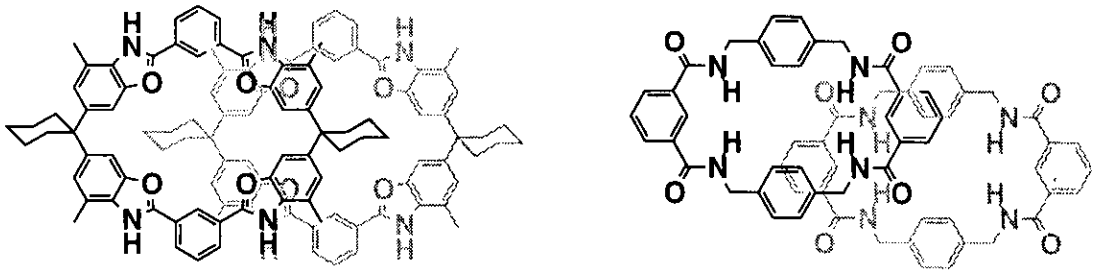

Figure 4. Non-statistical catenation via hydrogen bonding templates.

One-step synthesis of catenane via self-assembly was achieved in 1994.[6] From two identical macrocycles containing reversible Pd-N coordination bondings (Figure 5), the rings were immediately linked into a metal-linked catenane in an aqueous solution as a result of thermodynamic equilibration. The self-assembly of this catenane was driven by hydrophobic, π-π, and CH-π interaction.

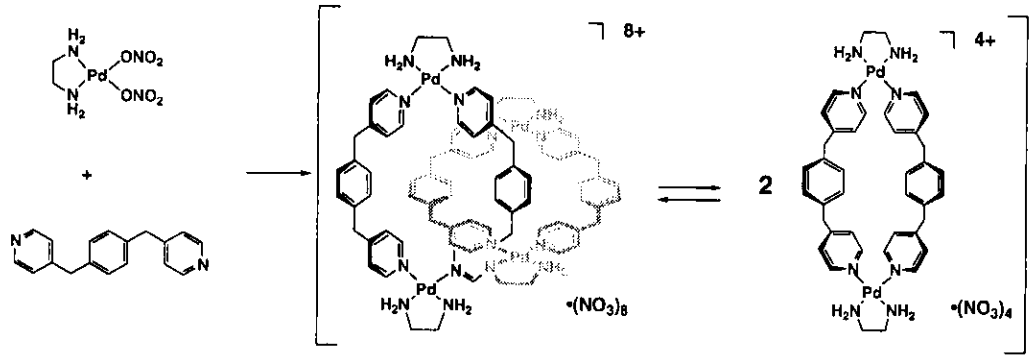

Figure 5. One-step catenane synthesis by self-assembling approach.

Recently, more complicated molecular topologies were synthesized in practical yields using the synthetic methodologies mentioned above. The examples of synthetic molecules possessing topological complexity are shown in the following figures. Sauvage extended the Cu(I) templated synthesis of [2]catenane into that of a trefoil knot and a doubly interlocked catenane as shown in Figure 6.[8] The methods involve the templating of doubly helicated precursors followed by ring closure, the reminiscent of Möbius strip approach which was first suggested by Frisch and Wasserman.[7a, 7b, 7c]

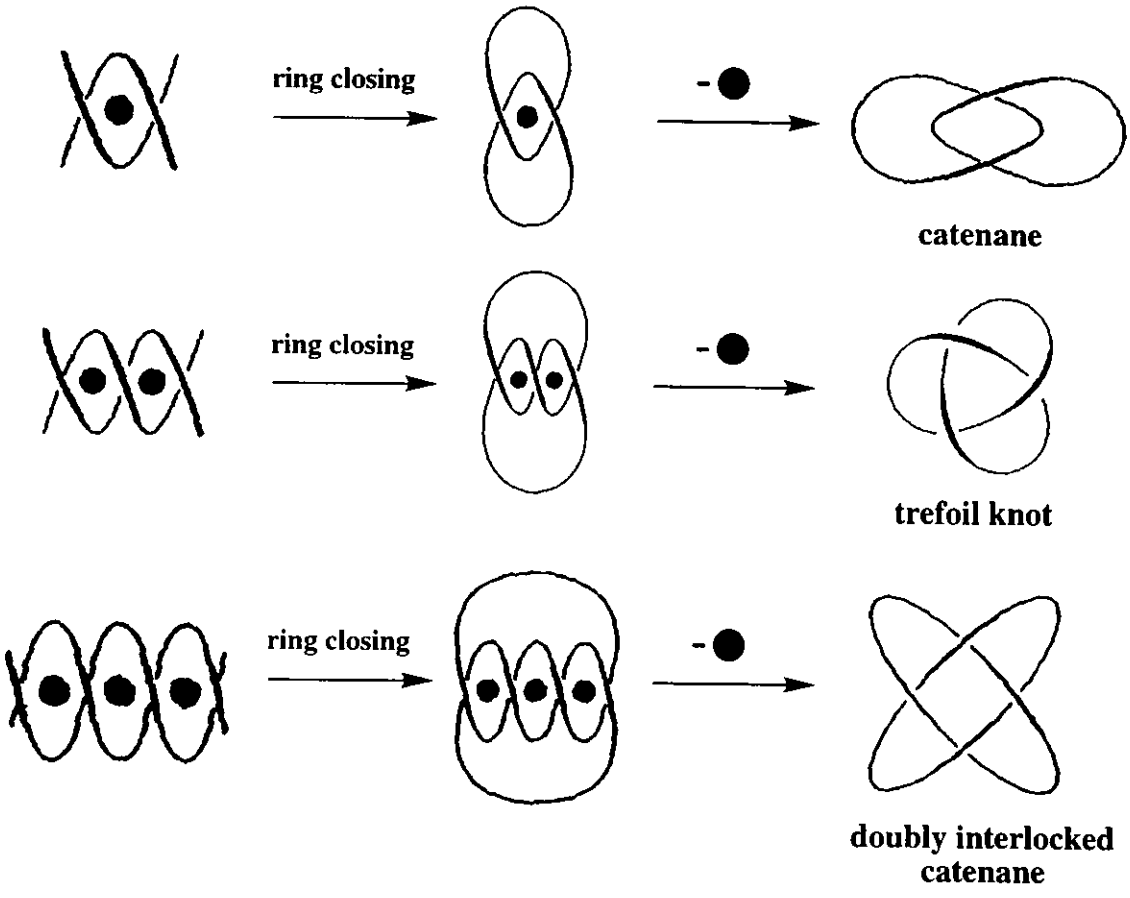

Figure 6. Sauvage's Möbius strip approach.

The approach established by Stoddart has been showing remarkable potential for the synthesis of a wide range of interlocked structures. Among them, a [5]catenane, or "Olympiadane" (Figure 7) and a [7]catenane strongly demonstrated the reliability of their method for the synthesis of versatile interlocked families.[9]

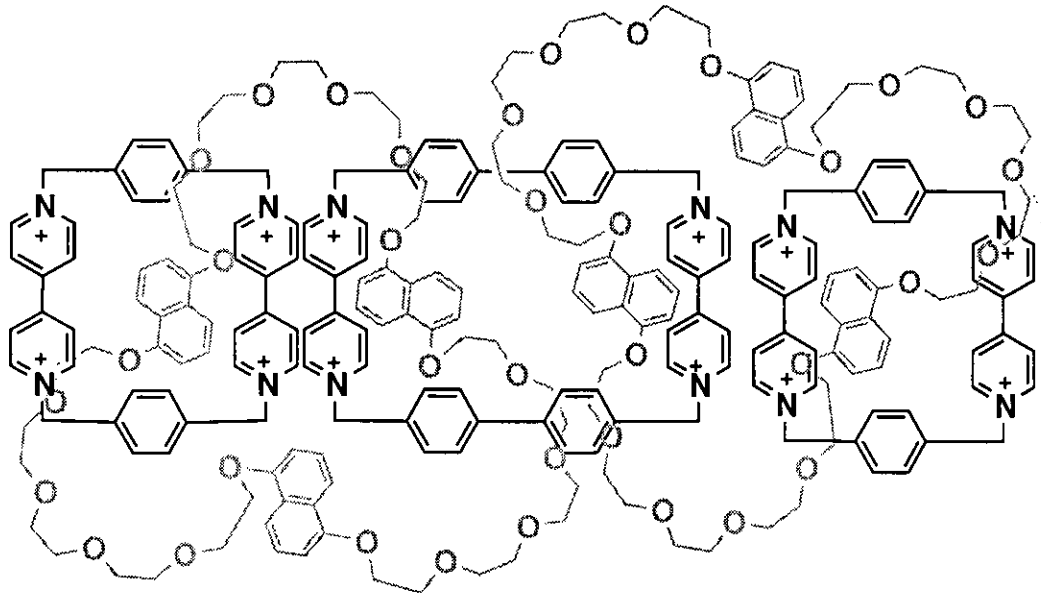

Figure 7. A [5]catenane: "Olympiadane", synthesized by Stoddart et al.

1.3 A Three-Dimensionally Interlocked Molecule

A [2]catenane is composed of two-dimensional composites: i.e., two macrocycles. A more complex molecular topology is that involving a three-dimensional macrobicyclic component in which three macrocycles are threading, one around each strand of the

macrobicyclic cage with the help of Cu(I) templated method.[10] This interlocked structure is composed of three macrocycles and a cage. On the other hand, there have been no report on an interlocked structure which consists of two three-dimensional cages. Thus, the author designed the self-assembly of a three-dimensionally interlocked structure which is composed of two identical cages.

In chapter 2, the author describes the quantitative synthesis of a three-dimensionally interlocked structure from two, identical coordination cages. Based on a rational synthetic design, two different exo-tridentate ligands were prepared and complexed with cis-protected Pd^{2+}. Spectroscopic and X-ray crystallographic analysis fully confirmed both the solution and the solid state structures of this complex. When the component cages possess molecular chirality (*P* and *M*), the 3-D interlocked complex from two units of these chiral coordination cages should be obtained as a diastereomeric mixture of a 3-D interlocked cages (*P•P, M•M)* and (*M•P*). Interestingly, these diastereo and enantioisomers are shown to be in rapid equilibrium on the NMR NOESY timescale.

1.4 Mechanistic Aspects

Chapter 3 deals with the mechanistic insight of the self-assembling process. The 3-D interlocked compound as discussed in chapter 2 consists of three species: two different ligands (L_1 and L_2) and a metal (M). Interestingly, each ligand gives its own assembled structure upon treatment with the metal. The author found that preformed (L_1+M) and (L_2+M) structures were reorganized into a 3-D interlocked (L_1+L_2+M) structure quantitatively when they were mixed together. This observation clearly showed the 3-D interlocked molecules were assembled under thermodynamic control and the yields were always quantitative regardless of the order of events, provided the ratio L_1:L_2:M were appropriate.

1.5 Catenanes: From Synthetic Challenges to Functional Systems

Functionalization of catenanes has became a topic of current interest. An electrically triggered swinging catenane, where geometry change of Cu(I) to Cu(II) drove the molecular motion, was synthesized by Sauvage et al. [11] (Figure 8) This molecule is a prototypical system for nano-devices.

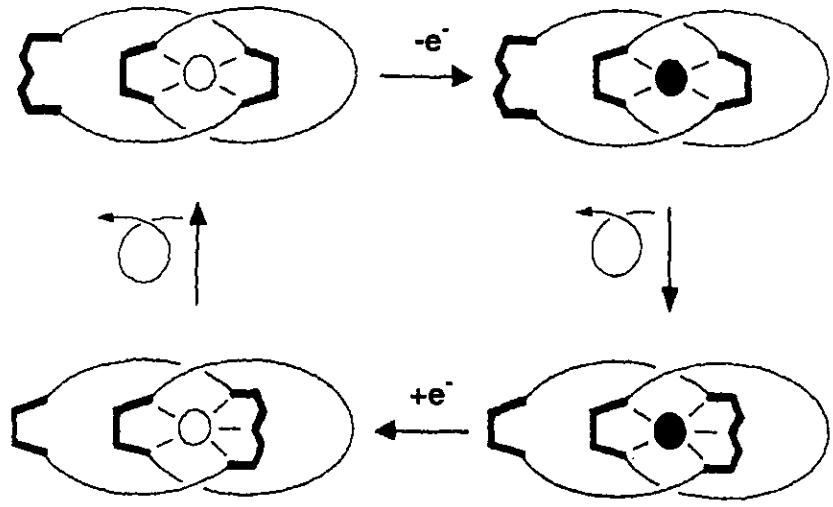

Figure 8. A [2]catenane swinging upon electrochemical stimulation by Sauvage et al. White and black circles denote Cu(I) and Cu(II) respectively.

Stoddart et al reported that the similar molecular motion triggered by electrochemical redox in [2]catenane on an electrode surface, which operated as a molecular-based semiconductor.[12]

The author designed a functionalization of interlocked structure by incorporating porphyrin units, which take essential roles in both functional, biological and artificial systems for oxygen transport, electron transfer, and energy migration and conversion. Chapter 4 describes the synthesis of a porphyrinic [2]catenane. The two macrocycles which have different metalloporphyrins were linked by the use of Cu(I)-phenanthlorin template method.

In this system, donor and acceptor porphyrins were incorporated in the two rings in such a way that the distance and the orientation are restricted. This system shows ultrafast electrontransfer from donor porphyrin to acceptor one against excitation, which is considered as a mimic of the charge separation function of photosynthetic proteins.

1.6 Porphyrin Assemblies: Previous Works

To design more functional systems, the author considered the construction of multi-porphyrin systems by metal-directed self-assembly. The construction of multi-porphyrin systems by conventional syntheses often requires multi-step syntheses with low yields. To solve the synthetic problem, templating and self-assembly strategies have offered efficient construction of multi-porphyrin systems. Prior to the study of Sanders, there exist some excellent works on covalent and non-covalent approaches to multi-porphyrin systems.

Sanders built up porphyrin dimers and trimers (Figure 9) using 4,4'-bipyridine and 1,3,5-tris(4-pyridyl)triazine, respectively, as templates. The addition of these templates led to an remarkable increase in yields.[13] The trimeric cage accelerated the Diels-Alder reaction by the "entropic trap" effect of the cage. The stereochemistry of product was altered from endo to exo selective.[14]

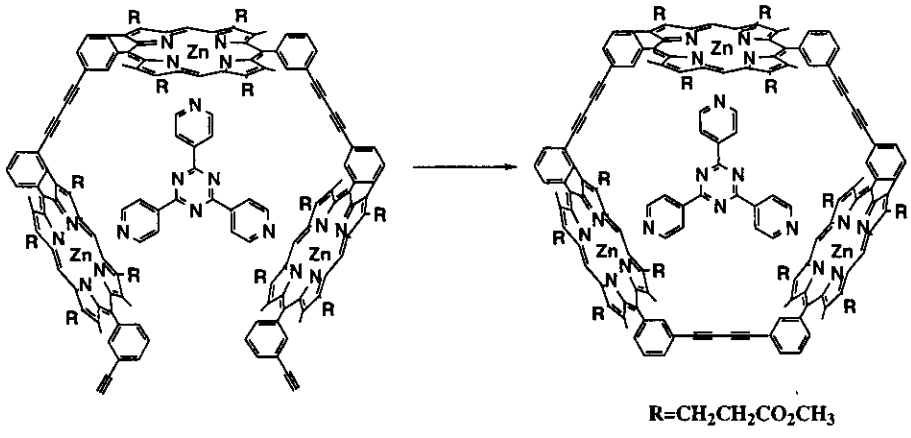

Figure 9. Template synthesis of porphyrin trimer by Sanders et al.

The metal-directed assembly of multi-porphyrin system was reported by Hunter.[15] Porphyrins with a pyridine-attached flexible side chain were dimerized into a porphyrin box structure (Figure 10) through the coordination of the pyridine nuclei to the axial position of zinc porphyrin. Quinone was bound in the cavity via hydrogen bonding to give porphyrin-quinone diad.

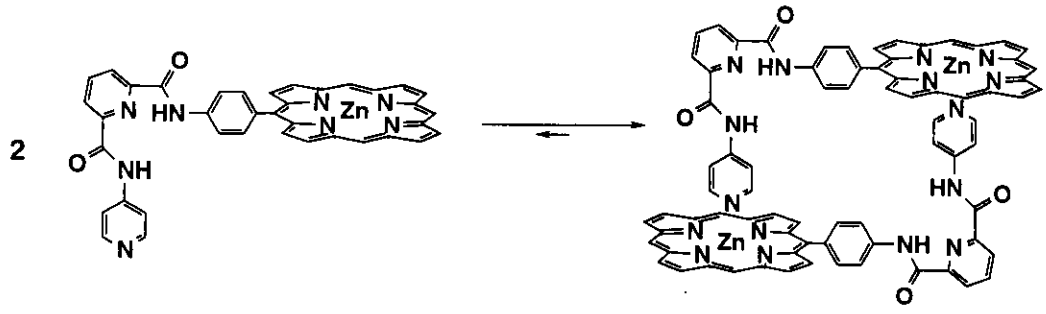

Figure 10. A stable porphyrin dimer designed by Hunter et al. The pentylphenyl substituents on the meso position are omitted for clarity.

Square complex containing pyridine substituted porphyrin ligands (Figure 11) were obtained by Lehn et al [16] and Stang et al [17] independently through coordination of Py-N and Pd(II), although their structures have not been determined by convincing methods. Furthermore, porphyrin rings in their complexes adopted cofacial conformation, giving no distinct hollow structures and guest inclusion properties.

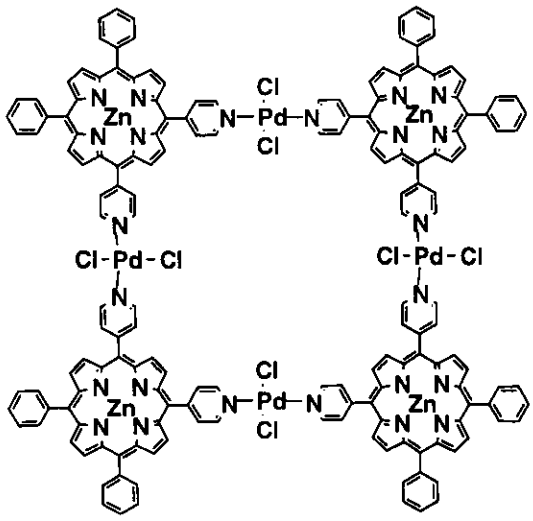

Figure 11. Lehn's tetranuclear porphyrin array supported by trans-substituted Pd(II).

1.7 A Porphyrin Prism

These examples discussed in earlier sections prompted the author to examine the metal-directed assembly of a multi porphyrinic system having a deep cavity within the framework where guest molecules could be strongly bound so that porphyrin-based functionalities could be enhanced or created through the host-guest interaction. Thus, he designed a panel-like porphyrin ligand to form discrete porphyrinic hollow structure having a deep cavity. In chapter 5, a porphyrin-based molecule having 3-pyridyl groups at *meso* positions was utilized as panel-like building block. Upon complexation with cis-protected Pd(II) in aqueous solution, a prism-like large hollow structure was obtained quantitatively. Both solution and solid state structures were confirmed by convincing methods. A large hydrophobic cavity surrounded by porphyrin units was found to include organic molecules through hydrophobic interaction. When pyrene was included in the porphyrin prism, a strong affinity between porphyrin and pyrene induced a remarkable conformational change from a D_{3h} to C_2 structure. Chiral pyrene

molecule induced optical activity of the host framework. A chirality memory effect was observed when the guest was exchanged with a free pyrene molecule, where the chirality of the host skeleton remained as observed by CD spectrum.

References

(1) Wasserman, E. *J. Am. Chem. Soc.* **1960,** *82,* 4433.

(2) Buchecker, C. O.; Sauvage, J.-P.; Kintzinger, J.-P. *Tetrahedron Lett.,* **1983**, 24, 5095.

(3) Ashton, P. R.; Goodnow, T. T.; Kaiser, A. E.; Reddington, M. V.; Slawin, A. M. Z.; Spencer, N.; Stoddart, J. F.; Vincent, C.; William, D. J. *Angew. Chem., Int. Ed. Engl.* **1989,** *28,* 1396.

(4) Hunter, C. A. *J. Am. Chem. Soc.* **1992,** *114,* 5303.

(5) Vögtle, F.; Meier, S.; Hoss, R. *Angew. Chem., Int. Ed. Engl.* **1992,** *31,* 1619.

(6) Fujita, M.; Ibukuro, F.; Hagihara, H.; Ogura, K. *Nature* **1994**, *367*, 720.

(7) (a) Van Gulick, N. *New J. Chem.* **1993**, *17*, 619. Preprint of this paper was first written in 1960. See the preface to this paper by Walba on p. 618 of this issue. (b) Frisch, H. L.; Wassereman, E. *J. Am. Chem. Soc.* **1961,** *83,* 3789. (c) Schlill, G. "Catenanes, Rotaxanes and Knots," Academic Press, New York, 1971.

(8) (a) Sauvage, J.-P.; Dietrich-Buchecker, C. O. *Molecular Topology: Catenane, Rotaxanes, and Knots*; VCH and Wiley: New York, 1998. (b) Sauvage, J.-P. *Acc. Chem. Res.* **1990**, *23*, 319. (c) Sauvage, J.-P.; Dietrich-Buchecker, C. O.; Chambron, J.-C. *Comprehensive Supramolecular Chemistry* (Ed. Lehn, J.-M.); Pergamon Press: Oxford, 1995; Vol 9, Chap 2. (d) Sauvage, J.-P. *Acc. Chem. Res.* **1998**, *31*, 611.

(9) Amabilino, D. B.; Ashton, P. R.; Reder, A. S.; Spencer, N.; Stoddart, J. F. *Angew. Chem., Int. Ed. Engl.* **1994,** *33,* 1286.

(10) Dietrich-Buchecker, C. O; Frommberger, B.; Lüer, I.; Sauvage, J.-P.; and Vögtle, F. *Angew. Chem., Int. Ed. Engl.* **1993,** *32,* 1434.

(11) Livoreil, A.; Dietrich-Buchecker, C. O; Sauvage, J.-P. *J. Am. Chem. Soc.* **1994**, *116*, 9399.

(12) Bissel, R. A.; Córdova, E.; Kaifer, A. E.; Stoddart, J. F. *Nature,* **1994**, *369*, 133.

(13) (a) Anderson, S.; Anderson, H. L.; Sanders, J. K. M. *J. Chem. Soc., Perkin Trans 1*, **1995**, 2247. (b) Anderson, S.; Anderson, H. L.; Sanders, J. K. M. *J. Chem. Soc., Perkin Trans 1*, **1995**, 2255. (c) Anderson, H. L.; Sanders, J. K. M. *Angew. Chem. Int. Ed. Engl.,* **1990**, *29*, 1400.

(14) (a) Bonar-Law, R. P.; Mackay, L. G.; Walter, C. J.; Marvaud, V.; Sanders, J. K. M. *Pure Appl. Chem.*, **1994**, *66*, 803. (b) Walter, C. J.; Sanders, J. K. M. *Angew. Chem. Int. Ed. Engl.,* **1995**, *34*, 217.

(15) (a) Hunter, C. A.; Sarson, L. D. *Angew. Chem. Int. Ed. Engl.* **1994**, *33*, 2313-2316. (b) Hunter, C. A.; Hyde, R. K. *Angew. Chem. Int. Ed. Engl.* **1996**, *35*, 1936-1939.

(16) Drain, C. M.; Lehn, J.-M. *J. Chem. Soc., Chem. Commun.* **1994**, 2313-2315.

(17) (a) Stang, P. J.; Fan, J.; Olenyuk, B. *J. Chem. Soc., Chem. Commun.* **1997**, 1453. (b) Fuss, M.; Siehl, H.-U.; Olenyuk, B.; Stang, P. J. *Organometalics* **1999,** *18,* 758. (c) Fan, J.; Whiteford, A.; Olenyuk, B.; Levin, M. D.; Stang, P. J.; Fleischer, E. B. *J. Am. Chem. Soc.* **1999,** *121*, 2741-2752.

Chapter 2

Spontaneous Assembly of Ten Components into Two Interlocked Coordination Cages

Nature **1999**, *400*, 52-55.

Abstract: Described here is the synthesis of a catenane which is composed of two macro bicyclic cages, and has a different framework as compared to a usual [2]catenane (composed from two macrocycles). This compound was obtained by metal-mediated self-assembly route. The framework of each C_{3v} cage was assembled from five components: two tridentate ligands (**3** and **4**) held together with three metal ions. Because each cage framework can bind an aromatic ring inside its cavity therefore, two cage units will bind one another during their assembly process through the formation of a quadruple aromatic stack, giving rise to the ten-component interlocked supermolecule. Convincing characterization of both solution and solid state structures were done by NMR, ESI-MS, and X-ray analyses. From a C_3 cage possessing molecular chirality, the three-dimensionally interlocked dimer was obtained as a mixture of diastereomers.

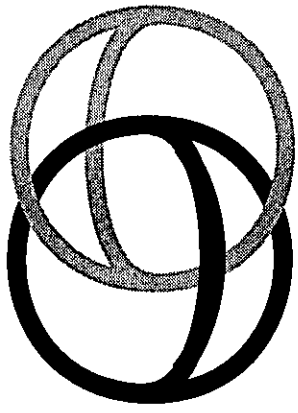

Schematic representation of an interlocked structure from three–dimensional bicyclic cages.

2.1 Introduction

Over the last few decades, continuous synthetic challenges to linked-ring molecule (or catenane)[1] and related compounds have intrigued not only the imaginations of chemists but also considerable development in synthetic and material chemistry[2]. In particular, noncovalent syntheses have been developed rapidly owing partly to the recent achievements of the efficient syntheses of catenanes by metal-templating[3,4] as well as by self-assembly[5-12]. While a catenane framework stems from the topological isomerism of two rings, no example has been reported to date for an interlocked molecule arising from the isomerism of two cages. Described here is such a three-dimensionally interlocked compound consisting of two cages, as schematically shown in Figure 1. The catenane was easily prepared by metal-mediated self-assembly[13-15]. The framework of each cage is assembled from five components, two different exo-tridentate ligands held together with three metal ions. The cage framework possesses an interspace ideal to bind an aromatic ring. Thus, the two cage units efficiently bind each other through the formation of an efficient quadruple aromatic stack giving rise to a ten-component self-assembly, an unprecedented three-dimensionally interlocked molecule[16,17].

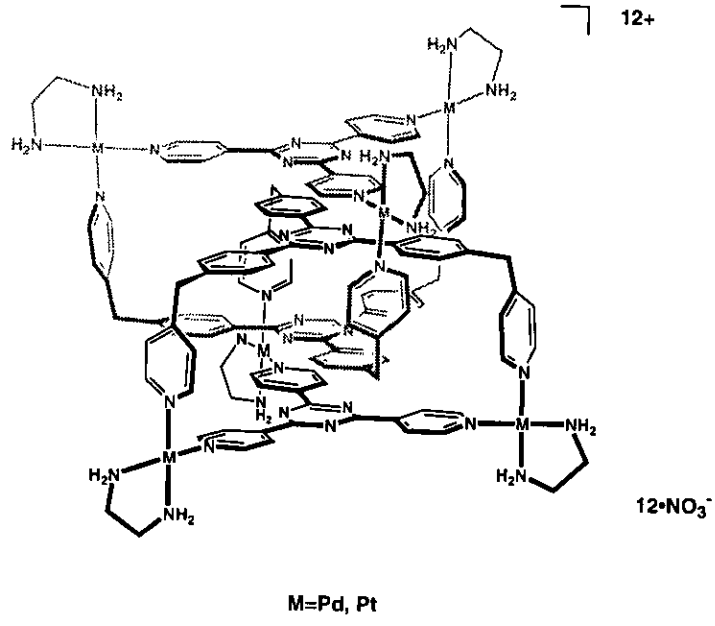

Figure 1. Chemical representation of 3–D interlocked structure.

2.2 Retrosynthetical Analysis of a 3–D Interlocked Compound

A strategy for constructing the 3–D interlocked compound is revealed by the retrosynthetical analysis of a target framework (Scheme 1). First, the interlocked cages (**A**) are divided into two separate cages (**B**), wherein labile metal-ligand bonds are put to make a reversible pathway (**A**⇄**B**). Second, the metal containing cage (**B**) is deformed so that it has a flat "floor" and a "ceiling" (**C**). The distance between the floor and the ceiling should be adjusted so that another copy of **B** would fit in the cavity. Thus, cagelike complex **1** is designed in which the interplanar surface-to-surface distance between the "floor" and the "ceiling" is *ca* 3.5 Å, an ideal distance for binding an aromatic ring. Finally, this cage compound **1** is disconnected into three component molecules **2**–**4**. Cis-protected Pd(II) and Pt(II) complexes **2** have been employed for metal-mediated self-assembly of discrete structures[14,15]. Quite recently, rectangular molecular boxes with the interplanar separation of *ca* 3.5 Å were shown to effectively self-assemble into catenated dimers[18].

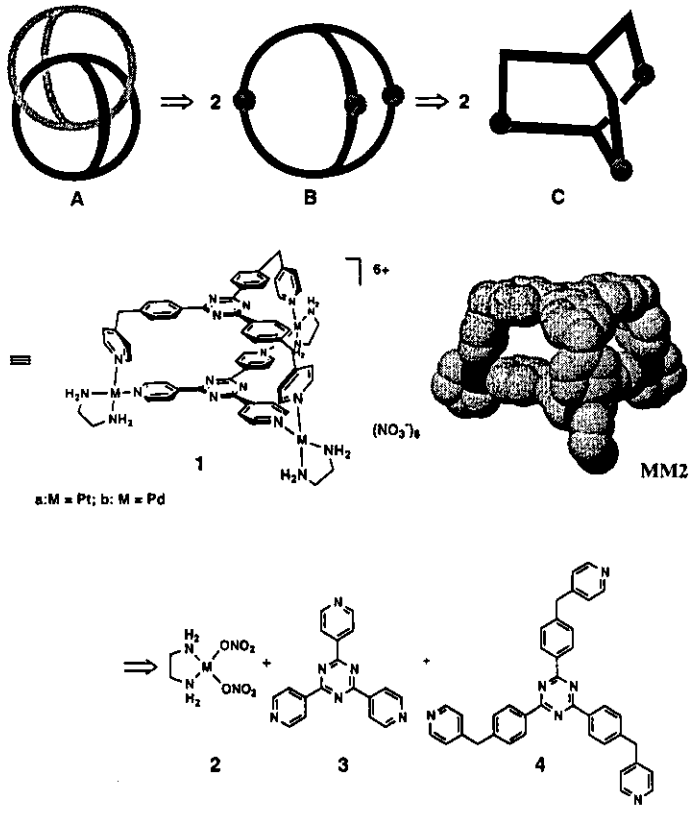

Scheme 1. Retrosynthetic analysis of the 3–D interlocked compound.

2.3 Synthesis of 3–D Interlocked Compound: Characterization of the Solution and Solid State Structure

Three components **2a**, **3**, and **4** were combined in a 3:1:1 stoichiometry in D_2O. At first, a kinetically distributed mixture was formed, which, however, gradually turned into a thermodynamically stable structure after heating the solution at 100 °C for 3 d. This slow conversion is due to the dual character of a Pt(II)-pyridine coordinate bond which is inert at room temperature but becomes labile at elevated temperature[19]. Therefore, thermodynamically favorable structure self-assembles at only elevated temperature. The nuclear magnetic resonance (NMR) spectrum of the crude reaction solution showed the formation of almost a single component, which was isolated in a pure form (65%). After converting to a PF_6 salt, the product was assigned as **5a** (PF_6 salt) by exact electrospray ionization mass spectrometry (ESI–MS). Similarly, Pd(II) counterpart **5b** was prepared, whose formula was confirmed by elemental analysis.

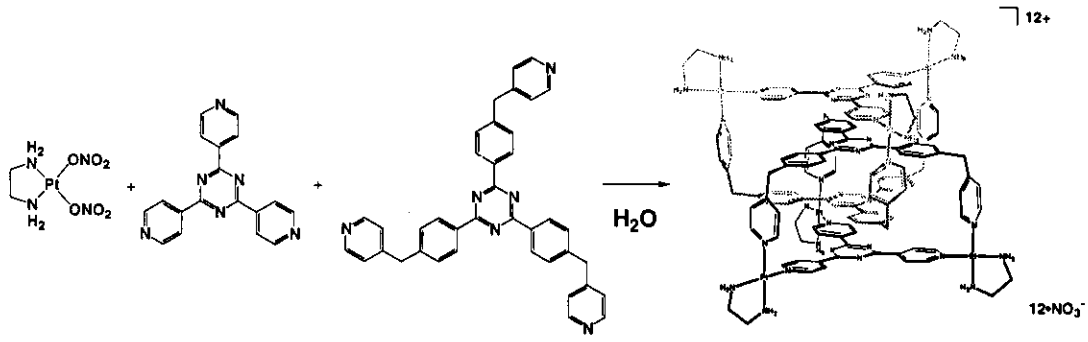

Scheme 2.

A reliable evidence for the 3–D interlocked structure of **5a** was obtained by an X–ray crystallographic analysis (Figure 2), which shows that **5a** consists of two identical cage frameworks interlocking with each other. The crystal system was assigned to be *C*–centered monoclinic (*C*2/c) and the crystallographically solved structure contained only one cage

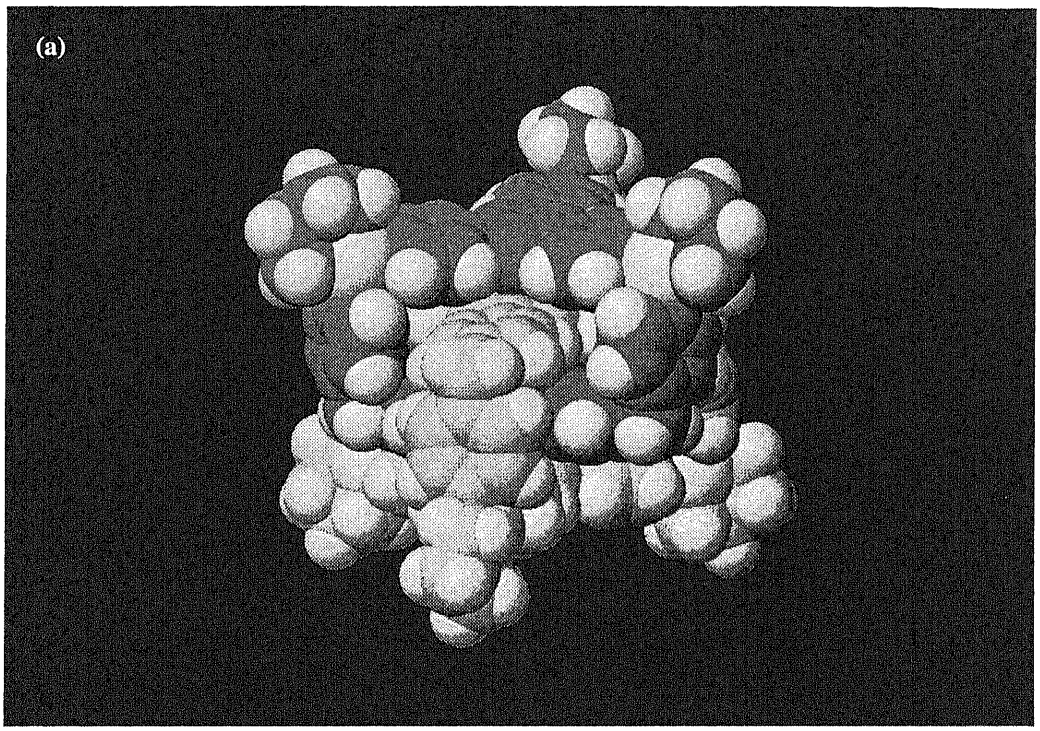

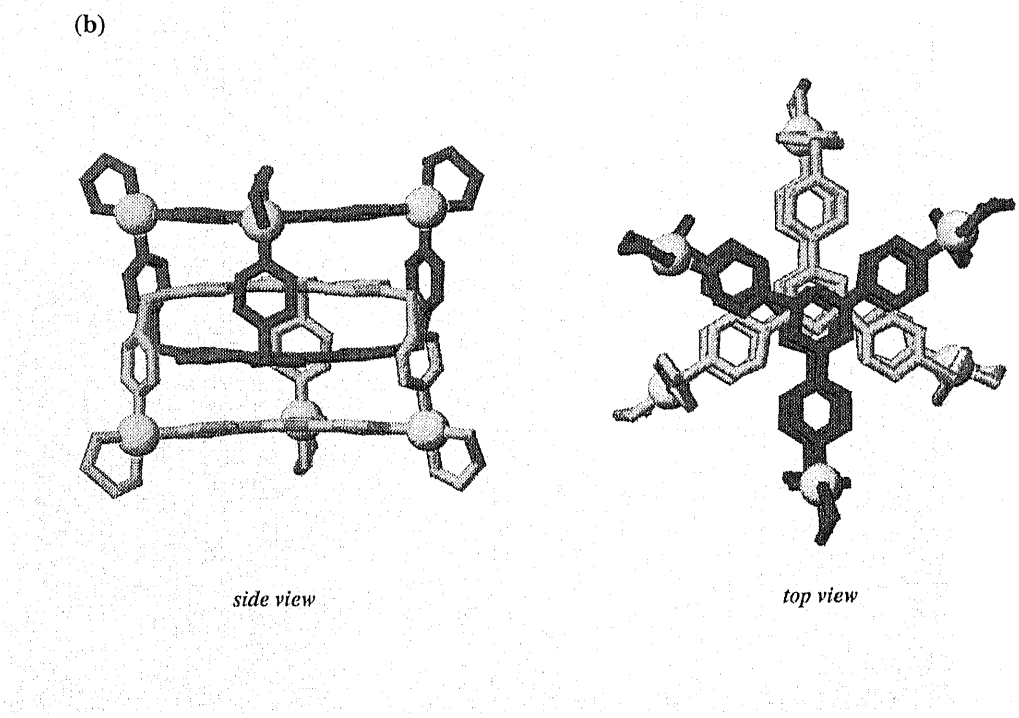

Figure 2. (a) A space–filling presentation and (b) ball–and–stick presentations of the X–ray structure of **5a** (BF_4 salt).

framework, which gave the interlocked structure after symmetry operation. From the side view of **5a** (Figure 2b), the efficient quadruple stacking of aromatic rings can be observed. This stacking makes the interlocked structure the most stable among any possible structures formed by the complexation of **2** with **3** and/or **4**. From the top view (Figure 2b), it is found that the triazine core rings of the two cage units are slightly displaced by *ca* 1.3 Å, probably due to efficient π-π stacking[20,21] or favorable crystal packing. Interestingly, interlocked cages are further stacked intermolecularly making one-dimensional infinite stacking of triazine π systems. Experimentally, a single crystal of the BF_4 salt of **5a** was obtained by adding excess amount of $NaBF_4$ to the aqueous solution of **5a** and standing the solution at ambient temperature for a few weeks.

The solution state structures of **5a** and **5b** were determined by NMR studies. Both ^1H and ^{13}C NMR agree well with the structure of **5a** and **5b** (Figure 3) and the assignments are fully supported by two-dimensional NMR measurements. The interlocked framework is consistent with (i) an outstanding upfield shift of C_6H_4(in) ($\Delta\delta$= 2.63) which is the most significantly shielded by another cage framework, and (ii) the observation of nuclear Overhauser effect (NOE) between Py_1-CH_2-C_6H_4

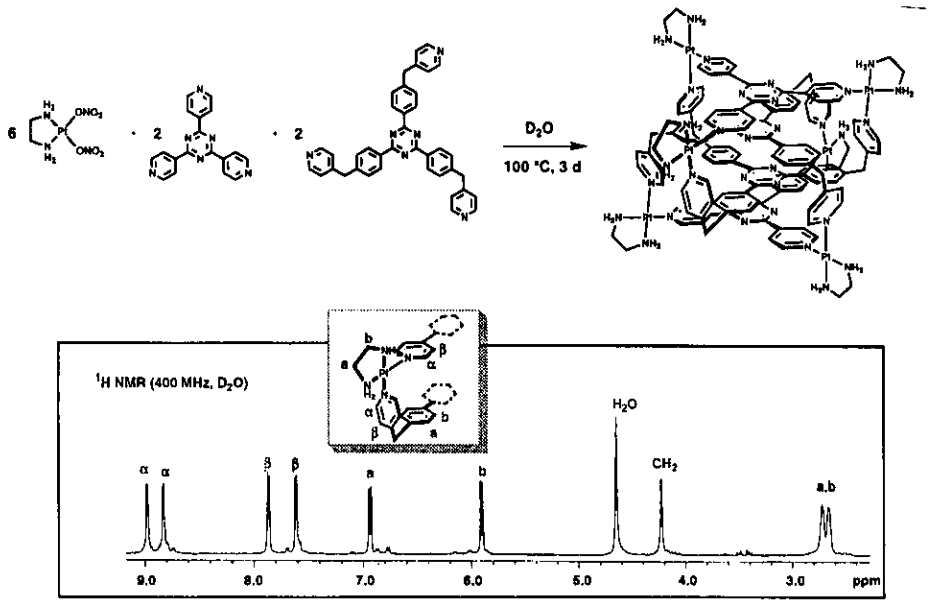

Figure 3. ^1H NMR spectrum of **5a** (400 MHz, D_2O).

and Py_2 units. Since the Pt(II)-Py bond is kinetically inert at room temperature, complex **5a** is stable at any concentrations and not in equilibration with other structures.

ESI-MS studies also confirmed the solution structure of **5a**. (Figure 4) When acetonitrile solution of **5a** (PF_6 salt) was subjected to the measurement, prominent peaks for $[M-(PF_6^-)_n]^{n+}\bullet m(CH_3CN)$ (n = 4–9, m = 2–18) were clearly observed with reasonable isotopic distribution. It is interesting that acetonitrile molecules seem to weakly solvate the cationic sphere of Pt^{2+} ions and the number of solvated acetonitrile (m) increases with positive charges (n). Furthermore, exact ESI-MS study shows good accordance with its theoretical distribution. Similarly, the ESI-MS study of BF_4 salt of **5a** afforded a series of peaks corresponding with $[M-(BF_4^-)_n]^{n+}\bullet m(CH_3CN)$.

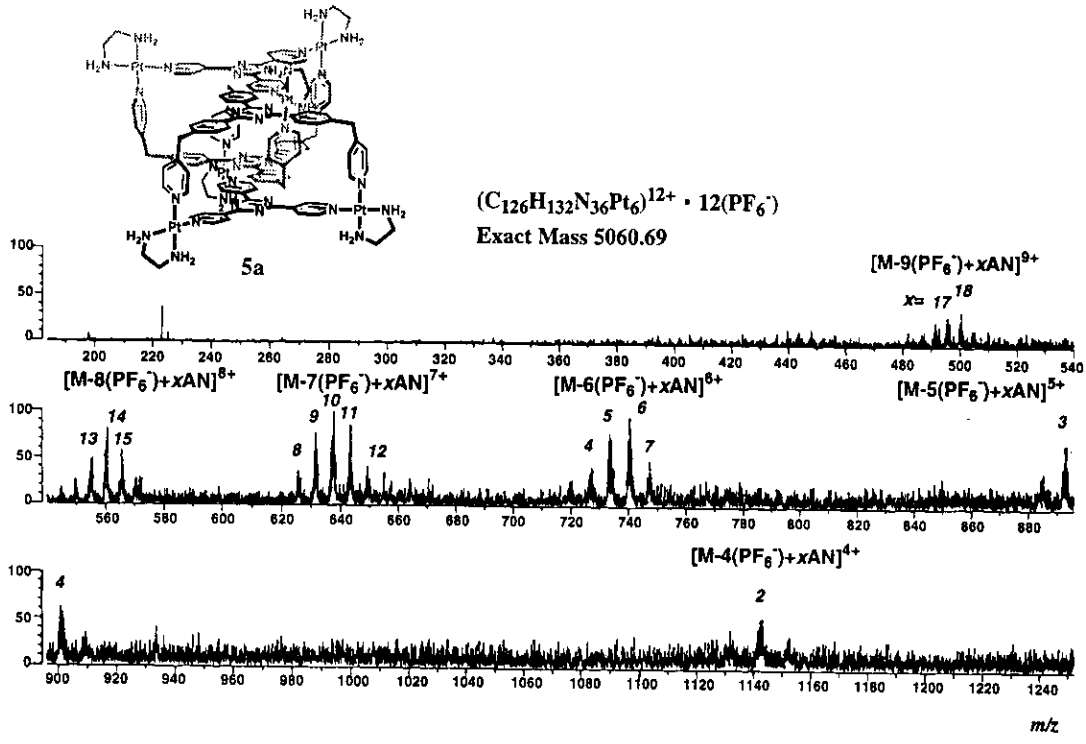

Figure 4. ESI-MS of **5a** (PF_6 salt).

2.4 A 3-D Interlocked Compound from Coordination Cages Having Molecular Chirality

Hexadentate ligand (**6**) having three pyrimidyl groups in combination with **2** and **4** is expected to give structures of diversed coordination fashions. While 1:1 complex of **6** and **4** gives enantiomer pair (*M* and *P*) of cage structures (D), double decker cage structure is expected from 1:2 complexation. These "imaginary" cages are subjected to bind each other to give expected discrete 3–D interlocked structure or one-dimensional chain structure.

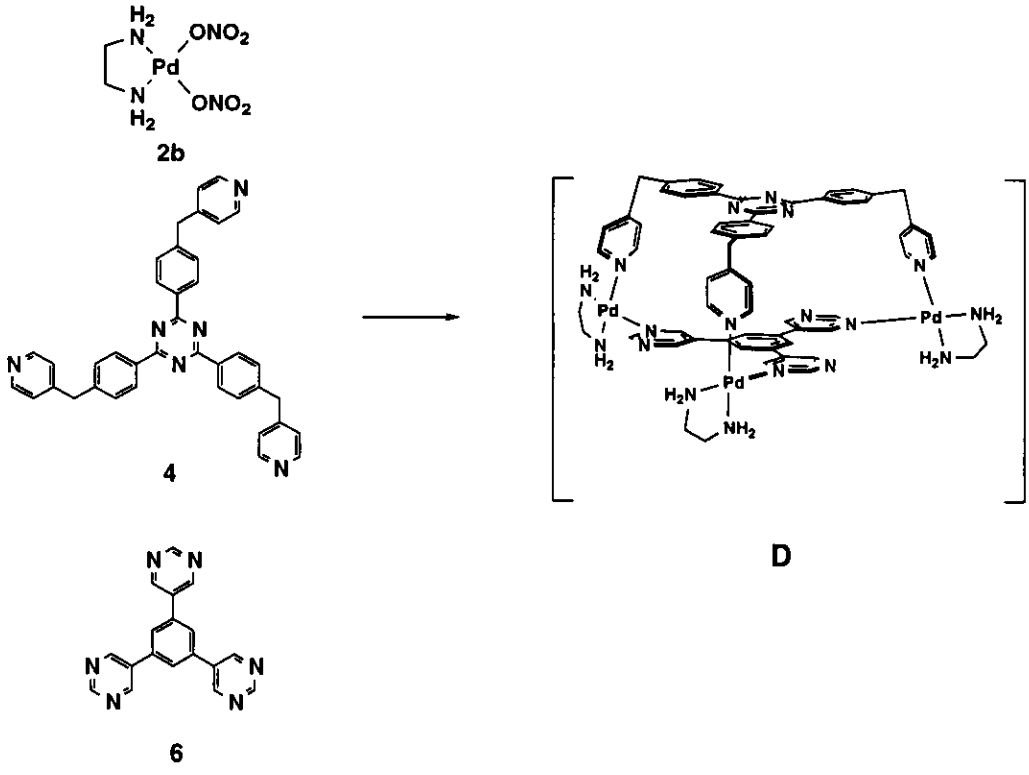

Scheme 3.

Thus, three components **2b**, **6**, and **4** were combined in a 6:1:2 stoichiometry in D_2O–CD_3OD (3:1) mixed solvent. After one day at 80 °C, the NMR spectrum (Figure 5) of the crude reaction solution gave more complex set of signals containing outstanding upfield shift for 8 protons. Those were assigned as phenylene protons that are significantly shielded by another cage framework, and implied formation of interlocked structure. The integration ratio showed that **4** and **6** complexed with **2b** in the ratio not of 6:1:2 but of 3:1:1, which is not

consistent with infinite 3–D interlocked structure but with discrete 3–D interlocked structure. Remaining **2b** and **4** could not be found in NMR spectrum, probably due to the formation of a mixture of oligomers in this condition (see chapter 3).

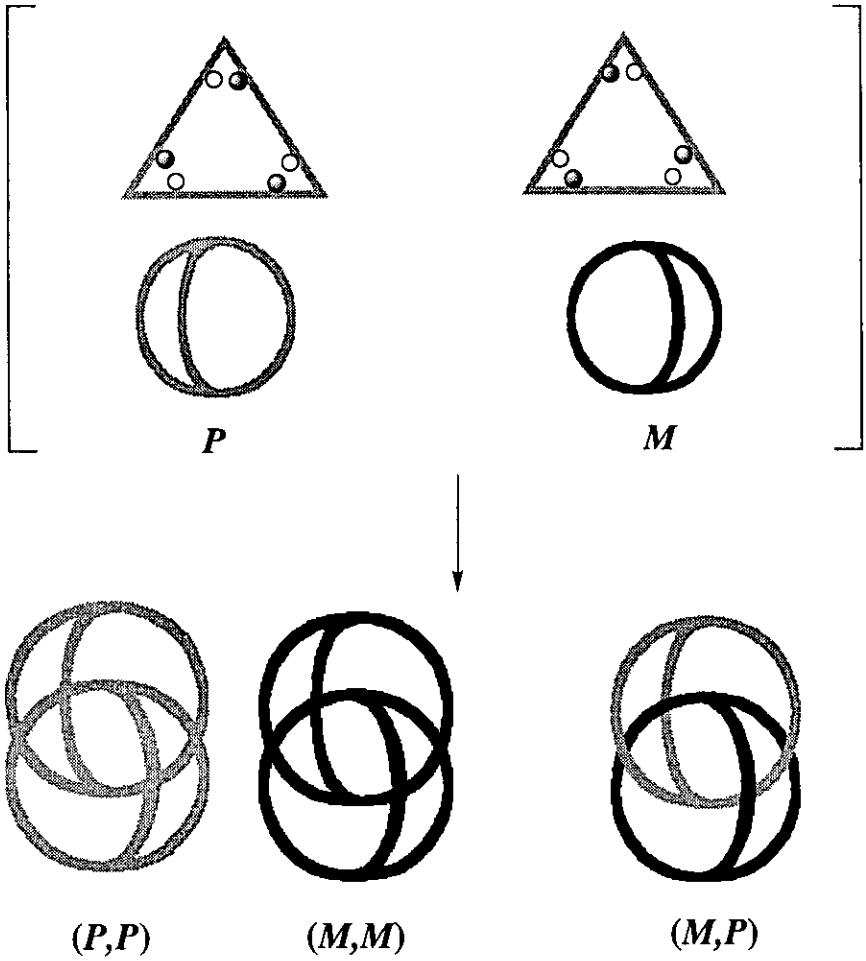

Scheme 4.

Since the cage has enantiomers (*M* and *P*), interlocked dimer should have diastereomers [(*M*• *M* and *P*•*P*) and (*M*•*P*)]. Careful assignment by 2D NMR affirmed the existence of the diastereomers pair and structural insight of this interlocked system. In the ^{1}H NMR spectrum, there were two sets of pyrimidyl, pyridyl and phenylene protons in same integration ratio corresponding to the diastereomers. Four protons on the phenylene ring were observed as

inequivalent eight doublets for diastereomer pair since their rotation was restricted due to the stacking structure, however pyridyl protons were observed not as eight doublets but as four doublets corresponding to two sets of pyridyl α and β protons, which implied free rotation of pyridyl rings.

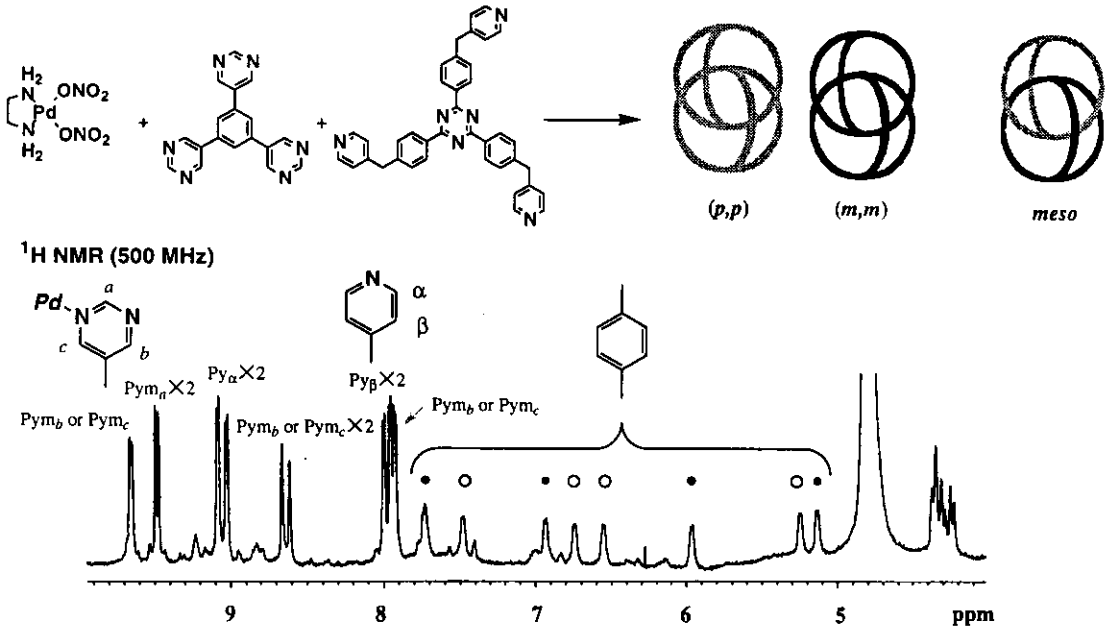

Figure 5. NMR spectrum of a mixture of diastereomers of 3–D interlocked compound.

2.5 The 3–D Interlocked Molecules in Motion

The resulting 3–D interlocked system, which was obtained as a mixture of diastereomers, showed an interesting dynamic behavior. The diastereomeric 3–D interlocked compound was obtained even at higher concentration using the following condition (**2b**:**4**:**6**=3:1:1, [**2b**]=50 mM, D_2O:CD_3OD=9:1). NMR NOESY experiment at 300 K gave intense corelational signals between phenyl protons of diastereomers. Observed chemical exchange as found from NMR study is strong evidence for a structural interchange between the diastereomers. Such structural interchange is due to rotation of hexadentate ligand coordinating to the metal by weak pyrimidine–Pd

bonding.

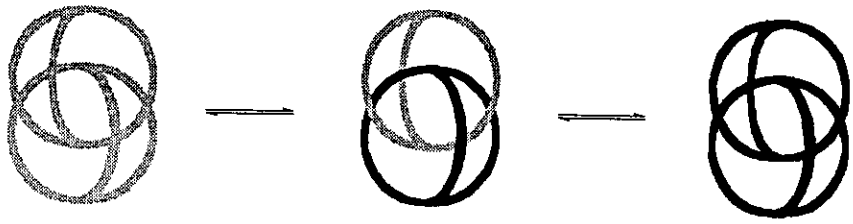

(P,P) *(M,P)* *(M,M)*

2.6 Conclusion

Topologically complex 3–D interlocked structures were constructed by metal–mediated self-assembly. Rational design (supramolecular retorosynthesis) successfully accesses the construction of unprecedented linked cage structures. From the cage components that don't possess C_{3v} symmetry, the interlocked dimer structure was obtained as a mixture of diastereomers. NMR NOESY experiment revealed an interesting dynamic behavior where a structural exchange between the diastereomers occurred within NOESY time scale.

2.7 Experimental Section

General: Thin layer chromatography (TLC) was performed on precoated silica plates (Merck, Kieselgel 60 F_{254} 2 mm). Column chromatography was performed on silicagel (Merck, Kieselgel 60, 70–230 mesh). Melting points were determined on a YANACO MP–500V without correction. FTIR spectra were recorded on JASCO–A–200 spectrometer or SHIMADZU FTIR 8300 spectrometer. ^{1}H NMR spectra were recorded on JEOL JNM–GSX 400 (400 MHz) spectrometer, JEOL JNM–GSX 500 (500 MHz) spectrometer, JEOL JNM–LA 500 (500 MHz) spectrometer, and Brucker (500 MHz) spectrometer. ^{13}C NMR spectra were recorded on, JEOL JNM–LA 500 (125 MHz) spectrometer. Chemical shifts are reported in parts par million (δ units) relative to tetramethylsilane served as an internal standard when $CDCl_3$ was used as a solvent. For other solvents, a solution of tetramethylsilane in $CDCl_3$ sealed in capillary was used as an external standard. Spectral splitting are designated as s,

singlet; d, doublet; t, triplet; q, quartet; m, multiplet; br, broad. Microanalyses were carried out on a Perkin–Elemer 240 B and 2400 CHN and YANACO MT-3. FAB MS (fast atom bombardment mass spectroscopy) were recorded on a JEOL JMS–HX 110A spectrometer. ESI–MS (electrospray ionization mass spectroscopy) were recorded on JEOL Type JMS–7000 (for CSI–MS) spectrometer. Preparative HPLC(GPC) was performed on a LC–908 C_{60} (Japan Analytical Industry, Co., Ltd.) with column (AJ2H J49–8F28, AJ1H J45–8F27). Solvents and reagents were purchased from TCI Co., Ltd., WAKO Pure Chemical Industries Ltd., Nacalai Tesque Ins., Tanaka kikinzoku Ltd., and Aldrich chemical., Ltd. These chemicals were used without purification, and a distillation and other purification procedures were done when it was needed.

Synthesis of ligand (4): 2,4,6–Tris[4– (4–pyridylmethyl)phenyl] –1,3,5–triazine (**4**). Butyllithium (1.60 M in hexane, 27.0 mL, 43.2 mmol) was added to a THF solution (50 mL) of diisopropylamine (5.05 mL, 36.0 mmol) at 0 °C. After 1 h, 4–picoline (2.95 mL, 30.0 mmol) was added and the solution was stirred for additional 1 h. Then, zinc chloride (0.5 M THF solution, 66.0 mL, 33.0 mmol) was added and the mixture was warmed to room temperature and stirred for 1.5 h. To this solution, tetrakis[triphenylphosphine]palladium(0) (1.04 g, 0.90 mmol), 2,4,6-tri(4–bromophenyl)–1,3,5–triazine (1.64 g, 3.00 mol), and 1,4–dioxane (70 mL) was added and the solution was heated at 100 °C for 3 d. Water (30 mL) and ethylenediamine (10 mL) were added and the mixture was stirred for 0.5 h. After usual workup (extraction with chloroform, drying over $MgSO_4$) purification by column chromatography on silica gel (eluent: $CHCl_3$–CH_3OH 20:1) and preparative gel–permeation chromatography gave **4** (596 mg, 1.02 mmol, 34%) as colorless crystals: mp 235–237 °C; ^1H NMR (300 MHz, $CDCl_3$) δ 8.70 (d, *J*=8.2 Hz, 2 H), 8.54 (d, *J*=5.9 Hz, 2 H), 7.38 (d, *J*=8.2 Hz, 2 H), 7.15 (d, *J*=5.9 Hz, 2 H), 4.09 (s, 2 H); ^{13}C NMR (125 MHz, $CDCl_3$) δ 171.4, 150.0, 149.3, 143.7, 134.8, 129.42, 129.40, 124.2, 41.2. IR (KBr) 3700, 2930, 1592, 1508, 1462, 1448, 1410, 1364, 800, 778, 720 (cm^{-1}). HRMS (FAB) *m/z* calcd. for $C_{39}H_{30}N_6 \cdot H^+$: 583.2602, found: 583.2606. Elemental

analysis calcd. for $C_{39}H_{30}N_6 \cdot 0.5H_2O$: C, 79.16; H, 5.28; N, 14.20; found C, 79.07; H, 5.20; N, 14.19.

Self-assembly of 5a: Ligands **3** (28 mg, 0.088 mmol) and **4** (51 mg, 0.088 mmol) were suspended in an aqueous solution (26 mL) of **2a** (100 mg, 0.26 mmol) and the mixture was stirred at 100 °C for 3 d. After the solution was condensed under reduced pressure to 5 mL, followed by addition of ethanol (20 mL) the compound **5a** was precipitated, which was isolated as a colorless powder upon filtration (116 mg, 0.029 mmol, 65%). ^{1}H NMR (500 MHz, D_2O, TMS in a sealed capillary as an external standard) δ 9.15 (d, J = 6.5 Hz, 12 H), 9.00 (d, J = 5.9 Hz, 12 H), 8.04 (d, J = 6.5 Hz, 12 H), 7.78 (d, J = 5.9 Hz, 12 H), 7.11 (d, J = 7.9 Hz, 12 H), 6.07 (d, J = 7.9 Hz, 12 H), 4.40 (s, 12 H), 2.8 - 2.9 (m, 24 H); ^{13}C NMR (125 MHz, D_2O, TMS in a sealed capillary as an external standard) δ 169.2 (*C*q), 169.0 (C_q), 158.2 (C_q), 153.6 (*C*H), 152.9 (*C*H), 146.9 (C_q), 144.6 (C_q), 132.5 (Cq_q), 129.4 (*C*H), 128.3 (*C*H), 127.8 (*C*H), 126.1 (*C*H), 48.4 (CH_2), 48.3 (CH_2), 42.2 (CH_2). IR (KBr) 1637, 1523, 1384, 1052, 810 cm^{-1}. Mass spectrometry was studied after **5a** was converted into its PF_6 salt by adding NH_4PF_6 to an aqueous solution of **5a**. Exact ESI-MS (PF_6 salt): prominent peaks for $[M\text{-}(PF_6^-)_n]^{m+} \cdot (CH_3CN)m$ (n = 4–9, m = 2–18) were clearly observed: e.g., *m/z* found for $[M\text{-}(PF_6^-)_8 + 14CH_3CN]_{8+}$ 559.3928 ; calcd 559.3953.

Crystallographic study of 5a. Slow evaporation of water from an aqueous solution (1.4 mL) of **5a** (20 mg) containing 0.2 M $NaBF_4$ at ambient temperature for 17 d gave a single crystal of **5a** (BF_4 salt) suitable for X–ray crystallographic analysis. Crystal data: monoclinic, *C*2/*c* (no. 15); a = 30.83 (1), b = 22.67 (1), c = 25.731(5) Å, β = 109.00(4), V = 17005(9) Å^3; z = 8; F(000) = 8880; μ(MoKα) = 50.14 cm^{-1}; λ = 0.71070; temp. = -150 °C; 17770 reflections measured (10686 independent), 6176 observed (I>4.00σ(I)); R = 0.119; R_w = 0.153. In this refinement, twelve counter ions and twelve water oxygens were taken into account for the refinement, including definitely assigned eight counter ions (four BF_4 ions in an asymmetric

unit) and four (two) BF_4^- fragments. Hydrogen atoms are located at the calculated positions (not refined). Despite the data collection at -150 °C, quality of the data was inferior due to high degree of disorder of BF_4 anions and solvent molecules. However, all heavy atoms involved in the cage framework are definitely identified.

Self-assembly of 5b. Ligand **3** (54 mg, 0.17 mmol) was added to an aqueous solution (26 mL) of **2b** (75 mg, 0.26 mmol) and the solution was stirred at 80 °C for 3 days. On the other hand, a CH_3OH (13 mL) solution of **4** (100 mg, 0.17 mmol) was added to an aqueous solution (1 mL) of **2b** (75 mg, 0.26 mmol). These two solution were combined and the mixture was stirred at 80 °C for 5 d. The addition of ethanol (600 mL) to this solution and stirring the solution at 4 °C for 1 d precipitated **5b,** which was isolated as colorless crystals (186 mg, 0.053 mmol, 61%) after filtration. Mp >300 °C; ^{1}H NMR (500 MHz, D_2O) δ 9.11 (d, J = 7.1 Hz, 12 H), 8.96 (d, J = 6.6 Hz, 12 H), 8.04 (d, J = 7.1 Hz, 12 H), 7.79 (d, J = 6.6 Hz, 12 H), 7.07 (d, J = 8.1 Hz, 12 H), 6.03 (d, J = 8.1 Hz, 12 H), 4.38 (s, 12 H); ^{13}C NMR (125 MHz, D_2O) δ 169.3 (*C*q), 169.0 (C_q), 158.3 (C_q), 152.6 (*C*H), 152.0 (*C*H), 146.9 (C_q), 144.9 (C_q), 132.5 (C_q), 129.4 (*C*H), 128.2 (*C*H), 127.4 (*C*H), 125.7 (*C*H), 47.6 (CH_2), 47.5 (CH_2), 42.3 (CH_2); IR (KBr) 1637, 1507, 1385, 1059, 826, 806 cm^{-1}. Anal. Calcd for $C_{126}H_{132}N_{48}O_{36}Pd_6 \cdot 12H_2O$: C, 40.36; H, 4.19; N, 17.93. Found: C, 40.16; H, 3.91; N, 17.65.

References and Notes

(1) Wasserman, E. *J. Am. Chem. Soc.* **1960,** *82,* 4433-4434.

(2) Amabilino, D. B.; Stoddart, J. F. *Chem. Rev.* **1995,** *95,* 2725-2728.

(3) Dietrich-Buchecker, C. O.; Sauvage, J.-P.; Kintzinger, J.-P. *Tetrahedron Lett.* **1983,** *24,* 5095-5098.

(4) Sauvage, J.-P.; Dietrich-Buchecker, C. O.; Chambron, J.-C. in Comprehensive Supramolecular Chemistry (Eds by Sauvage, J.-P.; Hosseini, M. W.) Vol. 9, 43-83 (Pergamon Press, Oxford, 1995; Chap 2).

(5) Ashton, P. R.; Goodnow, T. T.; Kaifer, A. E.; Reddington, M. V.; Slawin, A. M. Z.; Spencer, N.; Stoodart, J. F.; Vicent, C.; Williams, D. J. *Angew. Chem. Int. Edn Engl.* **1989**, *28*, 1396.

(6) Hunter, C. A. *J. Am. Chem. Soc.* **1992**, *114*, 5303-5311.

(7) Vögtle, F.; Meier, S.; Hoss, R. *Angew. Chem., Int. Edn Engl.* **1992**, *31*, 1619-1621.

(8) Fujita, M.; Ibukuro, F.; Hagihara; H.; Ogura, K. *Nature* **1994**, *367*, 720-723.

(9) Johnston, A. G.; Leigh, D. A.; Pritchard, R. J.; Deegan, M. D. *Angew. Chem., Int. Edn Engl.* **1995**, *34*, 1209-1212 .

(10) Hamilton, D. G. et al. *J. Am. Chem. Soc.* **1998**, *120*, 1096.

(11) Batten, S. R.; Robson, R. *Angew. Chem., Int. Edn Engl.* **1998**, *37*, 1460-1494.

(12) Drain, C. M.; Nifiatis, F.; Vasenko, A.; Batteas, J. D. *Angew. Chem., Int. Edn Engl.* **1998**, *37*, 2344-2347.

(13) Baxter, P. N. W. in Comprehensive Supramolecular Chemistry (Eds by Sauvage, J.-P.; Hosseini, M. W.) Vol. 9, 165-211 (Pergamon Press, Oxford, 1996; Chap. 5).

(14) Fujita, M. *Acc. Chem. Res.*, **1999**, *32*, 53-61.

(15) Fujita, M. *Chem. Soc. Rev.*, **1998**, *27*, 417-425.

(16) Dietrich-Buchecker, C.; Frommberger, B.; Lüer, I.; Sauvage, J.-P.; Vögtle, F. *Angew. Chem., Int. Edn Engl.* **1993**, *32*, 1434-1437.

(17) Ashton, P. R. et al. *Angew. Chem., Int. Edn Engl.* **1997**, *36*, 59-62.

(18) Fujita, M.; Aoyagi, M.; Ibukuro, F.; Ogura, K.; Yamaguchi, K. *J. Am. Chem. Soc.* **1998**, *120*, 611.

(19) Ibukuro, F.; Kusukawa, T.; Fujita, M. *J. Am. Chem. Soc.*, **1998**, *120*, 8561-8562.

(20) Jorgensen, W. L.; Severance, D. L. *J. Am. Chem. Soc.* **1990**, *112*, 4768-4774.

(21) Hunter, C. A.; Sanders, L. K. M. *J. Am. Chem. Soc.* **1990**, *112*, 5525-5534.

Chapter 3

Reconstruction of Three-Dimensionally Interlocked Structure from Two, Preorganized Three-Dimensional Cages

Nature **1999**, 400, 52-55.

Abstract: As described in chapter 2, the 3-D interlocked cages are assembled quantitatively from three species-ten components as a most stable compound among many possible structures. The extraordinary thermodynamic stability was demonstrated in an NMR experiment. Symmetrical cage-like complexes **4** and **5** which are assembled from each ligand (**2** and **3**, respectively) and Pd(II) complex **1** are also possible structures and formed as most stable structures in each system. After combining them, the preformed cage-like complexes gradually reorganized into a single product of 3-D interlocked compound **6**, which is constructed from the two ligands (**2** and **3**) and the metal ion (**1**), as shown by ^{1}H NMR time-dependence experiment.

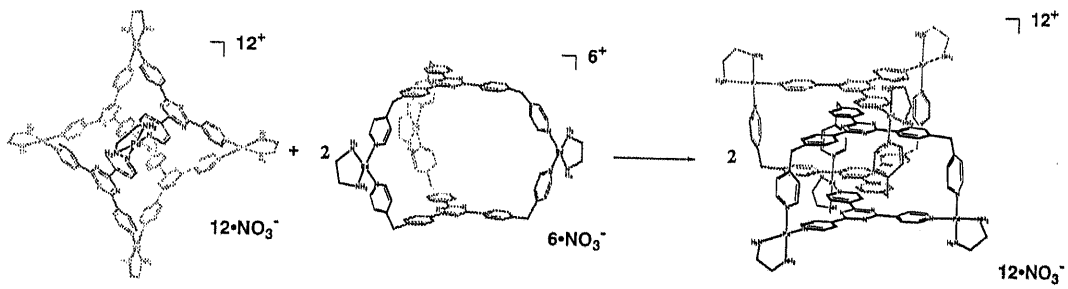

3.1 Introduction

Due to lack of complementary between metals and ligands, it has been quite difficult to establish a reliable approach for designing multi-component assemblies in coordination reactions. Concerning the assembling process, dominant assembling into single product in multi-component systems has to overcome a combination problem. Namely, multi-component coordination reactions of multidentate ligands (L_1, L_2, $\cdots$, L_n) with metals (M_1, M_2, $\cdots$, M_m) give complex mixtures due to a statistical distribution if there is no controlling force. Even at the most simple case (L_1+L_2+M_1), the reaction will result in a complex mixture of numerous number of products (xL_1+yL_2+zM_1: x, y, z=0, 1, $\cdots$, ∞) ranging from discrete to infinite structures. In some cases, the most stable compounds form in symmetrical fashion where each ligand coordinate to the metal [(xL_1•zM_1) or (yL_2•zM_1)] independently. However, if there exists the remarkable driving forces in the equilibrium reactions, it can push the equilibrium into the most stable species as thermodynamic products even if the compounds are composed of multi-species and assembled in non-symmetrical fashion.

3.2 Catenation Approach for Multi-Component Assemblies

As described in chapter 2, the 3-D interlocked compound is assembled very efficiently even from three species-ten component, where each coordination cage is composed of two kind of ligands and the metal ion. This method should be the new approach for a versatile way of synthesis for multi-component assemblies. As described above, catenation is one of the most promising driving forces for predominant production of multi-component structures. The author paid an attention to this point and revealed its remarkable efficiency for synthesizing a multi-component assembly.

3.3 Reorganization of the 3-D Interlocked Compounds

M_6L_4 type complex **4** is a very stable cage compound which assembles from ten components ($6 \cdot \mathbf{1} + 4 \cdot \mathbf{2}$)[1] (Scheme 1a). Despite of its high molecular weight, the NMR spectrum of **4** shows only two doublets in an aromatic region corresponding to pyridyl α and β protons (Figure 1a), which reflects the high symmetry nature of the compound. M_3L_2 type cage **5** is also found to assemble from five components ($3 \cdot \mathbf{1} + 2 \cdot \mathbf{3}$) concomitant with the formation of oligomeric products (Scheme 1b, Figure 1b).

Scheme 1

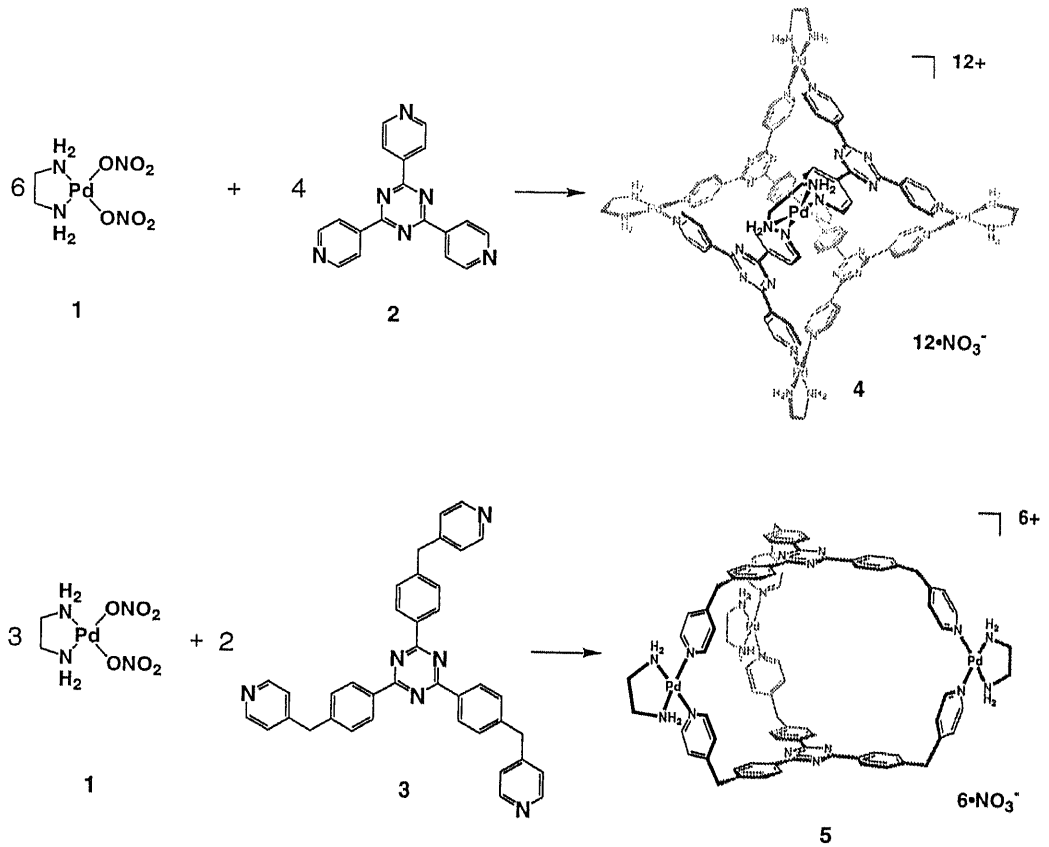

These cage compounds **4** and **5** were independently prepared in D_2O and then combined in 1:2 ratio so that component ratio **1**:**2**:**3** became 6:2:2. Two preformed Pd(II) cage

compounds **4** and **5** are reorganized into 3-D interlocked complex **6** in a high yield when they are mixed in an aqueous solution. (Scheme 2)

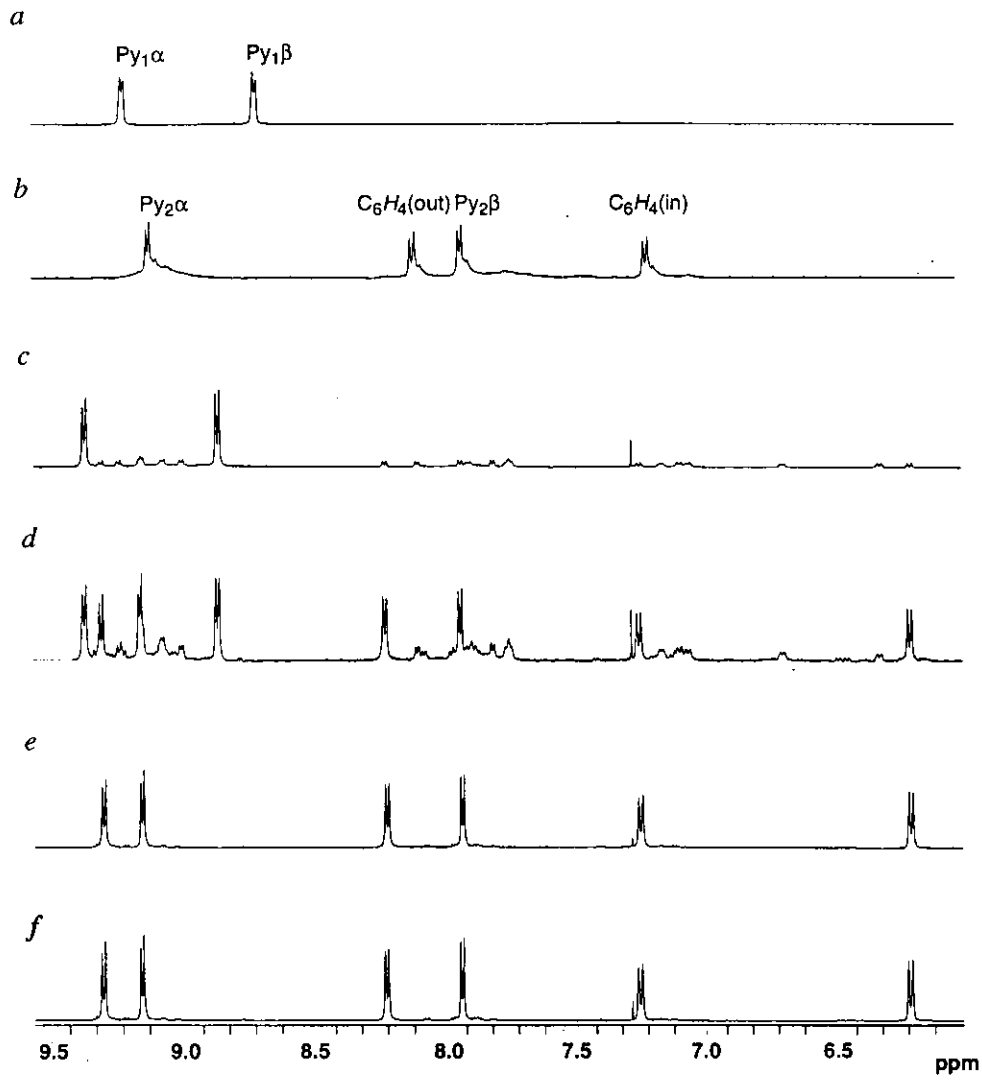

Figure 1. Formation of **6** via reorganization from **4** and **5**. NMR observation of the reorganization process: (*a*), **4**: A D_2O solution (1 mL) of **4** was prepared from **2** (2.1 mg, 6.7 x 10^{-3} mmol) and $enPd(ONO_2)_2$ (0.01 mmol) at 80 °C for a day. Py_1 = pyridine protons of

ligand **2**. (*b*), **5**: A D_2O-CD_3OD (1:1) solution (0.5 mL) of **5** was prepared from **3** (3.9 mg, 6.7 x 10^{-3} mmol) and $enPd(ONO_2)_2$ (0.01 mmol) at 80 °C for 5 d. Py2 = pyridine protons of ligand **3**. The assembly of cage **5** is slow and oligomeric products still remain even after 5 d. (*c*), The two solutions described above were combined and NMR was measured immediately. Cage **4** remained intact whereas cage **5** turned into oligomeric components probably due to interactions with components of **4**. (*d*), After 3 h at 20 °C. (*e*), After 24 h at 20 °C. (*f*), The two solutions described in *a* and *b* were combined and NMR was measured after 10 min at 80 °C. Chemical shift values are slightly different from those shown in Figure 3 because of the measurement in a mixed solvent (D_2O-CD_3OD 3:1).

The NMR spectrum of the mixture initially showed that cage **4** existed intact whereas cage **5** was considerably converted to oligomeric components (Figure 1c). After the solution was allowed to stand at room temperature, cages (**4**, **5**) and oligomers gradually disappeared; alternatively, another set of signals assignable to **6** appeared (Figure 1d). Finally, all components were completely reorganized into 3-D interlocked compound **6** after 1 d (Figure 1e). At an elevated temperature (80 °C), the reorganization process ($4+2\cdot5\rightarrow2\cdot6$) was significantly accelerated and completed within 10 min (Figure 1f). These results clearly showed that **6** is a thermodynamic product and is the most stable among all possible structures formed by numerous combination[2] of components **1**, **2**, and **3**. This quantitative reorganization of a 3-D interlocked compound which is a dimeric structure of coordination cages composed of three species demonstrates that catenation is a promising method for multi-component structures in coordination reactions where there is no complementary between ligands and metals.

Scheme 2.

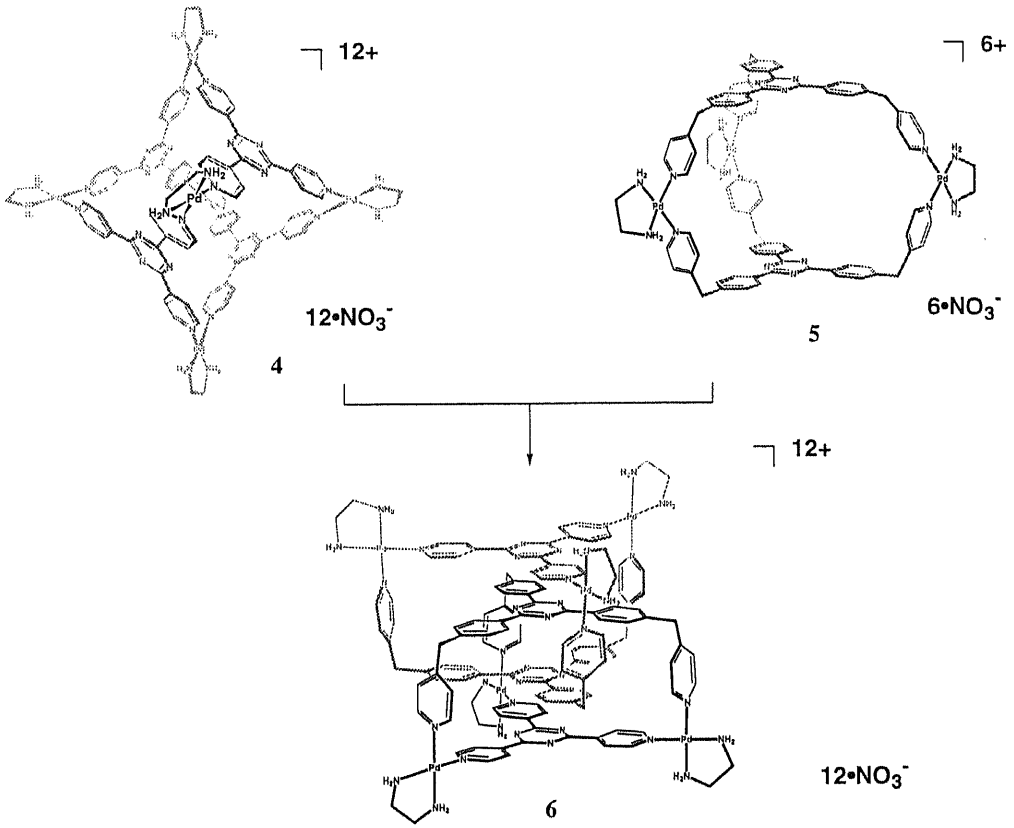

The group the author belongs to have already reported the guest-induced organization of 3-D cage compound **7** wherein the host framework was organized from its components only in the presence of a specific guest[3]. It is particularly interesting that, in the present study, the organization of a cage framework (3·**1** + **2** + **3**) is induced by another copy of itself through interlocking.

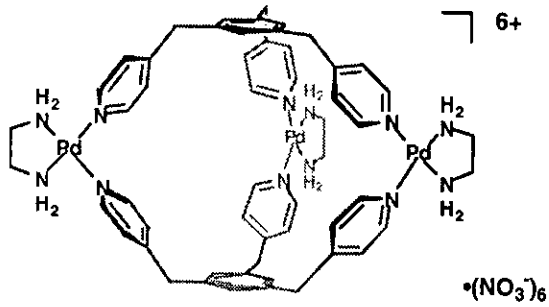

7

References

(1) Fujita, M.; Oguro, D.; Miyazawa, M.; Oka, H.; Yamaguchi, K.; Ogura, K. *Nature* **1995**, *378*, 469.

(2) Hasenknopf, B.; Lehn, J.-M.; Kneisel, B. O.; Baum, G.; Fenske, D. *Angew. Chem., Int. Edn Engl.* **1996**, *35*, 1838.

(3) Fujita, M.; Nagao, S.; Ogura, K. *J. Am. Chem. Soc.* **1995**, *117*, 1649.

Chapter 4

A [2]Catenane Whose Rings Incorporate Two Differently Metallated Porphyrins

New J. Chem. **2001**, *25*, 790-796.

Abstract: A [2]catenane made with Zn(II) and Au(III) porphyrin-incorporating macrocycles has been synthesized using the transition metal templated technique, starting from either preformed Au(III) or Zn(II) porphyrin-containing macrocycle. The highest yield (10%) was obtained in the latter case. Removal of the copper(I) template metal afforded the free [2]catenane, whose ^{1}H NMR properties differ dramatically from those of the parent Cu(I) complex, suggesting that a changeover of the molecule has taken place upon demetallation.

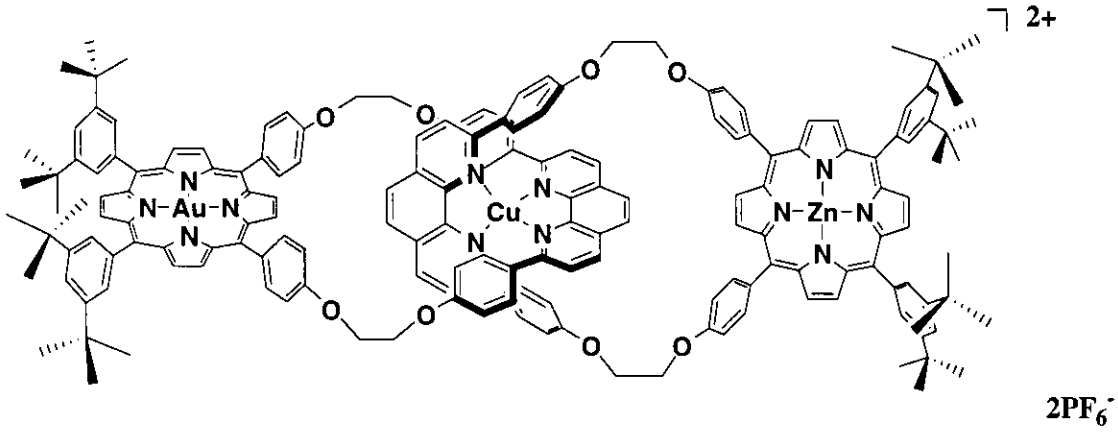

4.1 Introduction

Molecular systems capable of showing intramolecular photoinduced electron transfer between donor and acceptor components have been the subject of intense interest since the early eighties.[1] One of our approaches to this topic has been the use of Zn(II) porphyrin donors in the excited state and Au(III) porphyrin acceptors in the ground state[2] in combination with the so-called mechanical bond found in catenanes and rotaxanes. Only a few porphyrin-containing catenanes[3] and rotaxanes[4] have been described in the literature. As shown schematically in Figure 1, the compounds synthesized in our laboratory are either [2]rotaxanes[5] made with a Au(III) porphyrin-containing macrocycle threaded onto a Zn(II) porphyrin-stoppered dumbbell (Figure 1a and b) or a [2]catenane,[6] made from macrocycles with *pendent* Zn and Au porphyrins (Figure 1c).

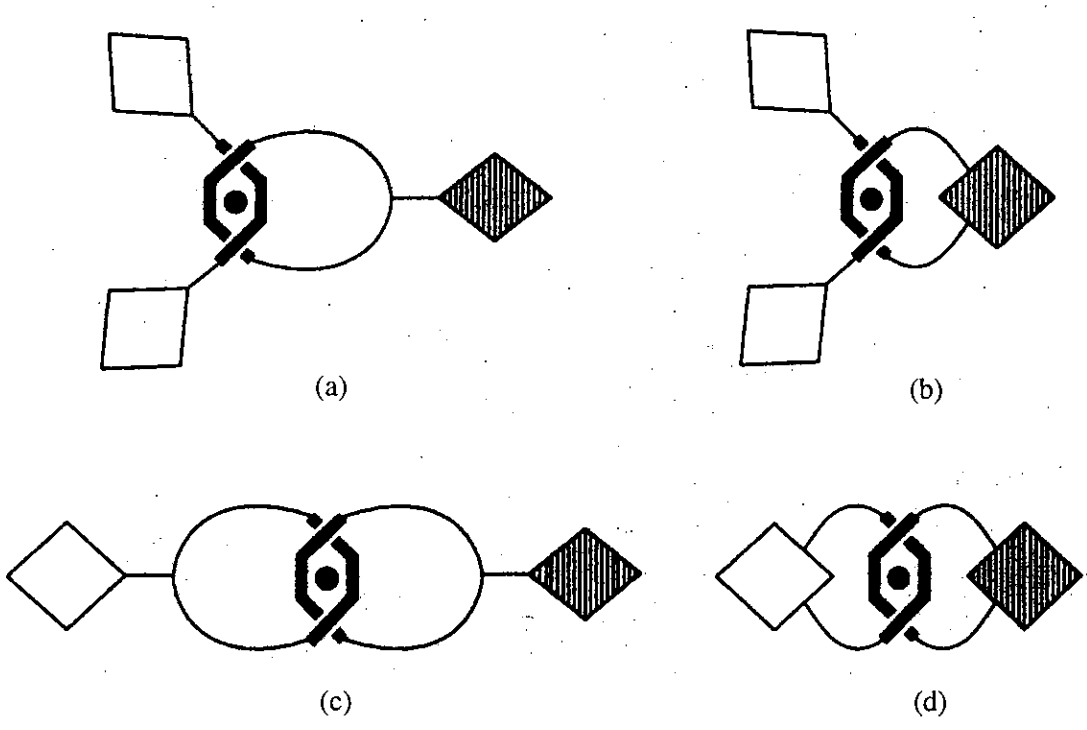

Figure 1. Schematic representation of metal-complexed [2]rotaxanes (a, b) and [2]catenanes (c,d). The thick lines represent chelating fragments, the black disk is a metal cation, the empty diamonds are Zn(II) porphyrins, and the hatched diamonds are Au(III) porphyrins. The black disk symbolises copper (I).

A natural extension of this work was the preparation of the analogous Cu(I)-complexed [2]catenane with macrocycles incorporating the Zn and Au porphyrins (Figure 1d). In this work, the author describe the different routes used for the preparation of this compound, and its demetallation to the [2]catenane species.

4.2 Synthesis of the Porphyrinic [2]Catenane

The target Cu(I)-complexed [2]catenane represented schematically in Figure 1d contains two different macrocycles. Therefore, two routes can be envisaged for its construction by the transition metal templated strategy.[7] They are shown in Figure 2. Both involve the preparation of an intermediate precatenane species, (C) or (F), in which either Zn or Au porphyrin-containing macrocycle (A) or (E) is threaded onto chelate (B), thanks to copper(I) coordination. Formation of the second, interlocking macrocycles, is achieved in the next step, by reaction of the precatenane with the appropriate porphyrin, (D) in the case of the (C), (G) in the case of (F), to produce the desired Cu(I)-complexed [2]catenane (H). Finally, removal of the metal template affords the free catenane species (I).

The precursors of the target Cu(I) complexed [2]catenane [Cu•**1**]$(PF_6)_2$ are shown in Figure 3. 5,10-di(*p*-hydroxyphenyl)-15,20-di(3,5-di-*tert*-butylphenyl)porphyrin **4** was obtained quantitatively by reaction of 5,10-di(*p*-anisyl)-15,20-di(3,5-di-*ter*-butylphenyl)porphyrin **3** with BBr_3 in CH_2Cl_2 at 0 °C, and its zinc complex **5** was obtained in 79% yield by treatment of **4** with $Zn(OAc)_2•2H_2O$ in refluxing $CHCl_3/CH_3OH$. Free base-incorporating macrocycle **7** was prepared by combining bis[2,9-(2-phenyloxy)iodoethyl]-1,10-phenanthroline **2** and **4** in DMF at 55 °C in the presence of Cs_2CO_3, and was obtained in 28% yield after chromatography. Reaction of **7** with $Zn(OAc)_2•2H_2O$ in the same conditions as above afforded the zinc porphyrin-containing macrocycle **8** in 85% yield. Alternatively, this compound could be prepared directly from phenanthroline **2** and Zn porphyrin **5** in condition similar to those described for **7**, and was obtained in 13% yield after chromatography.

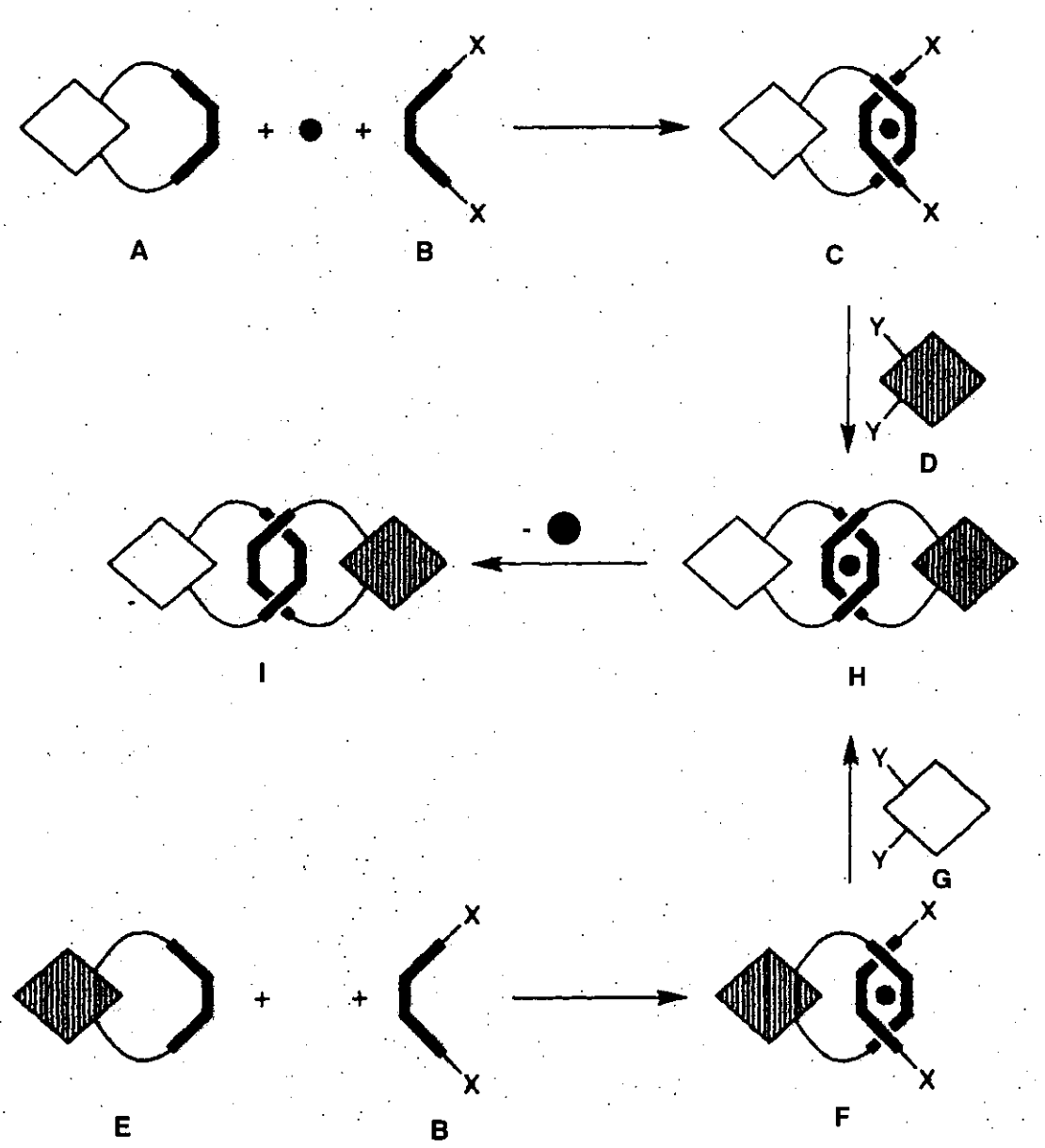

Figure 2. Two strategies for the transition metal-templated synthesis of a [2]catenane made with Zn and Au porphyrin-incorporating interlocked macrocycles. Symbols are as in Figure 1.

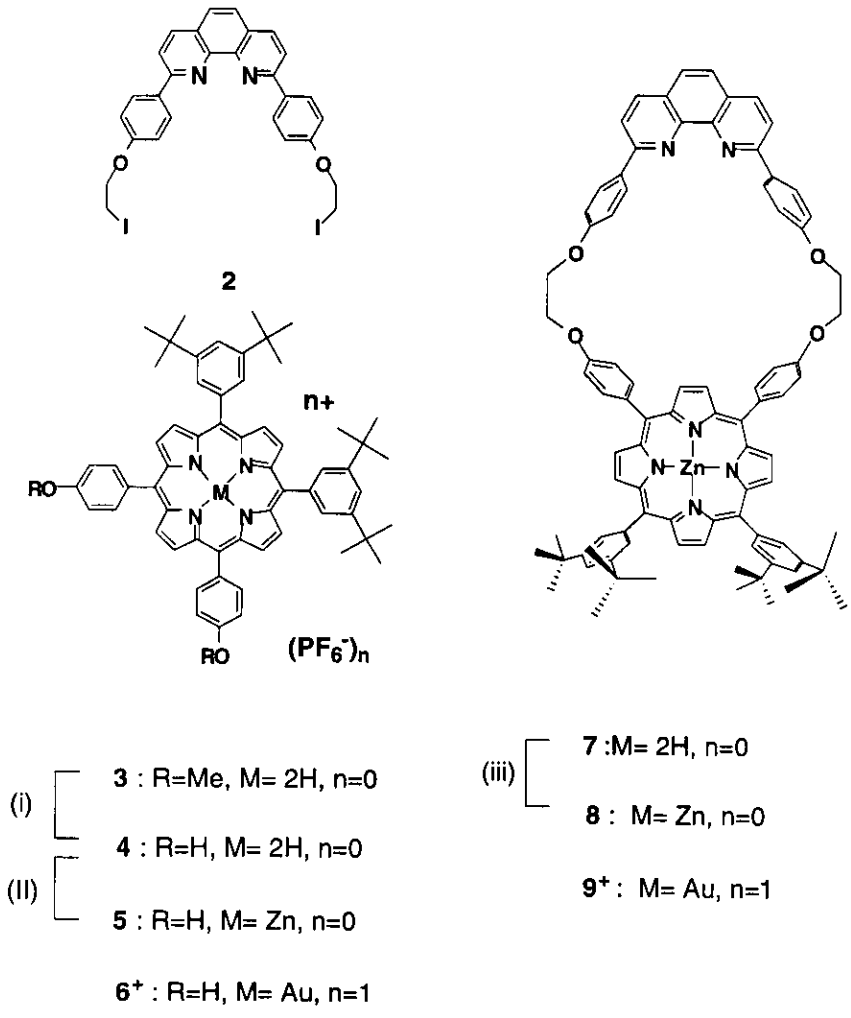

Figure 3. Precursors to [2]catenane **1**•PF_6. (i) BBr_3, CH_2Cl_2, 0 °C; (ii) $Zn(OAc)_2$•$2H_2O$; (iii) $Zn(OAc)_2$•$2H_2O$.

The three steps of the most efficient route leading to the Cu(I) complexed [2]catenate [Cu•**1**]$(PF_6)_2$ are shown in Figure 4. Mixing of equimolar solutions of $[Cu(CH_3CN)_4]PF_6$ in acetonitrile and Zn porphyrin-containing macrocycle **8** in dichloromethane, followed by addition of phenanthroline derivative **2** in dichloromethane, afforded in quantitative yield precatenate [Cu(**2**•**8**)]. Subsequently, this complex was combined with a stoichiometric

amount of gold(III) 5,10-di(*p*-hydroxyphenyl)-15,20-di(3,5-di-*ter*-butylphenyl)porphyrinate **6**•PF_6 in DMF. The resulting solution was treated portion wise with a suspension of Cs_2CO_3 in DMF. This procedure allows the relative instability of the prerotaxane in basic medium. In these condition, Cu(I) complexed [2]catenane [Cu•**1**]$(PF_6)_2$ was obtained in 10 % yield after chromatography.

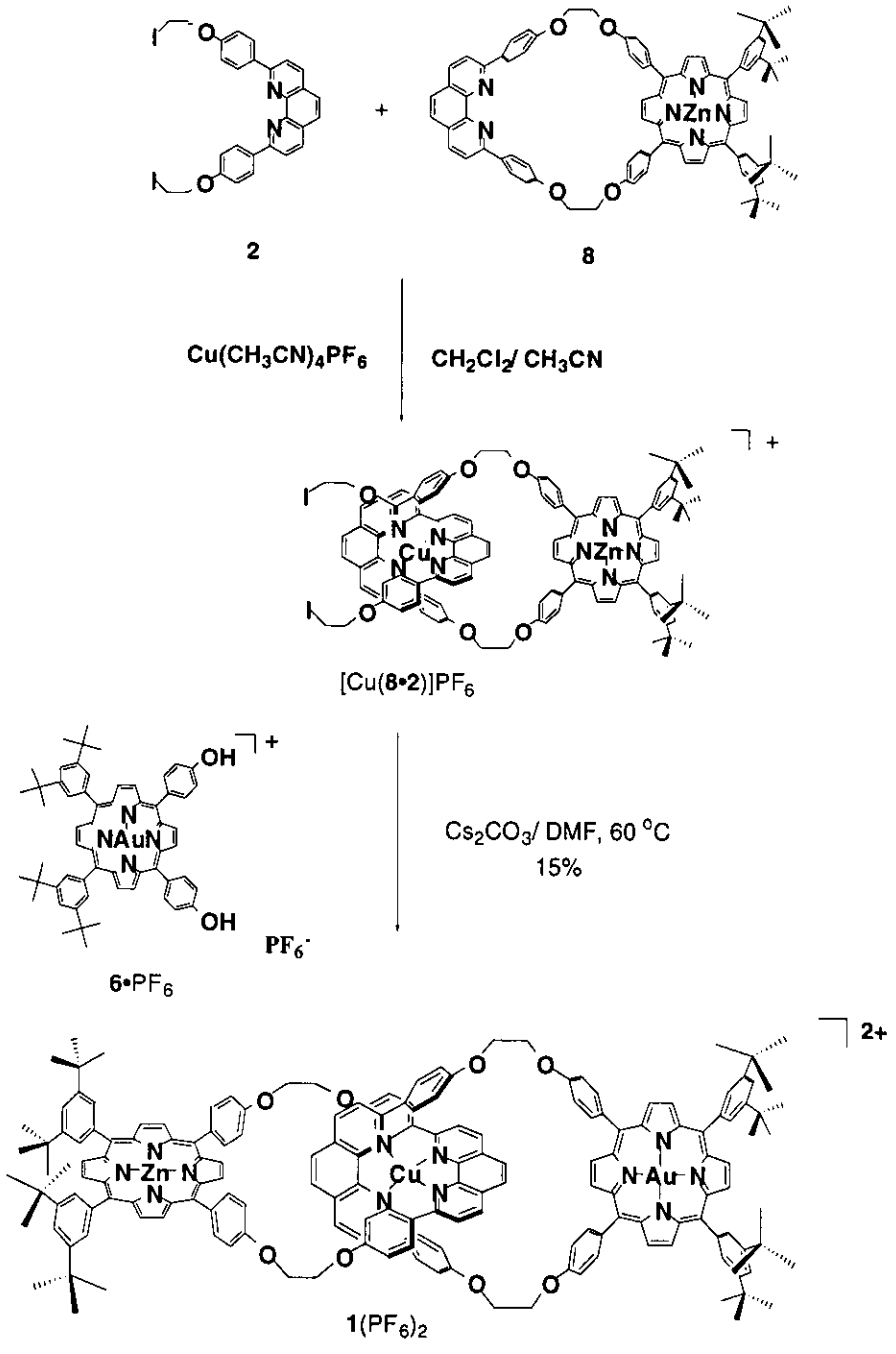

Figure 4: Two-step preparation of Cu(I)-complexed [2]catenane [Cu•**1**]$(PF_6)_2$.

The alternative route, which involves Au porphyrin-containing macrocycle **9** PF_6 and Zn porphyrin **5** as reactants afforded the same copper catenane in 5% yield. Demetallation leading to the free [2]catenane species **1**•PF_6, was carried out by treating the Cu(I) complex with 100 mol% KCN in a ternary mixture of $CHCl_3/CH_3CN/H_2O$ at 40 °C. [2]catenane **1**•PF_6 was obtained in 83 % yield after chromatography (Figure 5).

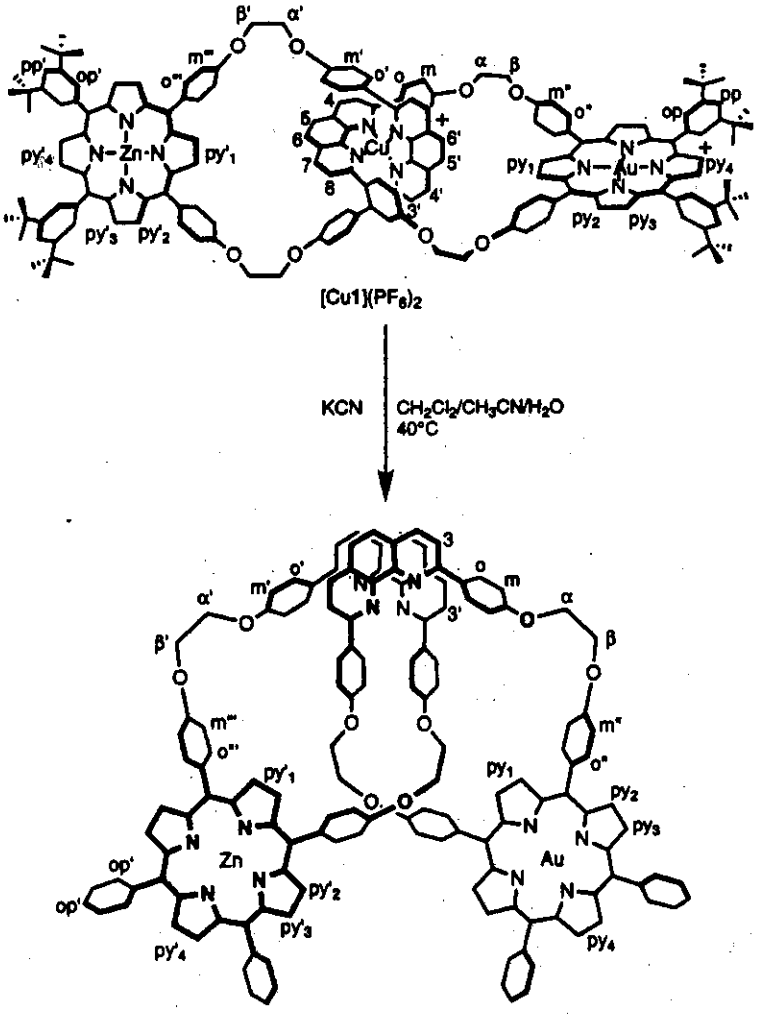

1•PF_6

Figure 5. Demetallation of [2]catenane [Cu•**1**]$(PF_6)_2$ to [2]catenane **1**•PF_6. Double bonds omitted for clarity.

4.3 Characterization of Porphyrinic [2]Catenane and its Dramatic Conformational Change upon Demetallation

The target compoounds, **2**•PF_6 and its Cu(I) complex were characterized by FAB-MS and ^{1}H NMR spectroscopy. The FAB mass spectra in the positive mode show the molecular peak corresponding to singly charged species resulting from the loss of one PF_6 anion, at 3041.0 amu for the Cu(I) [2]catenane, and 2832.2 amu for the [2]catenane. Peaks corresponding to the Au porphyrin-containing macrocycle $\mathbf{9}^+$ and the protonated Zn porphyrin-containing macrocycle **8** are observed at 1481.6 and 1349.5 amu, respectively.

Figure 6 shows a comparison of the room temperature ^{1}H NMR spectra (low field region) of [Cu•**1**]$(PF_6)_2$ (Figure 6). Labeling of the protons is indicated in Figure 5. The different signals could be assigned using 2D ROESY experiments. To distinguish between protons belonging to the interlocked Zn and Au porphyrin-containing macrocycles, it was assumed, as observed earlier, that the β-pyrrolic protons of the latter resonate at lower field than the former.[2b, 9] This is in agreement with the strong electron withdrawing effect of Au(III). Typical of the mutual 'fit in' of the 2,9-diphenyl-1,10-phenanthroline chelates in the Cu(I) complexed [2]catenane, are the upfield-shifted (6.4 ppm) signals of the meta protons (m and m') belonging to the phenyl substituents, as compared to the other aromatic protons.[10] With the exception of pyrrolic protons, which are the most sensitive to the nature of the porphyrinic metal, analogous protons of both macrocycles have similar chemical shifts. The spectrum of the free [2]catenane **1**•PF_6 is dramatically different from that of its parent Cu(I) complex. The signals of the pyrrolic protons have moved upfield, and the signals of proton o and o', and m and m' of the phenyl substituents belonging to the phenantroline nuclei have moved downfield by 0.8 ppm. This latter shift is typically observed when passing from metallocatenanes to free catenanes, and indicates that the phenyl substituent of a given phenanthroline upon removal of the metal template.[11] In addition to the above noted changes, the phenanthroline protons (3'-8') of the Zn porphyrin-containing macrocycle are shifted upfield to a much greater extent than the corresponding protons (3-8) of the Au porphyrin-containing macrocycle. This is true, in

particular, for the pairs 4', 7' and5', 6', which undergo shifts of –0.7 to –0.5 ppm. 2D ROESY maps of catenane $[Cu•\mathbf{1}](PF_6)_2$ indicate dipolar couplings between protons py1 of the Au porphyrin-containing macrocycle and protons 5', 6' of the Zn porphyrin-containing macrocycle. The same is true for protons py'1 and 5, 6. These observations are in agreement with the structure depicted in Figure 5. These correlations disappear in the case of catenane $\mathbf{1}•PF_6$, which shows only very weak cross peaks between protons of one macrocycle and protons of the other macrocycle, e.g., py'1 (py) and m (m') or m'' (m''). VT ^{1}H NMR spectra at temperature down to –95 °C performed on the free catenane $\mathbf{1}•PF_6$ show only increasing broadening of the peaks, indicating that the molecule exist in many exchanging conformations.

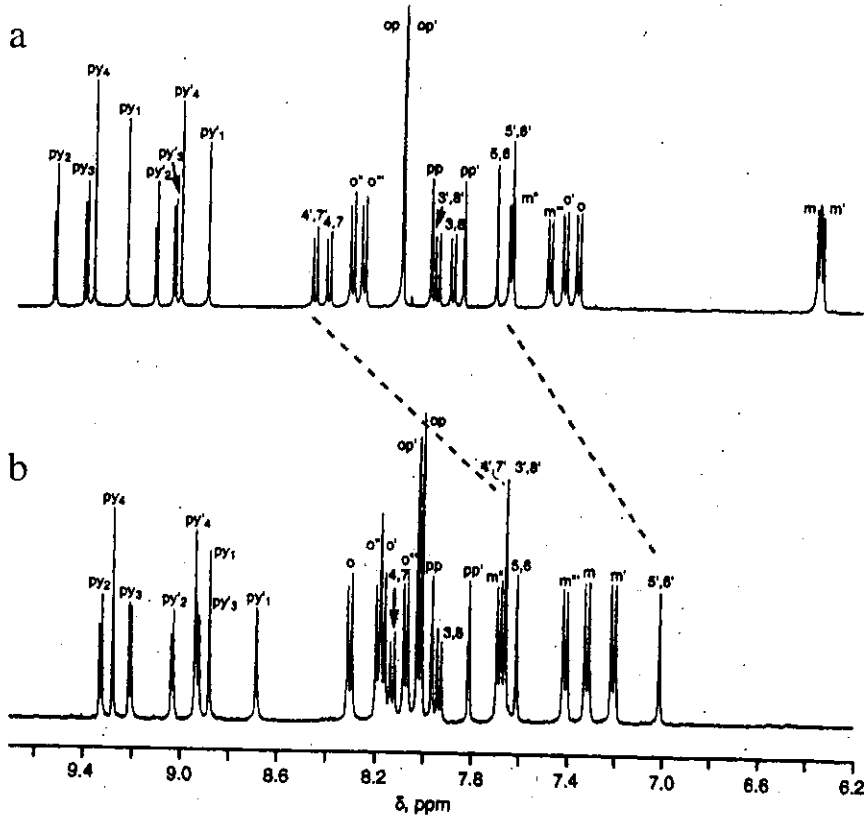

Figure 6. ^{1}H NMR spectra (500 MHz, CD_2Cl_2) of (a) $[Cu•\mathbf{1}]$ $(PF_6)_2$ and (b) $\mathbf{1}•PF_6$. Atom numbering as shown in Figure 5.

The study of photoinduced electron transfer between the Zn porphyrin component in the excited state and the Au porphyrin component in the ground state by fast laser flash photolysis techniques should allow to get more insight into the conformational properties of the [2]catenane, as shown recently for a related [2]rotaxane.[5]

4.4 Conclusion

A [2]catenane composed of two different macrocycles having donor and acceptor porphyrin was synthesized with help of metal-template effect. Among the diverse synthetic routes, the author found the most efficient ring closure step, which enable to obtain the [2]catenane in practical yield. The [2]catenane change its conformation dramatically upon removal of template Cu(I) metal to furnish a system where distance between donor and acceptor porphyrins change from ca 19 Å to 3～4 Å.

4.5 Experimental section

Precatenane [Cu(2•8)]PF_6: A solution of $Cu(CH_3CN)_4$ (0.0385 g, 0.103 mmol) in CH_3CN (6 mL) under argon was transferred via cannula to a solution of macrocycle **8** (0.100 g, 0.074 mmol) in CH_2Cl_2 (34 mL) under argon. After 40 minutes stirring, a solution of **2** (0.050 g, 0.074 mmol) in CH_2Cl_2 (17 mL) was added via cannula to the reaction mixture. After stirring for 5h, the solvents were removed in vacuo, leaving pure precatenane [Cu(**2**•**8**)]PF_6 as a red solid quantitatively. ^{1}H NMR (300 MHz, CD_2Cl_2) 9.14 (d, 2H, ^3J =4.6 Hz, Hpy'2), 9.06 (d, 2H, ^3J =4.4 Hz, Hpy'3), 9.03 (s, 2H, Hpy'4), 8.94 (s, 2H, Hpy'1), 8.52 (d,2H, ^3J =8.2 Hz, H4,7 or H4',7'), 8.45 (d, 2H, ^3J =8.2 Hz, H4', 7' or H4, 7), 8.28 (d, 4H, ^3J =8.2 Hz, Ho'''), 8.12 (d, 4H, ^4J =1.8 Hz, Hop'), 8.05 (s, 2H, H5',6'), 7.91 d, 2H, ^3J =8.4 Hz, H3,8 or H3',8'), 7.89 (d, 2H, ^3J =8.4 Hz, H3',8' or H3,8), 7.86 (t, 2H, Hpp'), 7.81 (s, 2H, H5,6), 7.49 (d, 4H, ^3J =8.6 Hz, Hm'''), 7.44 (d, 4H, ^3J =8.8 Hz, Ho or Ho'), 7.43 (d, 4H, ^3J =8.8 Hz, Ho' or Ho), 6.30 (d, 4H, ^3J = 8.4 Hz, Hm'), 6.11 (d, 4H, ^3J = 8.6 Hz, Hm), 4.77 (br, t, 4H, Hβ'), 4.14 (br, t, 4H, Hβ'), 4.14

(br, t, 4H, Hα'), 3.89 (t, 4H, ^3J = 6.3 Hz, Hα), 3.33 (t, 4H, ^3J =6.2 Hz, Hβ), 1.55 (s, 36H, CH_3).

[2]catenane [Cu•1]$(PF_6)_2$: To a solution of precatenane [Cu(**2**•**8**)]PF_6 (0.074 mmol) and gold porphyrin **9**•PF_6 (0.090 g, 0.0744 mmol) in DMF (14 mL) at 60 °C under argon, was added portionwise, via cannula, a suspension of Cs_2CO_3 (0.112 g, 0.344 mmol) in DMF (6 mL) over 1h. Heating and stirring were maintained overnight. The reaction was stopped 20 h after the end of the addition of Cs_2CO_3. The solvent was rotary evaporated. The residue was taken up in CH_2Cl_2 (100 mL), washed with water, and stirred overnight with a 5% solution of KPF_6 in water (50 mL). The crude material was subjected to repeated column chromatography on alumina (CH_2Cl_2/CH_3OH : 100/0.5 as eluent), and pure [Cu•**1**$(PF_6)_2$ isolated in 10% yield (0.0235 g). ^{1}H NMR (500 MHz, CD_2Cl_2): 9.548 (d, 2H, ^3J =5.08 Hz, Hpy2), 9.420 (d, 2H, ^3J = 5.09 Hz, Hpy3), 9.386 (s, 2H, Hpy4), 9.253 (s, 2H, Hpy1), 9.136 (d, 2H, ^3J =4.47 Hz, Hpy'2), 9.058 (d, 2H, ^3J = 4.47 Hz, Hpy'3), 9.031 (s, 2H, Hpy'4), 8.920 (s, 2H, Hpy'1), 8.480 (d, 2H, ^3J = 8.32 Hz, H4', 7'), 8.424 (d, 2H, ^3J = 8.17 Hz, H4,7), 8.330 (d, 4H, ^3J = 8.79 Hz, Ho''), 8.283 (d, 4H, ^3J = 8.63 Hz, Ho'''), 8.124 (d, 4H, ^4J = 1.85 Hz, Hop or Hop'), 8.122 (d, 4H, ^4J = 1.70 Hz, Hop' or Hop), 8.004 (t, 2H, ^4J = 1.77 Hz, Hpp or Hpp'), 7.979 (d, 2H, ^3J = 8.32 Hz, H3', 8'), 7.915 (d, 2H, ^3J = 8.32 Hz, H3,8), 7.870 (t, 2H, ^4J = 1.85 Hz, Hpp' or Hpp), 7.733 (s, 2H, H5,6), 7.673 (d, 4H, ^3J = 8.79 Hz, 7.670 (s, 2H, H5',6'), 7.512 (d, 4H, ^3J = 8.63 Hz, Hm'''), 7.447 (d, 4H, ^3J = 8.64 Hz, H0'), 7.392 (d, 4H, ^3J = 8.64 Hz, Ho), 6.386 (d, 4H, ^3J = 8.79 Hz, Hm), 6.376 (d, 4H, ^3J = 4.23 Hz, Ha), 4.198 (t, 4H, ^3J = 4.08 Hz, Ha'), 1.566 (s, 36H, CH_3 or CH_3'), 1.555 (s, 36H, CH_3' or CH_3). FAB-MS: m/z = 3041.02 $[M\text{-}PF_6^-]^+$, calcd. 3042.1 (10%); 2896.07 $[M\text{-}2PF_6^-+e^-]^+$, calcd. 2897.17 (33%); 1545.5 [**9**+Cu^++e^-] $^+$, calcd. 1546.1 (13%); 1481.6 [**9**] $^+$, calcd 1482.6 (63%), 1448.6 $[M\text{-}2PF_6^-]^{2+}$/2, calcd. 1448.6 (61%), 1413.5 [**8**+Cu^+]$^+$, calcd. 1414.6 (23%), 1349.5 [8+H^+] $^+$, calcd. 1351.0 (8%).

[2]catenane 1•PF_6: A mixture of catenane [Cu1]$(PF_6)_2$ (0.01562 g, 4.904 μmol) and KCN

(0.0312 g, 0.4791 mmol) in a ternary mixture of $CH_3CN/CHCl_3/H_2O$: 5.5/1.5/1.5 (8.5 mL) was heated at 40 °C for 50 min. The reaction mixture was diluted with CH_2Cl_2, the organic layer washed twice with water, and evaporated to dryness. The residue was retaken in CH_2Cl_2 (10 mL) and stirred 8 h with a 5% solution of KPF_6 in water (10 mL). The product was purified by column chromatography on alumina (CH_2Cl_2 as eluent) and isolated in 83% yield (0.01208 g). ^{1}H NMR (500 MHz, CD_2Cl_2): 9.329 (d, 2H, ^3J = 5.08 Hz, Hpy2), 9.280 (s, 2H, Hpy4), 9.209 (d, 2H, ^3J = 5.24 Hz, Hpy3), 9.034 (d, 2H, ^3J = 4.63 Hz, Hpy'2), 8.942 (s, 2H, Hpy'4), 8.929 (d, 2H, ^3J = 4.62 Hz, Hpy'3), 8.882 (s, 2H, Hpy1), 8.686 (s, 2H, Hpy'1), 8.304 (d, 4H, ^3J = 8.79 Hz, Ho), 8.188 (d, 4H, ^3J = 8.63 Hz, Ho''), 8.169 (d, 4H, ^3J = 8.78 Hz, Ho'), 8.128 (d, 4H, ^3J = 8.63 Hz, H4,7), 8.075 (d, 4H, ^3J = 8.48 Hz, Ho'''), 8.027 (d, 4H, ^4J = 1.69 Hz, Hop'), 8.010 (d, 4H, ^4J = 1.70 Hz, Hop), 7.966 (t, 2H, ^4J = 1.77 Hz, Hpp), 7.935 (d, 2H, ^3J = 8.33 Hz, H3,8), 7.813 (t, 2H, ^4J = 1.77 Hz, Hpp'), 7.686 (d, 4H, ^3J = 8.48 Hz, Hm), 7.661 (br s, 4H, H3', 8' and H4', 7'), 7.613 (s, 2H, H5,6), 7.409 (d, 4H, ^3J = 8.63 Hz, Hm'''), 7.318 (d, 4H, ^3J = 8.79 Hz, Hm), 7.208 (d, 4H, 3J = 8.78 Hz, Hm'), 7.014 (s, 2H, H5', 6'), 4.979 (t, 4H, 3J= 3.47 Hz, Hb), 4.880 (t, 4H, ^3J = 3.00 Hz, Hb'), 4.728 (t, 4H, ^3J =3.70 Hz, Ha), 4.658 (t, 4H, ^3J = 3.85 Hz, Ha'), 1.522 (s, 36H, CH_3), 1.494 (s, 36H, CH_3'). FAB-MS: m/z=2832.2 $[M\text{-}PF_6^-]^+$, calcd. 2833.6 (31%); 1481.6 $[\mathbf{9}]^+$, calcd. 1482.6 (100%); 1350.6 $[\mathbf{8}+H^+]^+$, calcd. 1351.0 (18%).

References and Notes

(1) For early references, see: (a) Ho, T.-F.; McIntosh, A. R.; Bolton, J. R. *Nature*, **1980**, *286*, 254-256. (b) Migita, M.; Okada, T.; Mataga, N.; Nishitani, S.; Kurta, N.; Sakata, Y.; Misumi, S. *Chem. Phys. Lett.* **1981**, *84*, 263-266. (c) Pasman, P.; Rob, F.; Verhoeven, J. W. *J. Am. Chem. Soc.* **1982**, *104*, 5127-5133. (d) Miller, J. R.; Calcaterra, L. T.; Closs, G. L. *J. Am. Chem. Soc.* **1984**, *106*, 3047-3049. (e) Joran, A. D.; Leland, B. A.; Geller, G. G.; Hopfield, J. J.; Dervan, P. B. *J. Am. Chem. Soc.* **1984**, *104*, 6090-6092. (f) Moore, T. A.; Gust, D.; Mathis, P.; Mialocq, J.-C.; Chachaty, C.; Bensasson, R. V.; Land, E. J.; Doizi, D.; Liddell, P. A.; Nemeth, G. A.; Moore,

A. L. Nature (London) 1984, 307, 630-632. (g) Wasielewski, M. R.; Niemczyk, M. P.; Svec, W. A.; Pewitt, E. B. *J. Am. Chem. Soc.* **1985**, *107*, 5562-5563. (h) Heitele, H.; Michel-Beyerle, M. E. *J. Am. Chem. Soc.* **1985**, *107*, 8286-8288.

(2) (a) Brun, A. M.; Harriman, A.; Heitz, V.; Sauvage, J.-P *J. Am. Chem. Soc.* **1991**, *113*, 8657-8663. (b) Brun, A. M.; Atherton, S. J.; Harriman, A.; Heitz, V.; Sauvage, J.-P *J. Am. Chem. Soc.* **1992**, *114*, 4632-4639.

(3) (a) Gunther, M. J.; Johnston, M. R. *J. Chem. Soc., Chem. Commun.* **1992**, 1163-1165. (b)Le Bras, F.; Loock, B.; Momenteau, M. *Tetrahedron Lett.* **1994**, *35*, 3289- . (c) Chambron, J.-C.; Heitz, V.; Sauvage, J.-P. *Bull. Soc. Chim. Fr.* **1995**, *132*, 340-347.

(4) (a)Ashton, P. R.; Johnston, M. R.; Stoddart, J. F.; Tolley, M. S. Wheeler, J. W. *J. Chem. Soc., Chem. Commun.* **1992**, 1128-1131. (b) Chambron, J.-C.; Heitz, V.; Sauvage, J.-P. *J. Chem. Soc., Chem. Commun.* **1992**, 1131-1133. (c) Vögtle, F.; Ahuis, F.; Baumann, S.; Sessler, J. L. *Leibigs Ann.* **1996**, 921-926. (d) Chichak, K.; Walsh, M. C.; Branda, N. R. *Chem. Commun.* **2000**, 847-848.

(5) (a) Linke, M.; Chambron, J.-C.; Heitz, V.; Sauvage, J.-P. *J. Am. Chem. Soc.* **1997**, *119*, 11329-11330. (b) Linke, M.; Chambron, J.-C.; Heitz, V.; Sauvage, J.-P.; Semetey, V. *Chem. Commun.*, **1998**, 2469-2470. (c) Linke, M.; Chambron, J.-C.; Heitz, V.; Sauvage, J.-P.; Encinas, S.; Bargelletti, F.; Flamigni, L. *J. Am. Chem. Soc.* **2000**, *122, in the press*..

(6) (a) Amabilino, D. B.; Sauvage, J.-P. *Chem. Commun,* **1996**, 2441-2442. (b) Amabilino, D. B.; Sauvage, J.-P. *New J. Chem.*, **1998**, 395-409.

(7) Dietrich-Buchecker, C. O.; Sauvage, J.-P. *Tetrahedron*, **1990**, *46*, 503-512.

(8) (a) Jørgensen, T.; Becher, J.; Chambron, J.-C.; Sauvage, J.-P. *Tetrahedron Lett.* **1994**, *35*, 4339-4342. (b) Raehm, L.; Kern, J.-M.; Sauvage, J.-P. *Chem. Eur. J.* **1999**, *5*, 3310-3317.

(9) Chardon-Noblat, S.; Sauvage, J.-P. *Tetrahedron*, **1991**, *47*, 5123-5132.

(10) Dietrich-Buchecker, C. O.; Marmot, P. A.; Sauvage, J.-P. Kintzinger, J. -P.; Maltese, P. *New J. Chem.* **1984**, *8*, 573-582.

(11) Dietrich-Buchecker, C. O.; Sauvage, J.-P. *Chem. Rev.* **1987**, *87*, 795-810.

Chapter 5

Self-Assembly of A Porphyrin Prism - Characterization of Both Solid and Solution State Structures-

Angew. Chem. Int. Ed. **2001**, *40*, 1718-1721.

Abstract: Described here is the quantitative synthesis of a prism-like structure composed of panel-like porphyrin ligands and cis-protected Pd(II)complexes. Porphyrin ligands having 3-pyridyl groups at the meso positions were complexed with a cis-protected Pd(II) complex to give a D_{3h} symmetrized prism-like structure in which the side of the prism is made up of the three porphyrin units held together with the six Pd(II) centers. The structure was stable enough to determine both solid and solution state structures by NMR, ESI-MS and X-ray analyses. Exact ESI-MS revealed that one NO_3^- was strongly entrapped inside the cavity.

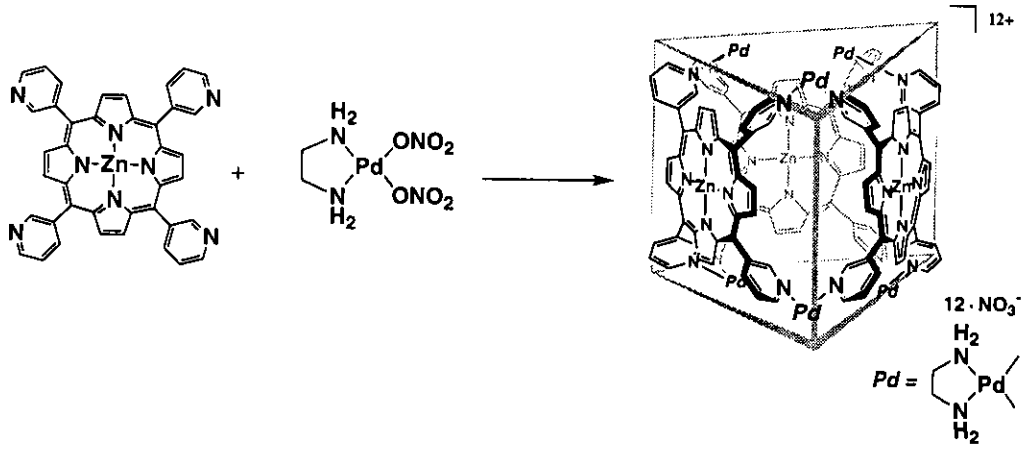

5.1 Introduction

Porphyrin assemblies play an essential role in biological systems for oxygen transport,[1] electron transfer, and energy migration and conversion.[2] In this regard, designing molecular assemblies using porphyrin units is a promising approach for constructing artificial functional systems. Both covalent[3] and non-covalent[4] syntheses of polyporphyrins have offered some novel classes of compounds with respect to their structures and functions. Here, the author reports a porphyrin-based hollow framework that is expected to open a new porphyrin chemistry through host-guest interaction. The strategy employed here is the molecular paneling[5] of a pyridine-functionalized porphyrin via metal-coordination. As shown in Scheme 1, a prism-like hollow structure is quantitatively assembled from three porphyrin ligands and six $(en)Pd^{2+}$ building blocks.

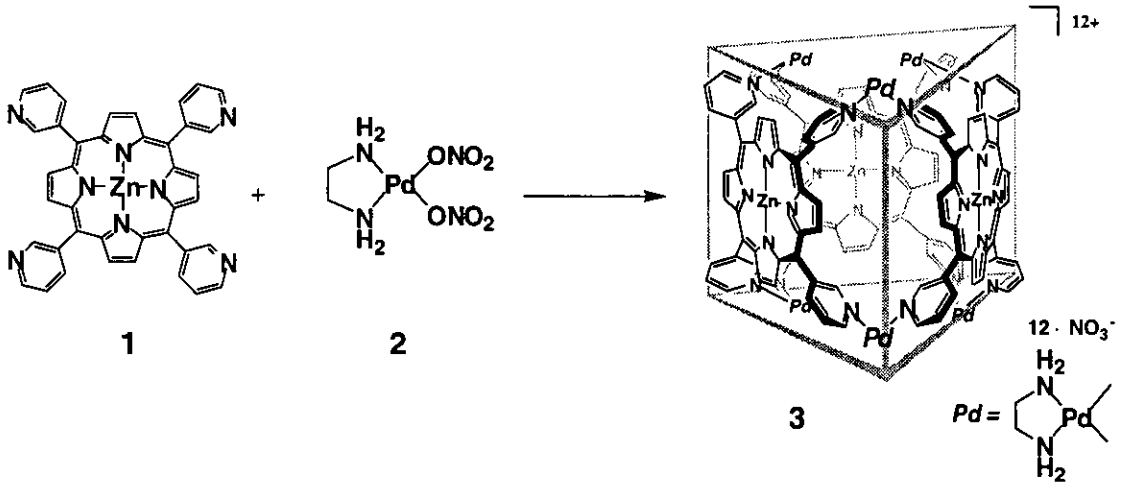

Scheme 1.

The spatially fixed porphyrin ligands surround a large hydrophobic cavity which can accommodate neutral organic molecules such as pyrene and perylene in an aqueous solution. Though metal-linked porphyrinic square arrays have been reported by several groups,[6] the porphyrin cores in the arrays seem to adopt cofacial rather than perpendicular conformation providing no distinct hollow structures and guest inclusion property. Quite recently, a Pd(II)-

lnked porphyrin cage which bound diamines was reported by Shinkai.[7]

5.2 Synthesis and Characterization of the Porphyrin Prism

The ligand designed here is (3-pyridyl)-functionalized porphyrin **1**. This square panel-like ligand can be hinged by (en)Pd^{2+} units **2** at two opposite ridges of the square and hence is anticipated to give a discrete porphyrin box structures.[8] Thus, the treatment of porphyrin ligand **1** with **2** (2 mol equiv) in H_2O-CH_3CN at 80 °C gave purple homogeneous solution after 1 d. NMR showed the formation of a single product that was isolated as a violet precipitate in 96% yield by adding acetone to the solution. After exchange of NO_3^- with PF_6^- anion, the structure of the product was assigned as $\mathbf{3}^{12+}$ by coldspray-ionization mass spectrometry (CSI-MS) and NMR analyses. CSI-MS displayed prominent peaks correspond to [M-n(PF_6^-)]•mCH_3CN[9]. (m is the number of the solvated acetonitrile molecules.)

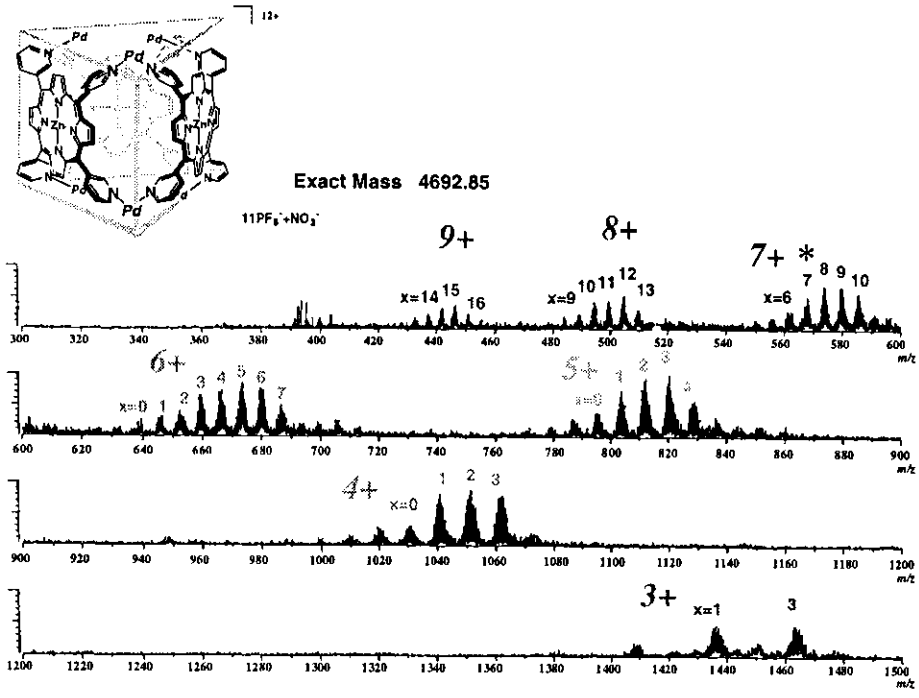

Figure 1. CSI-MS spectrum of $\mathbf{3}^{12+}$•$(PF_6^-)_{11}$•(NO_3^-). X is the number of the solvated acetonitrile molecules.

Interestingly, one NO_3^- ion did not exchanged by PF_6^- ion even if the complex was treated with a large excess amount of NH_4PF_6. The unexchanged NO_3^- ion could be strongly trapped by the prism $\mathbf{3}^{12+}$. This was clearly evidenced by exact mass measurement.[10] For example, the highest peak at *m/z*=567.7613 (7^+ charge) corresponds to $[M\text{-}6PF_6^-\text{-}NO_3^-+7CH_3CN]^{7+}$ (calcd. 567.7561) and not to $[M\text{-}7PF_6^-+5CH_3CN]^{7+}$ (calcd. 567.8879) though both of them showed the same *m/z* (568) in low resolution CSI-MS.

^{1}H NMR spectrum fully agreed with the D_{3h} structure of $\mathbf{3}^{12+}$ showing all equivalent pyridyl groups and two inequivalent pyrrole units (δ 9.01 and 8.89 as singlets: Figure 2).

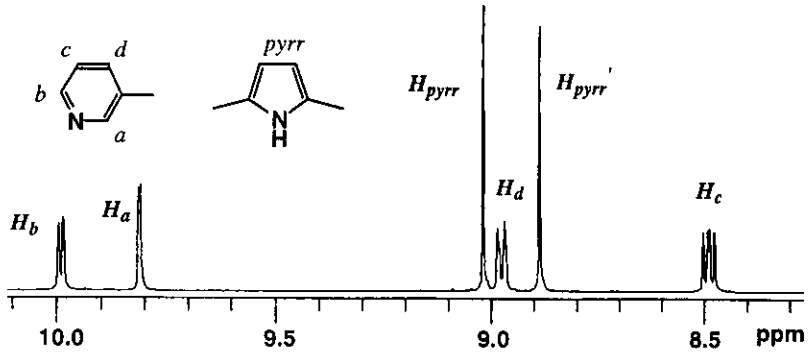

Figure 2. ^{1}H NMR spectrum of $\mathbf{3}^{12+}\bullet(NO_3^-)_{12}$ (500 MHz, D_2O:CD_3CN=1:1).

For D_{3h} porphyrin prism structure there are two possible conformations: one with Pd centers at the apical positions of the prism (conformation **A**) and another one at the equatorial positions (conformation **B**). Structural optimization of $\mathbf{3}^{12+}$ by Cerius^2 program[11] revealed that **A** was

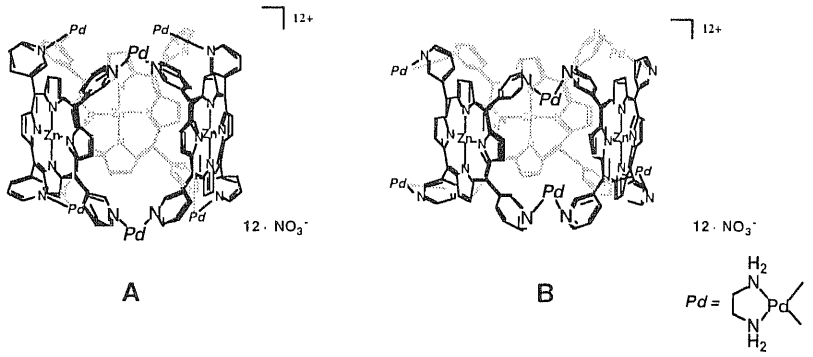

more stable than **B** by 67.6 kcal/mol. In fact, conformation **A** was confirmed by an X-ray crystallographic analysis. A single crystal of $\mathbf{3}^{12+}\bullet(NO_3^-)_{12}$ was obtained by slow diffusion of ethanol into an aqueous solution of $\mathbf{3}^{12+}\bullet(NO_3^-)_{12}$ (8.3 mM) at 23 °C for 1 week. The crystal structure of $\mathbf{3}^{12+}\bullet(NO_3^-)_{12}$ shown in Figure 2 clearly demonstrated

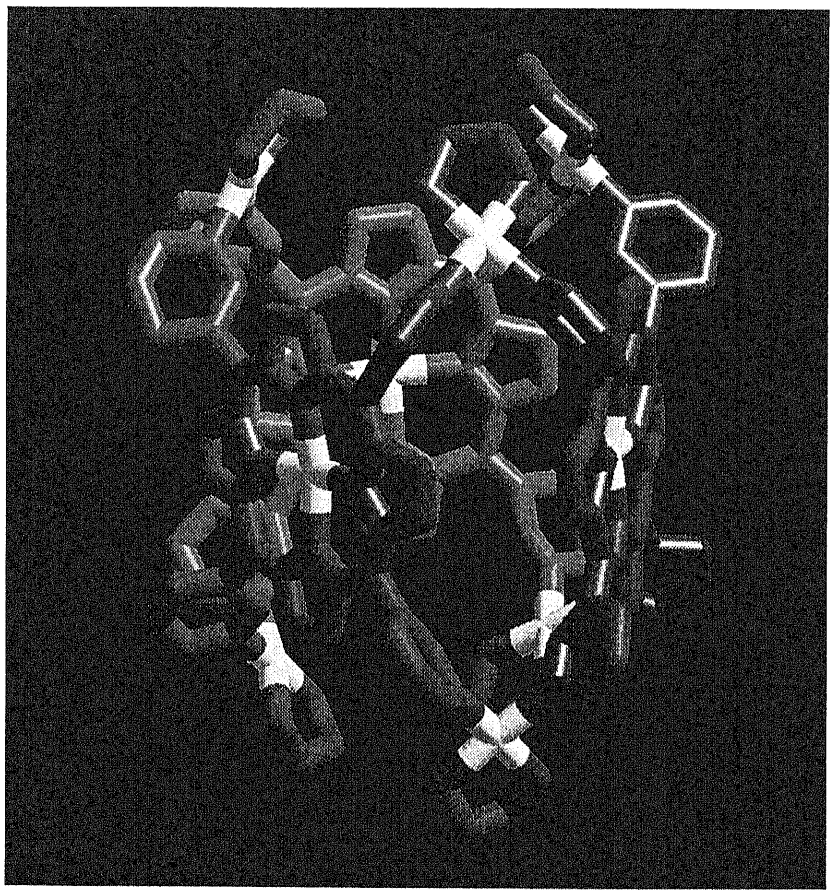

Figure 2. The X-ray crystal structure of $\mathbf{3}^{12+}\bullet(NO_3^-)_{12}$. Water molecules on Zn^{2+} are omitted for clarity.

that the three porphyrin-based ligands were hinged by six palladium atoms at the apical positions of the prism structure. The bite angles of Py-Pd-Py were close to ideal 90° (83-91°); 3-pyridine rings were twisted by 48-73 ° with respect to porphyrin planes. The shortest Pd-Pd distances was ca. 9 Å. Though this prism structure is composed of three porphyrn molecules, cationic nature makes it possible to dissolve the compound in water. Furthermore, the three porphyrin molecules surrounds the large hydrophobic cavity where is expected to host neutral organic molecules in aqueous solution.

5.3 Conclusion

Incorporation of a functional molecule, porphyrin, into artificial system was achieved using self-assembling method. Panel-like porphyrin ligands were complexed with cis-protected Pd(II) to give a prism-like structure in quantitative yield. Convincing characterization by NMR, ESI-MS, and X-ray crystallography revealed the nature of the prism structure. The water-soluble hollow structure expected to show a remarkable inclusion property which realizes enclathlation of guest substrates in the cavity surrounded by porphyrin molecules.

5-4 Experimental Section

Assembly of porphyrin prism [3^{12+}•(NO_3^-)$_{12}$]: Zinc 5,10,15,20-tetra(3-pyridyl)-21*H*,23*H*-porphin (**1**) (1.10 g, 1.62 mmol) was treated with (en)Pd(NO_3)$_2$ (**2**) (0.939 g, 3.23 mmol) in water-acetonitrile 1:1 mixed solvent (324 mL) at 80 °C for 1 d. The addition of acetone (2.5 L) to the resulting purple solution precipitated a purple powder which was separated by centrifuging and dried in vacuo to give $\mathbf{3}^{12+}$•(NO_3^-)$_{12}$ (1.95 g, 0.515 mmol, 96%). Mp >480 °C. ^{1}H NMR (500 MHz, CD_3CN:D_2O=1:1) δ 9.99 (d, *J*=5.7 Hz, 12 H), 9.81 (s, 12 H), 9.01 (s, 12 H), 8.97 (d, *J*=8.1 Hz, 12 H), 8.89 (s, 12 H), 8.49 (dd, *J*=8.1, 5.7 Hz, 12 H), 3.56~3.51, 3.48~3.42 (m, 24 H) (ppm). ^{13}C NMR (125 MHz, CD_3CN:D_2O=1:1) δ 153.856 (*C*H), 150.585 (*C*H),

149.439 (*C*q), 149.226 (*C*q), 144.948 (*C*H), 141.199 (*C*q), 131.944 (*C*H), 131.510 (*C*H), 124.940 (*C*H), 114.231 (*C*q) (ppm). IR (KBr) 1578. 1364, 1192, 1059, 995, 797, 718 (cm^{-1}). UV-vis (H_2O) λ_{max} (ε) [nm (cm^{-1} M^{-1})] 322 (49460), 422 (424600), 561 (31200), 601 (9620). An aqueous solution of $\mathbf{3}^{12+}\bullet(NO_3^-)_{12}$ (100 mg, 0.026 mmol in 40 mL) was poured into saturated NH_4PF_6 aqueous solution. The violet precipitate was separated by centrifuging, washed with water three times, and then dried in vacuo to give $\mathbf{3}^{12+}\bullet(PF_6^-)_{11}\bullet\ NO_3^-$ (102 mg, 0.021 mmol, 81%). Elemental analysis (%) calcd for $C_{122}H_{120}F_{66}N_{37}O_3P_{11}Pd_6Zn_3\bullet 23H_2O$: C, 30.99; H, 3.27; N, 10.13; found: C, 30.86; H, 2.89; N, 9.79.

Crystal data for $\mathbf{3}^{12+}\bullet(NO_3^-)_{12}$: The single crystal of $\mathbf{3}^{12+}\bullet(NO_3^-)_{12}$ was prepared by slow diffusion of ethanol into the aqueous solution of $\mathbf{3}^{12+}\bullet(NO_3^-)_{12}$ (8.3 mM) at 23 °C for 1 week. Triclinic, *P*-1, a=20.6267(14), b=20.7442(14), c=28.1631(19) Å, α=72.8840(10), β=74.0620(10), γ=66.2070(10)°, V=10369.3(12) $Å^3$, Z=2, ρ_{calcd}=1.452 g cm^{-3}, 23102 unique reflections out of 36032 with $I>2\sigma(I)$, $1.10<\theta<25.00°$, final R factors R_1=0.1068, wR_2=0.2985.

References and Notes

(1) a) S. R. Simon, *J. Mol. Biol.* **1971**, *58*, 69-77; b) J. K. Moffat, *J. Mol. Biol.* **1971**, *58*, 79-88; c) J. K. Moffat, S. R., Simon, W. H. Konigsberg, *J. Mol. Biol.* **1971**, *58*, 89-101.

(2) a) J. Deisenhofer, H. Michael, *Angew. Chem. Int. Ed. Engl.* **1989**, *28*, 829-847 and references therein; b) R. Huber, *Angew. Chem. Int. Ed. Engl.* **1989**, *28*, 848-869 and references therein; c) G. McDermott, S. M. Prince, A. A. Freer, A. M. Hawthornthwaite-Lawless, M. Z. Papiz, R. J. Cogdell, N. W. Isaacs, *Nature*, **1995**, *374*, 517-521.

(3) a) I. Tabushi, N. Koga, M. Yanagita, *Tetrahedron Lett.* **1979**, 257-260; b) T. Nagata, A. Osuka, K. Maruyama, *J. Am. Chem. Soc.* **1990**, *112*, 3054-3059; c) M. R. Wasielewski, *Chem. Rev.* **1992**, *92*, 435-461 and references therein; d) S. Prathapan, T. E. Johnson, J. S. Lindsey *J. Am. Chem. Soc.* **1993**, *115*, 7519-7520; e) V. S.-Y. Lin, S. G. DiMagno, M. J. Therien, *Science*,

1994, *264*, 1105-1111; f) J. K. M. Sanders in *Comprehensive Molecular Chemistry*; *Vol. 9* (Eds.: J.-P. Sauvage, M. W. Hosseini), Pergamon, Oxford, **1995**, chap. 4 and references therein; g) N. Bampos, V. Marvaud, J. K. M. Sanders, *Chem. Eur. J.* **1998**, *4*, 335-343; h) K. Tashiro, T. Aida, J.-Y. Zheng, K. Kinbara, K. Saigo, S. Sakamoto, K. Yamaguchi, *J. Am. Chem. Soc.* **1999**, *121*, 9477-9478; i) M. Nakash, Z. Clyde-Watson, N. Feeder, J. E. Davies, S. J. Teat, J. K. M. Sanders, *J. Am. Chem. Soc.* **2000**, *122*, 5286-5293.

(4) a) J.-C. Chambron, V. Heitz, J.-P. Sauvage, *J. Am. Chem. Soc.* **1993**, *115*, 12378-12384; b) M. Linke, J.-C. Chambron, V. Heitz, J.-P. Sauvage, *J. Am. Chem. Soc.* **1997**, *119*, 11329-11330; c) M. Andersson, M. Linke, J.-C. Chambron, J. Davidsson, V. Heitz, J.-P. Sauvage, L. Hammarström, *J. Am. Chem. Soc.* **2000**, *122*, 3526-3527; d) Y. Kobuke, H. Miyaji, *J. Am. Chem. Soc.* **1994**, *116*, 4111-4112; e) Y. Kobuke, H. Miyaji, *Bull. Chem. Soc. Jpn.* **1996**, *69*, 3563-3569; f) C. A. Hunter, L. D. Sarson, *Angew. Chem. Int. Ed. Engl.* **1994**, *33*, 2313-2316; g) C. A. Hunter, R. K. Hyde, *Angew. Chem. Int. Ed. Engl.* **1996**, *35*, 1936-1939; h) K. Funatsu, T. Imamura, A. Ichimura, Y. Sasaki, *Inorg. Chem.* **1998**, *37*, 179; i) K. Funatsu, T. Imamura, A. Ichimura, Y. Sasaki, *Inorg. Chem.* **1998**, *37*, 4986-4995.

(5) a) M. Fujita, D. Oguro, M. Miyazawa, H. Oka, K. Yamaguchi, K. Ogura, *Nature* **1995**, *378*, 469-471; b) N. Takeda, K. Umemoto, K. Yamaguchi, M. Fujita, *Nature*, **1999**, *398*, 794-796; c) K. Umemoto, K. Yamaguchi, M. Fujita, *J. Am. Chem. Soc.* **2000**, *122*, 7150-7151.

(6) a) C. M. Drain, J.-M. Lehn, *J. Chem. Soc., Chem. Commun.* **1994**, 2313-2315; b) P. J. Stang, J. Fan, B. Olenyuk, *J. Chem. Soc., Chem. Commun.* **1997**, 1453; c) M. Fuss, H.-U. Siehl, B. Olenyuk, P. J. Stang, *Organometalics* **1999**, *18*, 758; d) J. Fan, A. Whiteford, B. Olenyuk, M. D. Levin, P. J. Stang, E. B. Fleischer, *J. Am. Chem. Soc.* **1999**, *121*, 2741-2752.

(7) A. Ikeda, M. Ayabe, S. Shinkai, S. Sakamoto, K. Yamaguchi, *Org. Lett.* **2000**, 2, 3707-3710.

(8) Similar box structures can not be expected from an analogous 4-pyridyl-attached porphyrin ligand because of its two dimensional diversity, which is frequently employed in the assembly of infinite structures. a) E. B. Fleischer, A. M. Shachter, *Inorg. Chem.* **1991**, *30*, 3763-3769; b) B. F. Abrahams, B. F. Hoskins, R. Robson, *J. Am. Chem. Soc.* **1991**, *113*, 3606-

3607; c) Y. Diskin-Posner, S. Dahal, I. Goldberg, *Angew. Chem. Int. Ed. Engl.* **2000**, *39*, 1288-1292 and references therein.

(9) CH_3CN solvent enhanced the peak intensities in the ESI-MS study, probably due to its effective solvation of the cationic core facilitating the separation of PF_6^- counter ion.

(10)Exact mass by ESI-MS: K. Yamaguchi, S. Sakamoto, T. Imamoto, T. Ishikawa, *Anal. Sci.* **1999**, *15*, 1037-1038. The coordination number (m) of CH_3CN can be easily determined by using CD_3CN. For example, a 4^+ charged fragment at *m/z* 1051.3 was shifted to 1052.8 in CD_3CN corresponding to 6 Da increase or to the coordinating of two CD_3CN molecules in this fragment.

(11) A. K. Rappé, C. J. Casewit, K. S. Colwell, W. A. III, Goddard, W. M. Skiff, *J. Am. Chem. Soc.* **1995**, *114*, 10024-10025.

Chapter 6

A Porphyrin Prism: Structural Switching Triggered by Guest-Inclusion

Angew. Chem. Int. Ed. **2001**, *40*, 1718-1721.

Abstract: Cationic surface of the porphyrin prism makes it possible to dissolve itself in aqueous solution even though it is composed of three porphyrin units, which provides a large hydrophobic cavity inside the structure where various organic molecules can be bound with remarkable efficiency. Especially, inclusion of a pyrene molecule induced the transformation of the D_{3h} host structure into less symmetrical C_2 structure with a C_2 axis passing vertically through the center of one porphyrin unit. Careful assignment of the NMR spectrum clearly showed that the guest-induced $D_{3h} \rightarrow C_2$ transformation of the host took place through the flipping of two diagonal 3-pyridyl groups of the porphyrin. Pyrene molecule is allowed to spin rapidly inside the cavity.

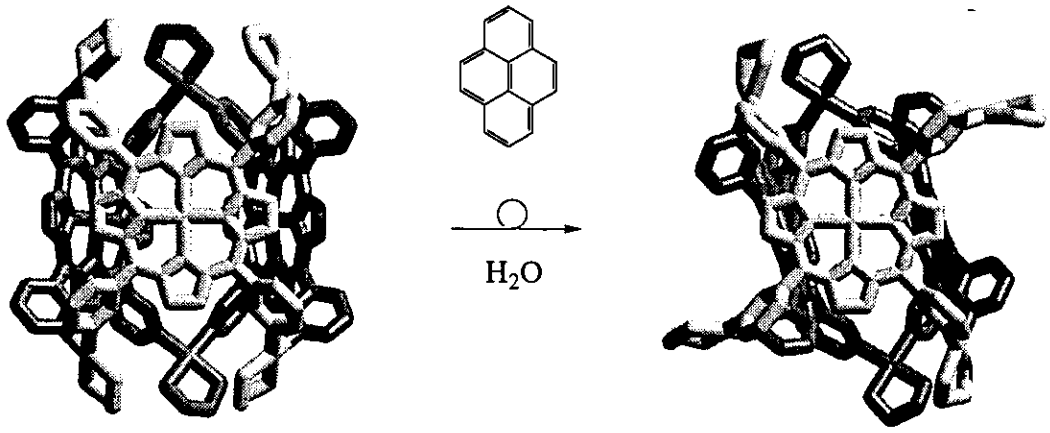

D_{3h} C_2

Pyrene is included.

6.1 Introduction

Studies on the guest inclusion property of host molecules is rapidly growing recently because the host-inclusion complexes possess potential for the data storage devices. Furthermore, establishment of the system which can read out an information in molecular level is one of the most important topic for the progress of nano-technology on going. Recently, data storing systems in molecular level where chirality is the information were reported from several groups.[1] This chapter describes the guest inclusion property of the porphyrin prism and its dynamic behavior which shows memory storage ability with lifetime of several hours.

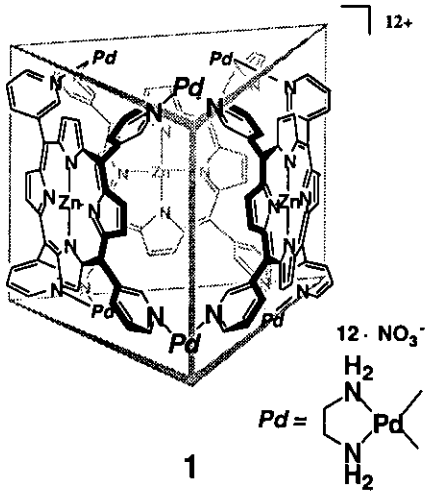

Figure 1. The porphyrin prism **1** (conformation **A**).

6.2 Structural Change of the Porphyrin Prism upon Pyrene Inclusion

The porphyrin prism (**1**) has a large hydrophobic cavity which is expected to show efficient guest inclusion property in aqueous solution. Upon the addition of pyrene as a guest, the D_{3h} conformation **A** of the prism dramatically changed as monitored by NMR. Thus, powdered pyrene (5 mol equiv) was suspended in the solution of $\mathbf{3}^{12+}\bullet(NO_3^-)_{12}$ (1.67 mM in

CD_3OD-D_2O=1:1). After 3 h at 80 °C, NMR became very complex (Figure 2) suggesting the dissymmetrization of the prism structure triggered by the guest binding (see appendix).

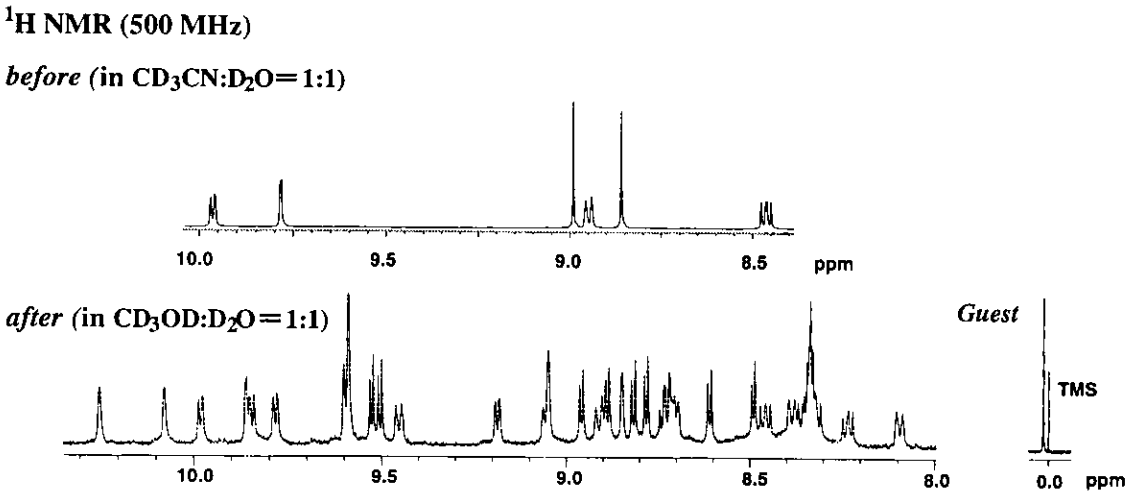

Figure 2. ^{1}H NMR (500 MHz) spectra of **1** and **1**•pyrene complex. Another two guest's signals are omitted. (see appendix)

Interestingly, the guest molecule was not dissymmetrized: pyrene signals were observed as three signals at δ 5.42, 2.97, 0.04 with outstanding upfield shift[2] ,which showed that pyrene molecule was allowed to spin rapidly inside the cavity. The outstanding upfield shift of the guest signals is a strong evidence for the inclusion of pyrene in the cavity. The 1:1 host-guest ratio was clearly confirmed by ESI-MS.[3] Detailed analysis by 800 MHz NMR spectroscopy (^{1}H, HH-COSY: see appendix) elucidated that the guest binding triggered the conformational change of the host from D_{3h} to C_2 symmetry. As shown in Figure 3, twelve pyridyl groups in the prism are placed on six different environments. Similarly, twelve pyrrole rings were also placed on six different environments (each pyrrole is dissymmetrized). These NMR observation fully agreed with the C_2 symmetry.

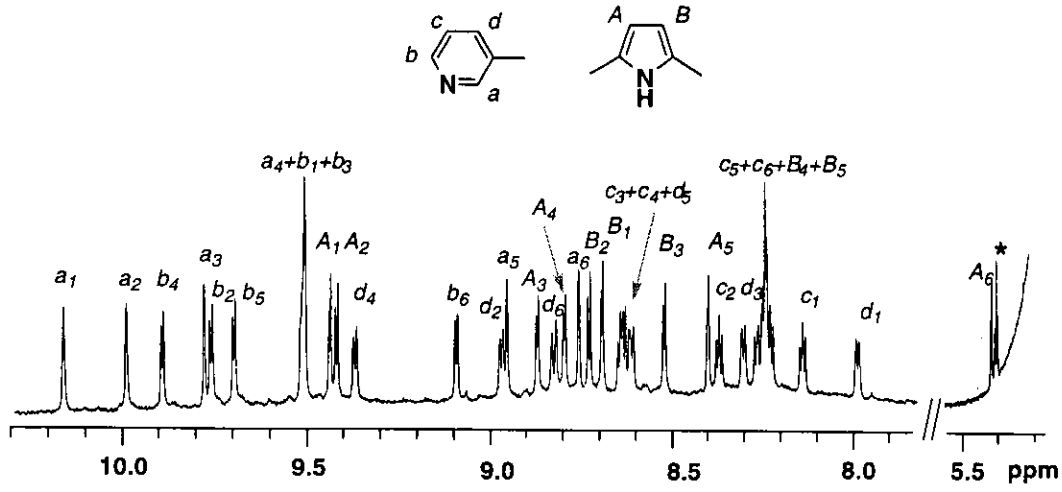

Figure 3. ^{1}H NMR (800 MHz) spectrum of $\mathbf{3}^{12+}\bullet(NO_3^-)_{12}\bullet$pyrene complex. For pyrrole protons, coupled pairs (A_1-B_1, A_2-B_2, ··· A_6-B_6) were assigned. B_6 proton was missing due to overlap with H_2O signal around 5.0 ppm. For 3-Py protons, six corelated pairs b_1-c_1-d_1, b_2-c_2-d_2, ··· b_6-c_6-d_6 were assigned while correlations with a_1-a_6 were not assigned. [Asterisk (*): pyrene]

We suggest that the guest binding triggered the apical-to-equatorial flipping of two Py-Pd-Py hinges at a diagonal position providing C_2-symmetrized conformation C (Figure 4). This transformation was strongly supported by molecular modeling using Cerius^2 program. In conformation C, two porphyrin faces are almost parallel to each other with an interplane distance of ca. 7.1 Å, which is an ideal distance to bind an aromatic ring in the box.

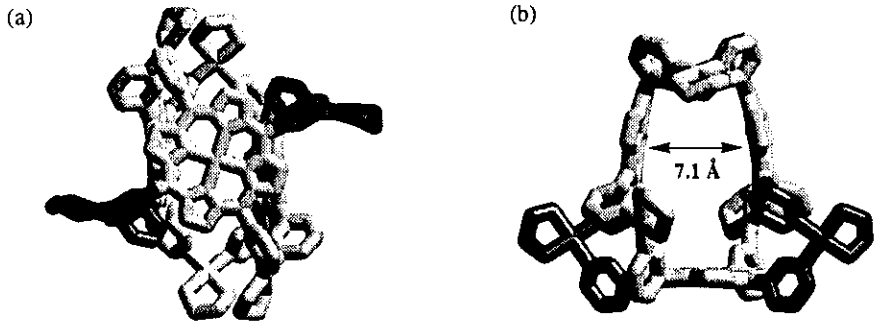

Figure 4. Optimised structure of $\mathbf{3}^{12+}\bullet(NO_3^-)_{12}\bullet$pyrene complex; (a) side view and (b) top view. The pyrene molecule exists inside is omitted for clarity.

In the UV spectrum of $3^{12+}\bullet(NO_3^-)_{12}\bullet$pyrene complex, Q-band was dramatically red-shifted about 13 nm in comparison to empty prism $3^{12+}\bullet(NO_3^-)_{12}$. This observation strongly suggests that there is a strong π-π interaction between the aromatic rings of host and guest molecule.

6.3 The Porphyrin Prism Possessing the Memory Storage Property

Since the porphyrin prism has molecular chirality originated from its C_2 symmetry, a chiral pyren molecule is expected to induce the optical activity on host framework. Upon addition of excess amount of chiral pyrene (**2**) as a powder form, to an aqueous solution of **1**, guest **2** was successfully included as monitored by ^{1}H NMR. After removal of excess **2** by filteration, symmetrical Cotton effect around Q-band area was obserbed on CD spectrum of **1**•(*R*)-**2** and **1**•(*S*)-**2** complexes (FIgure 5), which suggested the chiral induction of the host framework.

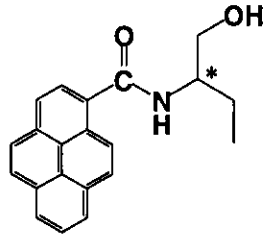

2

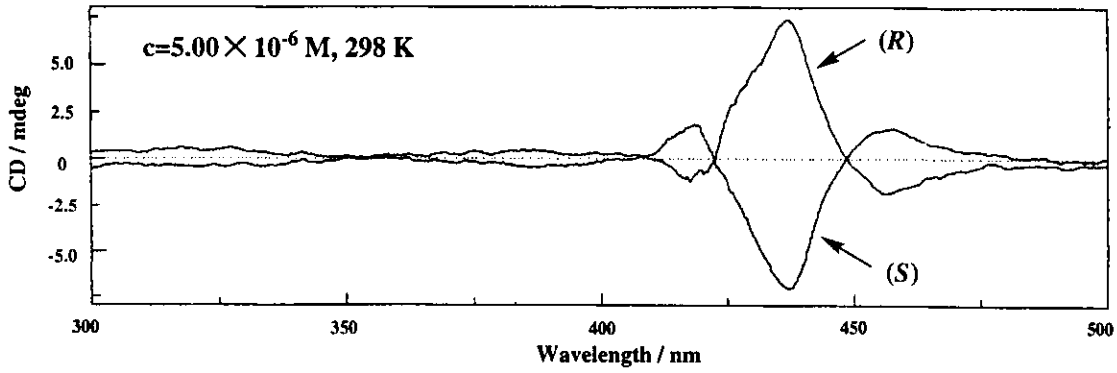

Figure 5. Chemical structure of **2** and CD spectrum of **1**•**2** in H_2O.

Even after exchange of included **2** by adding 5 equivalent of pyrene, the Cotton effect still remained with almost same intensity as before guest exchange as monitored by CD. Interestingly, slow decreasing of the cotton effect of the host-guest complex was observed. The half lifetime of this memory storage ability was found to be 8 hours at room temperature. (Figure 6)

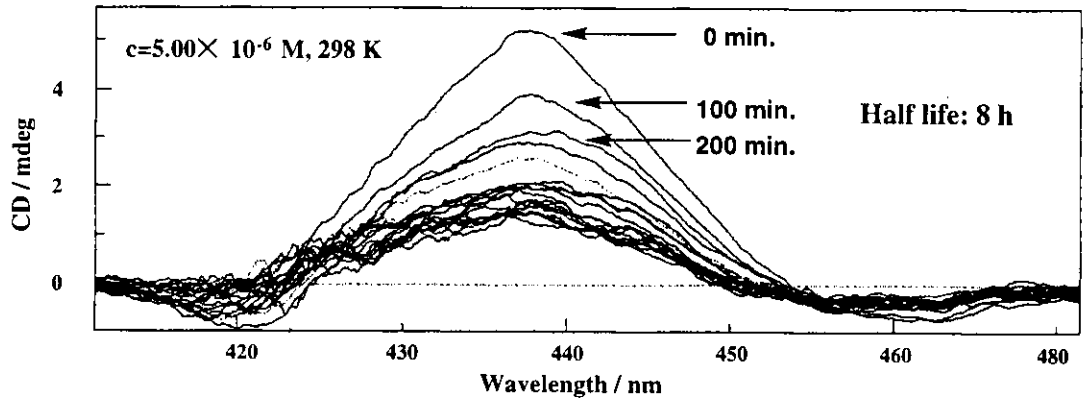

Figure 6. Time-dependence CD observation of guest exchanged **1**•**2** into **1**•pyrene.

6.4 Conclusion

Dramatic conformational change from D_{3h} to C_2 symmetry of the porphyrin prism upon pyrene inclusion was revealed by careful assignment of NMR spectrum. The chiral induction of the host framework was achieved by addition of chiral pyrene molecules. Interesting memory property of the prism compound was observed when included chiral pyrene molecule was exchanged by free pyrene molecule. Time-dependence CD observation revealed that the half-lifetime of the memory effect was ca. 8 hours at room temperature.

References and Notes

(1) Chirality memory: a) Furusho, Y; Kimura, T.; Mizuno, Y.; Aida, T. *J. Am. Chem. Soc.* **1997**, *119*, 5267-5268. b) Yashima, E; Maeda, K.; Okamoto, Y. *Nature* **1999**, *399*, 449-451. c) Suenaga, A.; Ikeda, M.; Takeuchi, M.; Robertson, A.; Shinkai, S. *J. Chem. Soc., Perkin Trans. 1*, **1999**, 3259-3264.

(2) The assignment was confirmed by the disappearance of these peaks with pyrene-d_{10} guest.

(3) CSI-MS data of compound $\mathbf{3}^{12+}\bullet(NO_3^-)_{12}\bullet$pyrene complex: CSI-MS ($CH_3CN$-$H_2O$=1:1) *m/z* 1267.9 $[\mathbf{3}^{12+}\text{-}3(NO_3^-)+\text{pyrene}]^{3+}$, 935.4 $[\mathbf{3}^{12+}\text{-}4(NO_3^-)+\text{pyrene}]^{4+}$, 736.0 $[\mathbf{3}^{12+}\text{-}5(NO_3^-)+\text{pyrene}]^{5+}$, 603.33 $[\mathbf{3}^{12+}\text{-}6(NO_3^-)+\text{pyrene}]^{6+}$.

Appendix

X-ray Crystallographic data

Chapter 2 3-D Interlocked compound 5a

Experimental

Data Collection

A clear prism crystal of $C_{126}H_{156}B_{12}F_{48}N_{36}Pt_6O_{12}$ having approximate dimensions of 0.35 x 0.20 x 0.18 mm was mounted on a glass fiber. All measurements were made on a Rigaku RAXIS II imaging plate area detector with graphite monochromated Mo-Ka radiation.

Indexing was performed from 4 oscillations which were exposed for 4.0 minutes. The crystal-to-detector distance was 86.30mm. The detector swing angle was zero. Readout was performed in the 0.203mm pixel mode.

Cell constants and an orientation matrix for data collection corresponded to a C-centered monoclinic cell with dimensions:

a = 30.83(1) ≈
b = 22.67(1) ≈ $\beta = 109.00(4)^{o}$
c = 25.731(5) ≈
V =17005(9) $Å^3$

For Z = 4 and F.W. = 4579.04, the calculated density is 1.79 g/cm^3. Based on the systematic absences of:

hkl: h+k = 2n+1
h0l: l = 2n+1

packing considerations, a statistical analysis of intensity distribution, and the successful solution and refinement of the structure, the space group was determined to be:

C2/c (#15)

The data were collected at a temperature of -150 ± 1°C to a maximum 2q value of 48.4°.A total of 30 oscillation images were collected, each being exposed for 4.0 minutes. The crystal-to-detector distance was 86.3 mm. The detector swing angle was 0°. Readout was performed in the 0.203mm pixel mode.

Data Reduction

A total of 17770 reflections was collected.

The linear absorption coefficient, μ, for Mo-Kα radiation is 50.1 cm^{-1}. The data were corrected for Lorentz and polarization effects.

Structure Solution and Refinement

The structure was solved by heavy-atom Patterson methods[1] and expanded using Fourier techniques[2]. Some non-hydrogen atoms were refined anisotropically, while the rest (including solvent atoms) were refined isotropically. Hydrogen atoms were included but not refined. The final cycle of full-matrix least-squares refinement[3] on F was based on 6176 observed reflections ($I > 4.00\sigma(I)$) and 882 variable parameters and converged (largest parameter shift was 4.93 times its esd) with unweighted and weighted agreement factors of:

$$R = \Sigma \, ||Fo| - |Fc|| \, / \, \Sigma \, |Fo| = 0.119$$

$$R_w = [\Sigma \, w \, (|Fo| - |Fc|)^2 / \Sigma \, w \, Fo^2]^{1/2} = 0.153$$

The standard deviation of an observation of unit weight[4] was 4.80. The weighting scheme was based on counting statistics and included a factor ($p = 0.030$) to downweight the intense reflections. Plots of $\Sigma \, w \, (|Fo| - |Fc|)^2$ versus $|Fo|$, reflection order in data collection, $\sin\theta/\lambda$ and various classes of indices showed no unusual trends. The maximum and minimum peaks on the final difference Fourier map corresponded to 4.80 and -3.09 $e^-/Å^3$, respectively.

Neutral atom scattering factors were taken from Cromer and Waber[5]. Anomalous dispersion effects were included in Fcalc[6]; the values for $\Delta f'$ and $\Delta f''$ were those of Creagh and McAuley[7]. The values for the mass attenuation coefficients are those of Creagh and Hubbell[8]. All calculations were performed using the teXsan[9] crystallographic software package of Molecular Structure Corporation.

References

(1) PATTY: Beurskens, P.T., Admiraal, G., Beurskens, G., Bosman, W.P., Garcia-Granda, S., Gould, R.O., Smits, J.M.M. and Smykalla, C. (1992). The DIRDIF program system, Technical Report of the Crystallography Laboratory, University of Nijmegen, The Netherlands.

(2) DIRDIF94: Beurskens, P.T., Admiraal, G., Beurskens, G., Bosman, W.P., de Gelder, R., Israel, R. and Smits, J.M.M.(1994). The DIRDIF-94 program system, Technical Report of the Crystallography Laboratory, University of Nijmegen, The Netherlands.

(3) Least Squares function minimized:

$$\Sigma w(|F_o|-|F_c|)^2$$

(4) Standard deviation of an observation of unit weight:

$$[\Sigma w(|F_O|-|F_C|)^2/(N_O-N_V)]^{1/2}$$

where: N_O = number of observations
N_V = number of variables

(5) Cromer, D. T. & Waber, J. T.; "International Tables for X-ray Crystallography", Vol. IV, The Kynoch Press, Birmingham, England, Table 2.2 A (1974).

(6) Ibers, J. A. & Hamilton, W. C.; Acta Crystallogr., 17, 781 (1964).

(7) Creagh, D. C. & McAuley, W.J .; "International Tables for Crystallography", Vol C, (A.J.C. Wilson, ed.), Kluwer Academic Publishers, Boston, Table 4.2.6.8, pages 219-222 (1992).

(8) Creagh, D. C. & Hubbell, J.H..; "International Tables for Crystallography", Vol C, (A.J.C. Wilson, ed.), Kluwer Academic Publishers, Boston, Table 4.2.4.3, pages 200-206 (1992).

(9) teXsan for Windows: Crystal Structure Analysis Package, Molecular Structure Corporation (1997).

EXPERIMENTAL DETAILS

A. Crystal Data

Empirical Formula	$C_{126}H_{156}B_{12}F_{48}N_{36}Pt_6O_{12}$
Formula Weight	4579.04
Crystal Color, Habit	clear, prism
Crystal Dimensions	0.35 X 0.20 X 0.18 mm
Crystal System	monoclinic
Lattice Type	C-centered
Indexing Images	3 oscillations @ 4.0 minutes
Detector Position	86.30 mm
Detector Swing Angle	0.0^o
Pixel Size	0.203 mm
Lattice Parameters	a = 30.83(1) ≈ b = 22.67(1) ≈ c = 25.731(5) ≈ β = 109.00(4) ≈ V = 17005(9) $≈^3$
Space Group	C2/c (#15)
Z value	4
D_{calc}	1.788 g/cm^3
F_{000}	8880.00
μ(MoKα)	50.14 cm^{-1}

B. Intensity Measurements

Diffractometer	RAXIS-II
Radiation	MoKα (λ = 0.71069 Å) graphite monochromated
Detector Aperture	200 mm x 200 mm
Data Images	30 exposures @ 4.0 minutes
Oscillation Range	7.0°
Detector Position	86.3.00 mm
Detector Swing Angle	0.0°
Pixel Size	0.203 mm
$2\theta_{max}$	48.4°
No. of Reflections Measured	Total: 17770 (10686 obs)
Corrections	Lorentz-polarization Absorption (trans. factors: 0.64 – 0.98)

C. Structure Solution and Refinement

Structure Solution	Patterson Methods (DIRDIF92 PATTY)
Refinement	Full-matrix least-squares on F
Function Minimized	Σ w (|Fo| - |Fc|)^2
Least Squares Weights	$1/\sigma^2(Fo) = 4Fo^2/\sigma^2(Fo^2)$
p-factor	0.0300
Anomalous Dispersion	All non-hydrogen atoms
No. Observations (I>4.00σ(I))	6176
No. Variables	882
Reflection/Parameter Ratio	7.00
Residuals: R; Rw	0.119 ; 0.153
Goodness of Fit Indicator	4.80
Max Shift/Error in Final Cycle	2.90
Maximum peak in Final Diff. Map	4.80 $e^-/\approx^3$
Minimum peak in Final Diff. Map	-3.09 $e^-/\approx^3$

Table 1. Atomic coordinates and B_{iso}/B_{eq}

atom	x	y	z	B_{eq}
Pt(1)	0.13170(5)	0.73995(8)	0.26777(5)	6.24(4)
Pt(2)	-0.25605(5)	0.44832(8)	0.06568(5)	5.77(4)
Pt(3)	0.11126(5)	0.15865(7)	0.23527(5)	5.22(3)
F(1)	0.300(1)	0.863(2)	0.250(1)	15(1)
F(2)	0.230(1)	0.838(1)	0.235(1)	10.6(7)
F(3)	0.277(1)	0.765(2)	0.248(1)	14(1)
F(4)	0.274(1)	0.818(2)	0.318(2)	17(1)
F(5)	-0.067(1)	1.000(2)	0.046(2)	15(1)
F(6)	-0.140(1)	0.995(2)	0.074(1)	15(1)
F(7)	-0.086(2)	0.938(3)	0.075(2)	14(2)
F(8)	-0.058(2)	0.983(2)	0.137(3)	15(4)
F(9)	-0.1865(9)	0.265(1)	0.0706(9)	9.6(7)
F(10)	-0.2424(9)	0.294(1)	0.1035(9)	9.6(6)
F(11)	-0.2426(9)	0.204(1)	0.0760(9)	9.4(6)
F(12)	-0.1904(8)	0.232(1)	0.1523(9)	9.0(6)
F(13)	0.959(1)	0.176(1)	0.099(1)	12.3(9)
F(14)	0.948(1)	0.147(2)	0.008(1)	14(1)
F(15)	0.895(1)	0.133(2)	0.052(1)	15(1)
F(16)	0.961(2)	0.087(2)	0.073(2)	20(2)
F(17)	1.004(3)	0.083(4)	0.714(3)	14(3)
F(18)	0.954(4)	0.102(5)	0.624(4)	23(3)
F(19)	0.943(3)	0.017(5)	0.696(3)	11(1)
F(20)	0.942(4)	0.116(5)	0.717(4)	11.(1)
F(21)	0.288(1)	0.561(1)	0.311(1)	11.7(8)
F(22)	0.208(2)	0.543(2)	0.296(2)	20(2)
F(23)	0.233(2)	0.582(2)	0.228(2)	17(2)
F(24)	0.237(1)	0.633(2)	0.291(1)	12.4(9)
O(1)	0.310(1)	0.146(2)	0.089(1)	12(1)
O(2)	0.240(1)	0.095(2)	0.131(2)	14(1)
O(3)	0.470(1)	0.263(2)	0.177(2)	14(1)
O(4)	0.902(1)	0.252(1)	0.132(1)	9.1(8)
O(5)	0.7711(9)	0.147(1)	0.204(1)	8.0(7)
O(6)	0.850(1)	0.093(2)	0.554(2)	15(1)
N(1)	0.166(1)	0.823(2)	0.290(1)	8(1)
N(2)	0.133(1)	0.734(2)	0.351(1)	17(1)
N(3)	0.1330(8)	0.745(1)	0.192(1)	4.9(6)
N(4)	0.0971(9)	0.662(1)	0.2459(9)	5.8(7)
N(5)	-0.3262(9)	0.442(1)	0.0403(9)	5.8(7)
N(6)	-0.264(1)	0.423(1)	0.137(1)	6.3(8)
N(7)	-0.2512(9)	0.476(2)	-0.0096(9)	5.9(7)

Table 1. Atomic coordinates and B_{iso}/B_{eq} (continued)

atom	x	y	z	B_{eq}
N(8)	-0.1872(7)	0.453(1)	0.0976(8)	3.8(5)
N(9)	0.108(1)	0.142(1)	0.311(1)	7.0(8)
N(10)	0.1462(9)	0.083(1)	0.2499(9)	5.3(7)
N(11)	0.0781(8)	0.235(1)	0.2254(8)	4.0(6)
N(12)	0.115(1)	0.169(1)	0.1629(8)	6.6(7)
N(13)	-0.0119(7)	0.539(1)	-0.0701(7)	3.7(5)
N(14)	-0.013(1)	0.431(1)	-0.0769(9)	5.4(6)
N(15)	0.0552(9)	0.482(2)	-0.0385(8)	7.1(8)
N(16)	-0.0243(8)	0.514(1)	0.1751(8)	3.8(5)
N(17)	-0.0283(8)	0.408(1)	0.1709(8)	5.4(7)
N(18)	0.0447(8)	0.454(1)	0.2101(8)	3.8(6)
C(1)	0.169(1)	0.721(2)	0.185(1)	5.3(8)
C(2)	0.175(1)	0.715(2)	0.130(1)	7(1)
C(3)	0.142(1)	0.744(2)	0.090(1)	7(1)
C(4)	0.105(1)	0.771(2)	0.105(2)	7(1)
C(5)	0.100(1)	0.768(2)	0.152(1)	10(1)
C(6)	0.138(1)	0.736(2)	0.027(1)	8(1)
C(7)	0.114(1)	0.686(1)	0.004(1)	5.1(8)
C(8)	0.072(1)	0.691(2)	-0.021(1)	8(1)
C(9)	0.046(1)	0.650(2)	-0.035(1)	7(1)
C(10)	0.061(1)	0.588(2)	-0.032(1)	8(1)
C(11)	0.109(1)	0.584(2)	-0.006(2)	8(1)
C(12)	0.133(1)	0.629(2)	0.012(1)	7(1)
C(13)	0.032(2)	0.533(2)	-0.049(1)	7(1)
C(14)	-0.031(1)	0.479(2)	-0.0782(7)	8.1(9)
C(15)	-0.0852(9)	0.501(2)	-0.104(1)	4.4(7)
C(16)	-0.103(1)	0.552(2)	-0.111(1)	5.4(8)
C(17)	-0.153(1)	0.558(2)	-0.132(1)	5.6(9)
C(18)	-0.175(1)	0.504(3)	-0.144(1)	10(1)
C(19)	-0.158(1)	0.456(2)	-0.144(1)	5.6(9)
C(20)	-0.113(1)	0.455(2)	-0.122(1)	8(1)
C(21)	-0.234(1)	0.509(2)	-0.163(1)	8(1)
C(22)	-0.243(1)	0.510(3)	-0.100(2)	11(1)
C(23)	-0.246(1)	0.445(2)	-0.095(2)	8(1)
C(24)	-0.2530(9)	0.431(2)	-0.043(1)	5.2(8)
C(25)	-0.246(1)	0.533(2)	-0.018(1)	9(1)
C(26)	-0.242(1)	0.545(2)	-0.059(2)	10(1)
C(27)	0.032(1)	0.438(2)	-0.052(1)	5.4(9)
C(28)	0.055(2)	0.378(1)	-0.040(1)	6.3(9)
C(29)	0.027(1)	0.321(2)	-0.050(1)	9(1)

Table 1. Atomic coordinates and B_{iso}/B_{eq} (continued)

atom	x	y	z	B_{eq}
C(30)	0.044(1)	0.271(2)	-0.039(1)	5.8(9)
C(31)	0.089(1)	0.264(2)	-0.0224(9)	7.0(9)
C(32)	0.116(1)	0.315(2)	-0.013(2)	7(1)
C(33)	0.100(1)	0.367(2)	-0.021(1)	7(1)
C(34)	0.113(1)	0.203(2)	-0.008(1)	7(1)
C(35)	0.111(1)	0.191(2)	0.052(1)	7(1)
C(36)	0.075(2)	0.168(2)	0.065(3)	14(2)
C(37)	0.082(1)	0.151(2)	0.1215(8)	18(1)
C(38)	0.151(1)	0.197(2)	0.152(1)	7(1)
C(39)	0.152(1)	0.205(2)	0.095(1)	7.8(9)
C(40)	0.053(1)	0.669(1)	0.217(1)	4.4(7)
C(41)	0.030(1)	0.615(1)	0.203(1)	4.5(7)
C(42)	0.0448(9)	0.564(1)	0.213(1)	3.2(6)
C(43)	0.093(1)	0.557(1)	0.244(1)	4.7(7)
C(44)	0.117(1)	0.606(2)	0.257(1)	5.3(8)
C(45)	0.022(1)	0.507(2)	0.1996(9)	5.2(8)
C(46)	-0.0438(9)	0.468(2)	0.166(1)	5.2(8)
C(47)	-0.097(1)	0.458(2)	0.1391(8)	5.8(8)
C(48)	-0.1205(8)	0.511(1)	0.1246(9)	3.5(6)
C(49)	-0.1676(9)	0.506(1)	0.1033(8)	3.4(6)
C(50)	-0.159(2)	0.407(2)	0.114(1)	8(1)
C(51)	-0.117(1)	0.407(2)	0.135(1)	4.7(8)
C(52)	0.020(1)	0.407(1)	0.195(1)	5.7(9)
C(53)	0.0416(9)	0.347(1)	0.2043(8)	3.6(7)
C(54)	0.015(1)	0.303(1)	0.189(1)	4.6(8)
C(55)	0.034(1)	0.250(2)	0.198(1)	7(1)
C(56)	0.103(1)	0.286(2)	0.239(1)	9(1)
C(57)	0.082(1)	0.342(2)	0.229(1)	6.8(9)
C(58)	0.143(2)	0.788(3)	0.373(2)	16(2)
C(59)	0.179(2)	0.824(2)	0.347(2)	14(1)
C(60)	-0.332(1)	0.408(2)	0.087(2)	10(1)
C(61)	-0.308(1)	0.422(2)	0.137(2)	8(1)
C(62)	0.141(2)	0.055(2)	0.297(1)	11(1)
C(63)	0.138(1)	0.097(2)	0.337(1)	6.2(9)
B(1)	0.267(4)	0.821(5)	0.271(4)	17(3)
B(2)	-0.102(4)	0.953(6)	0.098(5)	19(3)
B(3)	-0.214(1)	0.244(2)	0.098(1)	4.8(8)
B(4)	0.946(4)	0.145(5)	0.062(4)	19(3)
B(5)	0.970(2)	0.069(3)	0.703(2)	9(1)
B(6)	0.249(5)	0.579(6)	0.302(5)	20(3)

Table 1. Atomic coordinates and B_{iso}/B_{eq} (continued)

atom	x	y	z	B_{eq}
H(1)	0.1904	0.8240	0.2767	10.212
H(2)	0.1440	0.8529	0.2737	10.212
H(3)	0.1003	0.7285	0.3493	19.937
H(4)	0.1500	0.7039	0.3683	19.937
H(5)	-0.3390	0.4809	0.0387	7.048
H(6)	-0.3369	0.4254	0.0044	7.048
H(7)	-0.2537	0.3811	0.1434	7.145
H(8)	-0.2467	0.4451	0.1658	7.145
H(9)	0.1218	0.8143	0.3755	15.462
H(10)	0.1650	0.7826	0.4137	15.462
H(11)	0.2101	0.8116	0.3609	19.663
H(12)	0.1798	0.8672	0.3563	19.663
H(13)	-0.3674	0.4086	0.0787	11.162
H(14)	-0.3296	0.3647	0.0760	11.162
H(15)	-0.3126	0.3963	0.1619	10.921
H(16)	-0.3161	0.4614	0.1423	10.921
H(17)	0.1122	0.1799	0.3298	8.100
H(18)	0.0752	0.1322	0.3049	8.100
H(19)	0.1335	0.0578	0.2194	6.866
H(20)	0.1767	0.0904	0.2566	6.866
H(21)	0.1126	0.0332	0.2855	14.840
H(22)	0.1655	0.0297	0.3115	14.840
H(23)	0.1682	0.1146	0.3534	7.759
H(24)	0.1288	0.0794	0.3642	7.759
H(25)	0.0821	0.7930	0.0746	9.162
H(26)	0.0753	0.7905	0.1600	11.105
H(27)	0.1215	0.7712	0.0074	8.776
H(28)	0.1674	0.7368	0.0219	8.776
H(29)	-0.2401	0.5486	-0.1771	11.520
H(30)	-0.2471	0.4810	-0.1845	11.520
H(31)	0.0970	0.1770	-0.0348	8.586
H(32)	0.1436	0.2078	-0.0064	8.586
H(33)	0.1943	0.7036	0.2150	6.873
H(34)	0.1987	0.6991	0.1223	7.935
H(35)	0.0593	0.7284	-0.0276	8.519
H(36)	0.0120	0.6536	-0.0519	10.127
H(37)	0.1249	0.5476	-0.0016	8.351
H(38)	0.1659	0.6285	0.0258	7.136
H(39)	-0.0831	0.5838	-0.1009	6.073
H(40)	-0.1672	0.5952	-0.1299	7.134

Table 1. Atomic coordinates and B_{iso}/B_{eq} (continued)

atom	x	y	z	B_{eq}
H(41)	-0.1716	0.4197	-0.1558	7.937
H(42)	-0.0967	0.4168	-0.1166	8.186
H(43)	-0.0057	0.3289	-0.0631	7.807
H(44)	0.0243	0.2363	-0.0495	7.158
H(45)	0.1476	0.3128	-0.0034	9.129
H(46)	0.1212	0.4054	-0.0099	8.808
H(48)	0.0600	0.1209	0.1275	18.224
H(49)	0.1751	0.2082	0.1843	9.136
H(50)	0.1770	0.2253	0.0890	8.806
H(51)	-0.2402	0.4187	-0.1194	10.514
H(52)	-0.2633	0.3924	-0.0378	5.543
H(53)	-0.2476	0.5622	0.0076	11.346
H(54)	-0.2340	0.5833	-0.0666	12.573
H(55)	0.0389	0.7055	0.2104	6.326
H(56)	-0.0037	0.6168	0.1880	5.738
H(57)	0.1076	0.5200	0.2516	5.560
H(58)	0.1486	0.6047	0.2783	6.531
H(59)	-0.1071	0.5484	0.1270	4.331
H(60)	-0.1855	0.5403	0.0917	4.377
H(61)	-0.1732	0.3672	0.1106	8.636
H(62)	-0.1000	0.3742	0.1405	5.593
H(63)	-0.0184	0.3059	0.1705	7.251
H(64)	0.0156	0.2154	0.1788	8.990
H(65)	0.1352	0.2831	0.2554	7.488
H(66)	0.1042	0.3770	0.2383	5.727
H(67)	0.0461	0.1560	0.0447	20.925

$B_{eq} = 8/3\ p^2(U_{11}(aa^*)^2 + U_{22}(bb^*)^2 + U_{33}(cc^*)^2 + 2U_{12}(aa^*bb^*)\cos g + 2U_{13}(aa^*cc^*)\cos b + 2U_{23}(bb^*cc^*)\cos a)$

Table 2. Anisotropic Displacement Parameters

atom	U_{11}	U_{22}	U_{33}	U_{12}	U_{13}	U_{23}
Pt(1)	0.083(1)	0.085(1)	0.0758(8)	-0.0356(9)	0.0357(6)	-0.0224(7)
Pt(2)	0.0497(7)	0.095(1)	0.0728(7)	-0.0058(9)	0.0174(6)	0.0027(7)
Pt(3)	0.0648(8)	0.068(1)	0.0659(7)	0.0056(8)	0.0213(6)	0.0054(7)
N(1)	0.09(2)	0.11(3)	0.10(2)	-0.05(2)	0.01(2)	-0.06(2)
N(2)	0.16(2)	0.43(6)	0.10(2)	-0.23(3)	0.09(2)	-0.10(3)
N(3)	0.04(1)	0.05(2)	0.09(2)	-0.03(1)	0.02(1)	-0.03(1)
N(4)	0.06(2)	0.10(2)	0.06(1)	-0.07(2)	0.01(1)	-0.03(1)
N(5)	0.06(2)	0.08(2)	0.07(1)	-0.01(2)	0.01(1)	0.01(1)
N(6)	0.10(2)	0.07(2)	0.07(2)	0.01(2)	0.02(1)	0.02(1)
N(7)	0.04(1)	0.13(3)	0.04(1)	-0.01(2)	-0.01(1)	-0.01(2)
N(8)	0.01(1)	0.07(2)	0.06(1)	-0.01(1)	0.014(9)	0.01(1)
N(9)	0.12(2)	0.09(2)	0.07(2)	-0.01(2)	0.04(1)	-0.00(2)
N(10)	0.07(2)	0.08(2)	0.04(1)	0.02(2)	0.01(1)	0.00(1)
N(11)	0.07(2)	0.05(2)	0.05(1)	0.01(1)	0.039(9)	0.01(1)
N(12)	0.13(2)	0.09(2)	0.010(9)	0.05(2)	-0.02(1)	-0.01(1)
N(13)	0.03(1)	0.07(2)	0.04(1)	0.02(1)	0.012(8)	-0.01(1)
N(14)	0.12(2)	0.02(1)	0.09(1)	0.01(1)	0.08(1)	0.02(1)
N(15)	0.05(2)	0.18(3)	0.04(1)	-0.07(2)	0.01(1)	0.03(1)
N(16)	0.05(1)	0.05(2)	0.05(1)	-0.05(1)	0.024(9)	-0.02(1)
N(17)	0.03(1)	0.14(3)	0.03(1)	-0.02(2)	0.008(9)	-0.03(1)
N(18)	0.05(2)	0.03(2)	0.05(1)	-0.01(1)	0.01(1)	0.01(1)
C(1)	0.09(2)	0.07(3)	0.03(1)	0.02(2)	0.01(1)	-0.01(1)
C(2)	0.07(2)	0.17(4)	0.07(2)	0.01(2)	0.06(1)	-0.02(2)
C(3)	0.11(3)	0.09(3)	0.04(2)	-0.02(3)	0.02(2)	-0.01(2)
C(4)	0.05(2)	0.09(3)	0.15(3)	-0.00(2)	0.04(2)	-0.04(3)
C(5)	0.11(2)	0.26(6)	0.04(1)	-0.06(3)	0.06(1)	-0.04(2)
C(6)	0.08(3)	0.11(4)	0.09(2)	-0.04(3)	0.01(2)	0.02(2)
C(7)	0.08(2)	0.05(2)	0.05(2)	-0.05(2)	0.01(2)	-0.03(1)
C(8)	0.12(3)	0.05(2)	0.06(2)	-0.07(2)	-0.05(2)	0.01(2)
C(9)	0.09(2)	0.16(4)	0.04(1)	0.02(3)	0.03(1)	-0.03(2)
C(10)	0.04(2)	0.23(5)	0.03(1)	0.02(3)	0.01(1)	-0.05(2)
C(11)	0.11(3)	0.07(3)	0.14(2)	-0.05(2)	0.08(2)	-0.02(2)
C(12)	0.07(2)	0.12(4)	0.08(2)	-0.02(3)	0.03(2)	-0.04(2)
C(13)	0.16(4)	0.08(3)	0.01(1)	-0.02(3)	-0.01(2)	-0.02(1)
C(14)	0.11(2)	0.23(4)	-0.019(8)	-0.09(2)	0.024(8)	-0.03(1)
C(15)	0.04(2)	0.09(3)	0.04(1)	-0.02(2)	0.01(1)	-0.03(2)
C(16)	0.07(2)	0.07(2)	0.06(2)	0.04(2)	0.01(1)	-0.01(2)
C(17)	0.03(2)	0.11(3)	0.08(2)	-0.01(2)	0.01(1)	0.01(2)
C(18)	0.03(2)	0.29(6)	0.03(1)	-0.08(3)	-0.01(1)	0.03(2)
C(19)	0.04(2)	0.06(2)	0.13(2)	0.03(2)	0.05(1)	0.02(2)

Table 2. Anisotropic Displacement Parameters (continued)

atom	U_{11}	U_{22}	U_{33}	U_{12}	U_{13}	U_{23}
C(20)	0.13(3)	0.16(4)	0.05(2)	0.01(3)	0.05(2)	-0.01(2)
C(21)	0.08(2)	0.17(4)	0.07(2)	-0.02(3)	0.05(1)	0.05(2)
C(22)	0.07(3)	0.19(5)	0.19(3)	0.02(3)	0.05(2)	0.14(3)
C(23)	0.07(3)	0.14(4)	0.12(3)	0.02(3)	0.04(2)	0.02(3)
C(24)	0.02(1)	0.11(3)	0.08(2)	-0.04(2)	0.03(1)	-0.00(2)
C(25)	0.12(2)	0.23(4)	0.02(1)	-0.12(2)	0.03(1)	-0.02(2)
C(26)	0.06(2)	0.08(3)	0.23(4)	0.04(2)	0.06(2)	-0.06(3)
C(27)	0.03(1)	0.12(4)	0.07(2)	0.01(2)	0.04(1)	0.01(2)
C(28)	0.17(4)	0.04(2)	0.02(1)	0.01(2)	0.03(2)	-0.00(1)
C(29)	0.09(3)	0.19(4)	0.03(1)	0.09(3)	0.00(1)	-0.03(2)
C(30)	0.08(2)	0.08(3)	0.05(2)	0.04(2)	0.02(2)	0.00(2)
C(31)	0.12(2)	0.15(4)	0.01(1)	0.02(3)	0.04(1)	0.00(1)
C(32)	0.07(2)	0.08(3)	0.14(3)	0.04(2)	0.07(2)	-0.02(2)
C(33)	0.05(2)	0.08(3)	0.10(2)	0.02(2)	-0.01(2)	0.03(2)
C(34)	0.13(3)	0.08(3)	0.07(2)	0.03(3)	0.04(2)	-0.01(2)
C(35)	0.11(3)	0.07(3)	0.08(2)	-0.03(3)	0.01(2)	-0.01(2)
C(36)	0.07(3)	0.08(4)	0.38(9)	0.01(3)	0.05(4)	-0.04(5)
C(37)	0.29(3)	0.44(7)	-0.007(8)	0.12(4)	0.108(8)	0.07(2)
C(38)	0.07(2)	0.09(3)	0.12(3)	0.04(2)	0.05(2)	0.06(2)
C(39)	0.15(2)	0.12(3)	0.07(1)	0.09(2)	0.09(1)	0.04(2)
C(40)	0.05(2)	0.04(2)	0.07(2)	-0.01(2)	0.01(1)	-0.02(1)
C(41)	0.05(2)	0.05(2)	0.07(2)	0.03(2)	0.01(1)	0.03(1)
C(42)	0.05(2)	0.03(2)	0.06(1)	-0.00(1)	0.03(1)	0.00(1)
C(43)	0.10(3)	0.03(2)	0.04(1)	-0.01(2)	-0.01(1)	-0.02(1)
C(44)	0.08(2)	0.08(2)	0.05(1)	0.07(2)	0.04(1)	0.03(1)
C(45)	0.06(2)	0.12(3)	0.02(1)	-0.03(2)	0.02(1)	-0.01(1)
C(46)	0.04(1)	0.12(3)	0.05(1)	0.05(2)	0.04(1)	0.02(2)
C(47)	0.09(2)	0.13(3)	0.01(1)	-0.06(2)	0.039(9)	-0.03(1)
C(48)	0.01(1)	0.08(2)	0.04(1)	0.03(1)	0.00(1)	-0.01(1)
C(49)	0.06(2)	0.06(2)	0.016(9)	-0.01(2)	0.025(9)	0.00(1)
C(50)	0.12(3)	0.14(4)	0.03(2)	0.01(3)	0.00(2)	-0.01(2)
C(51)	0.05(2)	0.08(2)	0.05(2)	-0.03(2)	0.01(1)	-0.03(2)
C(52)	0.12(3)	0.04(2)	0.07(2)	0.04(2)	0.05(2)	0.03(2)
C(53)	0.05(2)	0.07(2)	0.02(1)	-0.01(2)	0.017(9)	0.00(1)
C(54)	0.07(2)	0.04(2)	0.08(2)	0.03(2)	0.04(1)	0.02(2)
C(55)	0.03(2)	0.12(4)	0.12(2)	-0.01(2)	0.05(2)	-0.00(2)
C(56)	0.08(2)	0.23(5)	0.03(1)	0.03(3)	0.02(1)	0.06(2)
C(57)	0.05(2)	0.07(2)	0.12(3)	0.06(2)	-0.01(2)	0.02(2)
C(58)	0.11(3)	0.29(6)	0.25(4)	-0.11(4)	0.11(3)	-0.20(4)
C(59)	0.24(4)	0.19(4)	0.14(3)	-0.19(3)	0.13(2)	-0.08(3)

Table 2. Anisotropic Displacement Parameters (continued)

atom	U_{11}	U_{22}	U_{33}	U_{12}	U_{13}	U_{23}
C(60)	0.10(2)	0.12(4)	0.23(3)	-0.02(3)	0.13(2)	0.04(3)
C(61)	0.02(2)	0.11(3)	0.15(3)	-0.00(2)	0.00(2)	0.01(3)
C(62)	0.21(4)	0.15(4)	0.05(2)	0.14(3)	0.03(2)	0.01(2)
C(63)	0.05(2)	0.10(3)	0.07(2)	0.04(2)	0.00(2)	0.04(2)

The general temperature factor expression:
$\exp(-2p^2(a^{*2}U_{11}h^2 + b^{*2}U_{22}k^2 + c^{*2}U_{33}l^2 + 2a^*b^*U_{12}hk + 2a^*c^*U_{13}hl + 2b^*c^*U_{23}kl))$

Table 3. Bond Lengths(≈)

atom	atom	distance	atom	atom	distance
PT1	N1	2.14(3)	PT1	N2	2.13(3)
PT1	N3	1.96(3)	PT1	N4	2.04(2)
PT2	N5	2.05(3)	PT2	N6	2.00(3)
PT2	N7	2.09(3)	PT2	N8	2.01(2)
PT3	N9	2.02(3)	PT3	N10	1.99(3)
PT3	N11	1.99(2)	PT3	N12	1.92(2)
N1	C59	1.40(5)	N2	C58	1.34(7)
N3	C1	1.30(4)	N3	C5	1.32(5)
N4	C40	1.34(4)	N4	C44	1.40(4)
N5	C60	1.48(5)	N6	C61	1.38(4)
N7	C24	1.33(4)	N7	C25	1.33(5)
N8	C49	1.33(4)	N8	C50	1.35(5)
N9	C63	1.39(4)	N10	C62	1.43(5)
N11	C55	1.34(4)	N11	C56	1.34(5)
N12	C37	1.31(4)	N12	C38	1.39(5)
N13	C13	1.30(5)	N13	C14	1.47(4)
N14	C14	1.30(5)	N14	C27	1.33(4)
N15	C13	1.32(5)	N15	C27	1.31(5)
N16	C45	1.37(4)	N16	C46	1.30(4)
N17	C46	1.43(4)	N17	C52	1.42(4)
N18	C45	1.38(4)	N18	C52	1.30(4)
C1	C2	1.49(4)	C2	C3	1.35(5)
C3	C4	1.46(5)	C3	C6	1.62(5)
C4	C5	1.31(5)	C6	C7	1.37(5)
C7	C8	1.30(5)	C7	C12	1.41(5)
C8	C9	1.30(5)	C9	C10	1.48(6)
C10	C11	1.43(5)	C10	C13	1.51(6)
C11	C12	1.304(5)	C14	C15	1.66(4)
C15	C16	1.30(4)	C15	C20	1.32(5)
C16	C17	1.46(4)	C17	C18	1.38(6)
C18	C19	1.29(6)	C18	C21	1.68(5)
C19	C20	1.31(5)	C21	C22	1.69(6)
C22	C23	1.48(7)	C22	C26	1.31(7)
C23	C24	1.45(5)	C25	C26	1.15(6)
C27	C28	1.52(5)	C28	C29	1.54(6)

C28	C33	1.32(5)	C29	C30	1.30(5)
C30	C31	1.31(5)	C31	C32	1.40(5)
C31	C34	1.54(5)	C32	C33	1.31(5)
C34	C35	1.57(5)	C35	C36	1.36(7)
C35	C39	1.42(5)	C36	C37	1.44(8)
C38	C39	1.49(4)	C40	C41	1.40(4)
C41	C42	1.23(4)	C42	C43	1.46(4)
C42	C45	1.45(4)	C43	C44	1.32(4)
C46	C47	1.58(4)	C47	C48	1.39(4)
C47	C51	1.31(4)	C48	C49	1.38(3)
C50	C51	1.29(5)	C52	C53	1.49(4)
C53	C54	1.30(4)	C53	C57	1.30(4)
C54	C55	1.34(5)	C56	C57	1.41(6)
C58	C59	1.69(7)	C60	C61	1.30(6)
C62	C63	1.44(5)			

Table 5. Bond Angles(°)

atom	atom	atom	angle	atom	atom	atom	angle
N1	PT1	N2	87(2)	N1	PT1	N3	93(1)
N1	PT1	N4	178(1)	N2	PT1	N3	178(1)
N2	PT1	N4	93(1)	N3	PT1	N4	87.1(9)
N5	PT2	N6	81(1)	N5	PT2	N7	96(1)
N5	PT2	N8	174.8(9)	N6	PT2	N7	177(1)
N6	PT2	N8	94(1)	N7	PT2	N8	88.7(9)
N9	PT3	N10	81(1)	N9	PT3	N11	96(1)
N9	PT3	N12	176(1)	N10	PT3	N11	176.5(9)
N10	PT3	N12	95(1)	N11	PT3	N12	87.9(9)
F8	F19	B5	88(2)	PT1	N1	C59	105(3)
PT1	N2	C58	108(4)	PT1	N3	C1	115(2)
PT1	N3	C5	123(2)	C1	N3	C5	122(3)
PT1	N4	C40	114(2)	PT1	N4	C44	125(2)
C40	N4	C44	121(3)	PT2	N5	C60	100(2)
PT2	N6	C61	114(2)	PT2	N7	C24	112(3)
PT2	N7	C25	119(2)	C24	N7	C25	129(3)
PT2	N8	C49	119(2)	PT2	N8	C50	125(3)
C49	N8	C50	116(3)	PT3	N9	C63	112(2)
PT3	N10	C62	110(2)	PT3	N11	C55	132(3)
PT3	N11	C56	119(2)	C55	N11	C56	108(3)
PT3	N12	C37	120(3)	PT3	N12	C38	124(2)
C37	N12	C38	117(3)	C13	N13	C14	106(3)
C14	N14	C27	107(3)	C13	N15	C27	115(3)
C45	N16	C46	112(3)	C46	N17	C52	110(3)
C45	N18	C52	117(3)	N3	C1	C2	123(3)
C1	C2	C3	112(3)	C2	C3	C4	118(3)
C2	C3	C6	120(3)	C4	C3	C6	120(3)
C3	C4	C5	125(4)	N3	C5	C4	118(4)
C3	C6	C7	112(3)	C6	C7	C8	119(4)
C6	C7	C12	124(3)	C8	C7	C12	117(3)
C7	C8	C9	125(4)	C8	C9	C10	123(4)

C9	C10	C11	110(4)	C9	C10	C13	129(3)
C11	C10	C13	121(4)	C10	C11	C12	122(4)
C7	C12	C11	122(4)	N13	C13	N15	127(4)
N13	C13	C10	118(4)	N15	C13	C10	116(4)
N13	C14	N14	132(3)	N13	C14	C15	95(3)
N14	C14	C15	132(3)	C14	C15	C16	132(3)
C14	C15	C20	111(3)	C16	C15	C20	117(3)
C15	C16	C17	120(3)	C16	C17	C18	113(3)
C17	C18	C19	127(3)	C17	C18	C21	114(4)
C19	C18	C21	118(4)	C18	C19	C20	114(4)
C15	C20	C19	128(4)	C18	C21	C22	102(2)
C21	C22	C23	96(4)	C21	C22	C26	142(5)
C23	C22	C26	121(4)	C22	C23	C24	110(4)
N7	C24	C23	116(3)	N7	C25	C26	115(4)
C22	C26	C25	129(5)	N14	C27	N15	132(4)
N14	C27	C28	109(3)	N15	C27	C28	119(3)
C27	C28	C29	121(4)	C27	C28	C33	127(4)
C29	C28	C33	112(3)	C28	C29	C30	123(4)
C29	C30	C31	121(4)	C30	C31	C32	117(4)
C30	C31	C34	124(4)	C32	C31	C34	118(3)
C31	C32	C33	124(4)	C28	C33	C32	123(4)
C31	C34	C35	103(3)	C34	C35	C36	128(4)
C34	C35	C39	115(4)	C36	C35	C39	118(4)
C35	C36	C37	120(5)	N12	C37	C36	125(4)
N12	C38	C39	122(3)	C35	C39	C38	117(3)
N4	C40	C41	112(3)	C40	C41	C42	131(3)
C41	C42	C43	117(3)	C41	C42	C45	131(3)
C43	C42	C45	111(3)	C42	C43	C44	115(3)
N4	C44	C43	124(3)	N16	C45	N18	125(3)
N16	C45	C42	111(3)	N18	C45	C42	124(3)
N16	C46	N17	133(3)	N16	C46	C47	127(3)
N17	C46	C47	100(3)	C46	C47	C48	112(3)
C46	C47	C51	124(3)	C48	C47	C51	124(3)
C47	C48	C49	115(3)	N8	C49	C48	120(3)
N8	C50	C51	128(4)	C47	C51	C50	116(4)
N17	C52	N18	123(3)	N17	C52	C53	116(3)
N18	C52	C53	121(3)	C52	C53	C54	116(3)
C52	C53	C57	120(3)	C54	C53	C57	124(4)
C53	C54	C55	115(3)	N11	C55	C54	130(4)
N11	C56	C57	123(3)	C53	C57	C56	120(4)
N2	C58	C59	111(4)	N1	C59	C58	113(3)
N5	C60	C61	120(4)	N6	C61	C60	104(4)
N10	C62	C63	111(4)	N9	C63	C62	109(3)

Table 7. Non-bonded Contacts out to 3.60 ≈ (selected)

atom	atom	distance	ADC	atom	atom	distance	ADC
N13	C52	3.38(3)	56503	N13	C45	3.41(3)	56503
N13	N18	3.41(3)	56503	N13	C27	3.42(3)	56503
N13	C46	3.43(3)	56503	N13	N17	3.44(3)	56503
N13	N16	3.46(3)	56503	N13	N15	3.50(3)	56503
N14	C41	3.28(4)	56503	N14	C42	3.31(3)	56503
N14	N16	3.34(3)	56503	N14	C45	3.38(3)	56503
N14	C13	3.57(4)	56503	N14	C10	3.58(4)	56503
N15	N16	3.33(3)	56503	N15	C46	3.37(3)	56503
N15	C14	3.44(4)	56503	N15	C48	3.45(3)	56503
N15	C15	3.49(3)	56503	N15	C47	3.52(3)	56503
N16	C45	3.21(3)	2	N16	C27	3.29(4)	56503
N16	C42	3.34(3)	2	N16	C13	3.35(3)	56503
N16	C14	3.45(3)	56503	N16	N18	3.49(3)	2
N16	C43	3.56(4)	2	N17	C52	3.37(3)	2
N17	C13	3.39(4)	56503	N17	C10	3.39(3)	56503
N17	N18	3.43(3)	2	N18	C46	3.22(3)	2
N18	C15	3.51(4)	56503	N18	C16	3.58(4)	56503
C10	C47	3.46(4)	56503	C10	C46	3.54(4)	56503
C10	C14	3.58(5)	56503	C11	C20	3.38(5)	56503
C11	C51	3.41(5)	56503	C11	C47	3.46(4)	56503
C11	C50	3.58(5)	56503	C13	C46	3.14(4)	56503
C13	C14	3.29(3)	56503	C13	C47	3.53(5)	56503
C14	C45	3.24(3)	56503	C14	C42	3.49(3)	56503
C20	C43	3.40(4)	56503	C23	C63	3.56(5)	45408
C34	C58	3.48(6)	56404	C41	C41	3.49(6)	2
C43	C48	3.37(3)	2	C45	C45	3.30(5)	2
C45	C46	3.43(4)	2	C52	C52	3.42(6)	2
C54	C54	3.55(6)	2				

The ADC (atom designator code) specifies the position of an atom in a crystal. The 5-digit number shown in the table is a composite of three one-digit numbers and one two-digit number: TA (first digit) + TB (second digit) + TC (third digit) + SN (last two digits). TA, TB and TC are the crystal lattice translation digits along cell edges a, b and c. A translation digit of 5 indicates the origin unit cell. If TA = 4, this indicates a translation of one unit cell length along the a-axis in the negative direction. Each translation digit can range in value from 1 to 9 and thus ± 4 lattice translations from the origin (TA=5, TB=5, TC=5) can be represented.

The SN, or symmetry operator number, refers to the number of the symmetry operator used to generate the coordinates of the target atom. A list of symmetry operators relevant to this structure is given below.

For a given intermolecular contact, the first atom (origin atom) is located in the origin unit cell and its position can be generated using the identity operator (SN=1). Thus, the ADC for an origin atom is always 55501. The position of the second atom (target atom) can be generated using the ADC and the coordinates of the atom in the parameter table. For example, an ADC of 47502 refers to the target atom moved through symmetry operator two, then translated -1 cell translations along the a axis, +2 cell translations along the b axis, and 0 cell translations along the c axis.

An ADC of 1 indicates an intermolecular contact between two fragments (eg. cation and anion) that reside in the same asymmetric unit.

Symmetry Operators:

(1)	+X,	+Y,	+Z	(2)	-X,	+Y,	1/2-Z
(3)	-X,	-Y,	-Z	(4)	+X,	-Y,	1/2+Z
(5)	1/2+X,	1/2+Y,	+Z	(6)	1/2-X,	1/2+Y,	1/2-Z
(7)	1/2-X,	1/2-Y,	-Z	(8)	1/2+X,	1/2-Y,	1/2+Z

Chapter 5 Porphyrin Prism $3^{12+}\bullet(NO_3^-)_{12}$

Table 1. Crystal data and structure refinement for $3^{12+}\bullet(NO_3^-)_{12}$.

Identification code	$3^{12+}\bullet(NO_3^-)_{12}$	
Empirical formula	C138 H184 N48 O74 Pd6 Zn3	
Formula weight	4533.84	
Temperature	173(2) K	
Wavelength	0.71073 Å	
Crystal system	Triclinic	
Space group	P-1	
Unit cell dimensions	a = 20.6267(14) Å	α= 72.8840(10)°.
	b = 20.7442(14) Å	β= 74.0620(10)°.
	c = 28.1631(19) Å	γ = 66.2070(10)°.
Volume	10369.3(12) $Å^3$	
Z	2	
Density (calculated)	1.452 Mg/m^3	
Absorption coefficient	0.941 mm^{-1}	
F(000)	4612	
Crystal size	0.15 x 0.15 x 0.15 mm^3	
Theta range for data collection	1.10 to 25.00°.	
Index ranges	-24<=h<=24, -21<=k<=24, -33<=l<=33	
Reflections collected	55466	
Independent reflections	36032 [R(int) = 0.0367]	
Completeness to theta = 25.00°	98.6 %	
Max. and min. transmission	0.8717 and 0.8717	
Refinement method	Full-matrix-block least-squares on F^2	
Data / restraints / parameters	36032 / 330 / 1964	
Goodness-of-fit on F^2	1.932	
Final R indices [I>2sigma(I)]	R1 = 0.1068, wR2 = 0.2985	
R indices (all data)	R1 = 0.1578, wR2 = 0.3176	
Largest diff. peak and hole	2.804 and -5.376 $e.Å^{-3}$	

Table 2. Atomic coordinates (x 10^4) and equivalent isotropic displacement parameters ($Å^2$x 10^3) for $3^{12+}\cdot(NO_3^-)_{12}$. U(eq) is defined as one third of the trace of the orthogonalized U^{ij} tensor.

	x	y	z	U(eq)
Pd(1)	9019(1)	6799(1)	-459(1)	33(1)
Pd(2)	1903(1)	8180(1)	182(1)	33(1)
Pd(3)	9813(1)	4998(1)	-3295(1)	47(1)
Pd(4)	2753(1)	6317(1)	-2783(1)	44(1)
Pd(5)	8803(1)	9926(1)	-3676(1)	54(1)
Pd(6)	1825(1)	10943(1)	-2978(1)	52(1)
Zn(1)	5917(1)	8188(1)	-4016(1)	43(1)
Zn(2)	5971(1)	5649(1)	-1080(1)	27(1)
Zn(3)	5113(1)	10048(1)	-1386(1)	69(1)
N(11A)	7072(4)	5246(4)	-1126(3)	32(2)
N(12A)	8508(4)	6095(4)	-102(3)	29(2)
C(10A)	7588(5)	4902(5)	-1494(4)	31(2)
C(11A)	8282(5)	4682(5)	-1379(4)	36(2)
C(12A)	8202(5)	4883(5)	-946(4)	35(2)
C(13A)	7435(5)	5251(5)	-795(4)	30(2)
C(14A)	7138(5)	5559(5)	-375(4)	31(2)
C(15A)	7631(5)	5597(5)	-89(4)	29(2)
C(16A)	8062(5)	6016(5)	-339(4)	32(2)
C(17A)	7659(6)	5272(6)	402(4)	37(3)
C(18A)	8106(6)	5370(5)	658(4)	37(2)
C(19A)	8528(5)	5772(5)	372(4)	38(3)
N(21A)	6107(4)	5212(4)	-1691(3)	29(2)
N(22A)	9110(5)	4500(5)	-2906(4)	44(2)
C(20A)	5578(6)	5189(6)	-1877(4)	38(3)
C(21A)	5871(6)	4966(7)	-2363(4)	47(3)
C(22A)	6599(6)	4818(7)	-2440(4)	50(3)
C(23A)	6742(5)	4963(6)	-2009(4)	37(2)
C(24A)	7431(5)	4803(6)	-1915(4)	37(2)
C(25A)	8069(5)	4445(6)	-2287(4)	36(2)
C(26A)	8539(5)	4796(6)	-2559(4)	36(2)
C(27A)	8192(6)	3762(7)	-2369(5)	49(3)
C(28A)	8756(7)	3464(9)	-2699(5)	70(4)
C(29A)	9206(6)	3858(7)	-2981(5)	52(3)
N(31A)	4920(4)	5700(4)	-898(3)	28(2)
N(32A)	3432(5)	5565(5)	-2327(3)	41(2)
C(30A)	4426(5)	5893(5)	-484(4)	30(2)
C(31A)	3748(5)	5832(5)	-482(4)	33(2)
C(32A)	3847(5)	5627(5)	-918(4)	35(3)
C(33A)	4560(5)	5541(5)	-1177(4)	29(2)
C(34A)	4852(5)	5325(5)	-1628(4)	33(2)
C(35A)	4383(6)	5158(6)	-1856(4)	43(3)
C(36A)	3895(5)	5694(6)	-2147(4)	37(2)
C(37A)	4382(9)	4464(7)	-1744(6)	81(5)
C(38A)	3897(9)	4325(8)	-1940(7)	95(6)
C(39A)	3434(8)	4894(7)	-2217(6)	72(5)
N(41A)	5857(4)	5798(4)	-356(3)	28(2)
N(42A)	2708(4)	7270(4)	440(3)	31(2)
C(40A)	6385(5)	5846(5)	-177(4)	29(2)
C(41A)	6075(5)	6215(5)	230(4)	35(2)
C(42A)	5354(6)	6376(6)	302(4)	40(3)

C(43A)	5222(5)	6102(5)	-60(4)	30(2)
C(44A)	4540(5)	6137(5)	-100(4)	28(2)
C(45A)	3908(5)	6431(5)	265(4)	29(2)
C(46A)	3310(5)	6970(5)	121(4)	30(2)
C(47A)	3895(5)	6189(5)	781(4)	37(3)
C(48A)	3298(5)	6498(6)	1126(4)	37(2)
C(49A)	2696(5)	7031(5)	942(4)	38(3)
N(11B)	5134(4)	9390(5)	-687(4)	44(2)
N(12B)	8124(4)	7593(4)	-228(3)	36(2)
C(10B)	4579(6)	9209(6)	-375(5)	49(3)
C(11B)	4842(6)	8632(7)	48(5)	54(3)
C(12B)	5551(6)	8467(6)	-23(5)	53(3)
C(13B)	5737(6)	8960(6)	-480(4)	44(3)
C(14B)	6441(6)	8973(5)	-674(4)	39(3)
C(15B)	6991(6)	8536(6)	-352(4)	42(3)
C(16B)	7596(6)	7995(6)	-511(4)	38(3)
C(17B)	6904(6)	8645(6)	126(4)	45(3)
C(18B)	7414(7)	8238(6)	418(4)	50(3)
C(19B)	8044(6)	7713(6)	226(4)	42(3)
N(21B)	6190(5)	9825(4)	-1477(3)	37(2)
N(22B)	7975(5)	10647(5)	-3318(4)	45(2)
C(20B)	6644(6)	9382(6)	-1136(4)	38(3)
C(21B)	7358(6)	9422(6)	-1328(4)	42(3)
C(22B)	7324(5)	9897(6)	-1783(4)	38(3)
C(23B)	6607(6)	10122(5)	-1876(4)	36(2)
C(24B)	6364(6)	10623(5)	-2311(4)	36(2)
C(25B)	6895(6)	10902(6)	-2703(4)	43(3)
C(26B)	7470(6)	10441(6)	-2957(4)	41(3)
C(27B)	6846(7)	11609(6)	-2812(5)	55(3)
C(28B)	7352(7)	11834(7)	-3172(5)	60(4)
C(29B)	7901(8)	11348(7)	-3421(5)	63(4)
N(31B)	5074(5)	10742(5)	-2072(3)	42(2)
N(32B)	2348(4)	11487(5)	-2833(3)	40(2)
C(30B)	5658(6)	10872(6)	-2391(4)	44(3)
C(31B)	5429(7)	11345(6)	-2879(5)	59(4)
C(32B)	4715(6)	11445(7)	-2820(5)	57(3)
C(33B)	4492(6)	11075(6)	-2319(4)	41(3)
C(34B)	3809(6)	11065(5)	-2127(4)	37(3)
C(35B)	3277(6)	11472(6)	-2441(4)	40(3)
C(36B)	2856(5)	11141(6)	-2539(4)	39(3)
C(37B)	3103(6)	12224(6)	-2640(5)	51(3)
C(38B)	2572(6)	12565(6)	-2953(5)	55(3)
C(39B)	2209(6)	12184(6)	-3038(4)	46(3)
N(41B)	4028(4)	10250(4)	-1283(3)	36(2)
N(42B)	2430(4)	8750(4)	303(3)	29(2)
C(40B)	3585(5)	10705(5)	-1628(4)	37(2)
C(41B)	2867(6)	10745(5)	-1404(4)	38(3)
C(42B)	2865(6)	10331(5)	-923(4)	38(3)
C(43B)	3599(6)	10023(6)	-870(4)	36(2)
C(44B)	3844(6)	9532(6)	-432(4)	39(3)
C(45B)	3308(5)	9309(5)	-10(4)	35(2)
C(46B)	2887(5)	8981(5)	-75(4)	32(2)
C(47B)	3210(7)	9414(7)	482(5)	55(3)
C(48B)	2736(7)	9172(6)	859(4)	46(3)
C(49B)	2358(6)	8858(6)	759(4)	42(3)

N(11C)	6988(5)	8076(5)	-4215(3)	45(2)
N(12C)	8178(5)	10084(5)	-4182(4)	48(2)
C(10C)	7556(6)	7428(7)	-4246(4)	46(3)
C(11C)	8235(7)	7555(8)	-4384(5)	61(4)
C(12C)	8076(6)	8278(7)	-4423(4)	50(3)
C(13C)	7285(7)	8586(7)	-4314(4)	50(3)
C(14C)	6888(6)	9323(6)	-4325(5)	46(3)
C(15C)	7335(7)	9784(7)	-4421(4)	49(3)
C(16C)	7755(6)	9695(6)	-4092(4)	43(3)
C(17C)	7385(9)	10306(8)	-4892(5)	70(4)
C(18C)	7803(9)	10667(8)	-4971(5)	73(4)
C(19C)	8235(7)	10559(7)	-4603(5)	63(4)
N(21C)	6193(5)	7126(5)	-4088(3)	42(2)
N(22C)	9256(5)	5354(6)	-3866(4)	53(3)
C(20C)	5721(6)	6792(6)	-3988(4)	48(3)
C(21C)	6120(7)	6016(7)	-3913(5)	52(3)
C(22C)	6818(7)	5921(8)	-3978(5)	56(3)
C(23C)	6853(6)	6637(6)	-4092(4)	41(3)
C(24C)	7503(6)	6749(6)	-4170(4)	43(3)
C(25C)	8193(6)	6139(7)	-4214(4)	48(3)
C(26C)	8637(6)	5912(6)	-3855(4)	47(3)
C(27C)	8411(6)	5768(7)	-4593(4)	55(3)
C(28C)	9068(7)	5176(8)	-4606(5)	63(4)
C(29C)	9479(6)	4982(7)	-4235(4)	51(3)
N(31C)	4874(5)	8360(5)	-4059(3)	42(2)
N(32C)	3583(5)	6250(5)	-3382(3)	41(2)
C(30C)	4305(6)	9009(7)	-4078(4)	47(3)
C(31C)	3655(6)	8897(7)	-4067(4)	50(3)
C(32C)	3827(6)	8193(6)	-4028(4)	45(3)
C(33C)	4582(6)	7847(6)	-4015(4)	43(3)
C(34C)	4969(6)	7125(6)	-3969(4)	43(3)
C(35C)	4539(6)	6653(6)	-3886(4)	41(3)
C(36C)	4008(6)	6638(6)	-3464(4)	41(3)
C(37C)	4658(7)	6226(7)	-4219(5)	55(3)
C(38C)	4228(8)	5816(8)	-4131(5)	66(4)
C(39C)	3687(7)	5854(7)	-3717(5)	59(3)
N(41C)	5690(5)	9276(5)	-4212(4)	48(2)
N(42C)	2513(5)	10871(6)	-3645(4)	52(3)
C(40C)	6179(7)	9627(7)	-4286(5)	53(3)
C(41C)	5730(7)	10429(8)	-4305(6)	73(4)
C(42C)	5072(9)	10500(8)	-4245(6)	79(5)
C(43C)	4998(7)	9807(6)	-4201(5)	50(3)
C(44C)	4361(6)	9679(7)	-4137(5)	48(3)
C(45C)	3662(7)	10303(6)	-4113(5)	48(3)
C(46C)	3145(6)	10335(7)	-3672(4)	47(3)
C(47C)	3494(7)	10870(7)	-4545(5)	56(3)
C(48C)	2838(8)	11424(8)	-4496(6)	71(4)
C(49C)	2366(7)	11414(7)	-4055(5)	59(3)
N(1A)	9537(5)	7486(5)	-824(4)	49(2)
N(2A)	9949(5)	6036(5)	-667(4)	47(2)
C(1A)	10345(6)	7060(6)	-915(6)	64(4)
C(2A)	10415(7)	6399(7)	-1066(6)	66(4)
N(1B)	1096(5)	9083(5)	-55(4)	47(2)
N(2B)	1326(5)	7660(5)	48(4)	48(3)
C(2B)	807(7)	8178(7)	-279(6)	64(4)

C(1B)	483(7)	8898(6)	-95(6)	62(4)
N(1C)	10573(6)	5434(8)	-3664(5)	87(4)
N(2C)	10386(5)	4636(6)	-2729(4)	58(3)
C(2C)	11101(7)	4712(9)	-2946(6)	74(4)
C(1C)	10943(9)	5449(10)	-3275(7)	89(5)
N(2D)	1897(5)	6447(6)	-2219(4)	63(3)
N(1D)	2036(6)	7017(6)	-3228(4)	63(3)
C(1D)	1294(7)	7111(10)	-2935(6)	88(6)
C(2D)	1274(8)	7045(10)	-2411(7)	98(6)
N(1E)	9664(6)	9196(8)	-4005(5)	92(5)
N(2E)	9466(6)	9755(8)	-3202(5)	84(4)
C(1E)	10285(8)	9008(9)	-3757(7)	88(5)
C(2E)	10126(11)	9178(19)	-3313(11)	202(18)
N(1F)	1141(5)	10959(6)	-2303(4)	58(3)
N(2F)	1261(6)	10395(8)	-3072(5)	87(4)
C(1F)	561(8)	10746(9)	-2300(6)	80(5)
C(2F)	856(9)	10149(10)	-2592(7)	90(5)
O(1A)	5813(6)	7985(6)	-3232(4)	90(3)
O(2A)	5833(5)	6714(4)	-1472(4)	72(3)
O(3A)	5323(10)	9058(9)	-1770(7)	172(7)
O(4A)	4925(11)	11073(10)	-1058(8)	179(8)
N(100)	-70(6)	4060(6)	-598(4)	65(3)
O(101)	112(7)	3445(6)	-342(5)	103(4)
O(102)	-276(5)	4573(5)	-389(3)	63(2)
O(103)	-19(7)	4118(6)	-1063(4)	105(4)
N(200)	-30(20)	-872(16)	4825(12)	350(20)
O(201)	432(14)	-1101(13)	4461(9)	248(11)
O(202)	-240(30)	-1330(20)	5138(16)	610(50)
O(203)	24(15)	-351(12)	4944(9)	228(11)
N(300)	7038(8)	5717(7)	3138(6)	101(5)
O(301)	6808(11)	5815(10)	3577(6)	189(8)
O(302)	6852(9)	6240(8)	2811(6)	141(5)
O(303)	7356(6)	5101(6)	3082(4)	87(3)
N(400)	11217(7)	975(6)	184(5)	80(4)
O(401)	10887(7)	1585(6)	-16(5)	109(4)
O(402)	11308(8)	924(7)	607(5)	130(5)
O(403)	11371(5)	419(5)	39(4)	74(3)
N(500)	7888(7)	3388(7)	891(4)	78(4)
O(501)	8022(7)	3627(6)	442(4)	100(4)
O(502)	7835(9)	2803(8)	998(6)	148(6)
O(503)	7810(5)	3742(5)	1206(4)	73(3)
N(600)	-212(6)	7055(5)	2172(4)	58(3)
O(601)	-655(5)	6932(5)	2553(4)	78(3)
O(602)	159(5)	6586(5)	1931(3)	63(2)
O(603)	-152(6)	7665(5)	2033(4)	87(3)
N(800)	1066(12)	1689(13)	2004(9)	202(11)
O(801)	445(12)	1958(14)	1947(10)	267(13)
O(802)	1420(14)	2060(16)	1752(11)	317(16)
O(803)	1241(10)	1234(10)	2407(7)	172(7)
N(900)	11976(12)	-520(14)	-1407(8)	221(12)
O(901)	12308(9)	-337(8)	-1841(6)	145(6)
O(902)	12393(11)	-965(12)	-1124(8)	214(9)
O(903)	11375(12)	-121(14)	-1199(9)	266(12)
N(110)	-1420(11)	6340(10)	4043(8)	158(8)
O(111)	-1801(10)	6860(9)	4243(7)	170(7)

O(112)	-857(10)	6381(11)	3796(8)	196(8)
O(113)	-1485(10)	5741(10)	4234(8)	188(8)
N(120)	8028(6)	1153(6)	3620(4)	65(3)
O(121)	8100(5)	518(5)	3827(4)	77(3)
O(122)	8100(7)	1333(6)	3172(4)	103(4)
O(123)	7859(5)	1624(5)	3864(4)	74(3)
N(130)	6706(5)	12802(5)	-2111(3)	50
O(131)	6013(8)	13133(11)	-2146(8)	221(9)
O(132)	7175(7)	12931(7)	-2401(5)	117(4)
O(133)	6695(4)	12342(4)	-1701(3)	50
O(1W)	1224(13)	3569(13)	1545(10)	235(10)
O(2W)	8566(6)	4776(6)	1858(4)	91(3)
O(3W)	55(11)	4634(10)	1794(8)	179(7)
O(4W)	8922(5)	1973(5)	-1512(3)	64(2)
O(5W)	9769(4)	2666(4)	-895(3)	55(2)
O(6W)	8130(20)	2160(20)	1785(15)	355(18)
O(7W)	9335(9)	-203(9)	-1364(6)	150(6)
O(8W)	10853(11)	1348(11)	-1002(8)	182(7)
O(9W)	10774(11)	-1999(11)	3239(8)	188(8)
O(10W)	12991(13)	-3749(13)	3287(10)	236(10)
O(11W)	4383(14)	5766(13)	4513(10)	236(10)
O(12W)	6920(20)	2180(20)	1048(14)	341(17)
O(13W)	9651(5)	652(5)	-952(4)	77(3)
O(14W)	516(18)	2338(18)	3650(13)	318(16)
O(15W)	6812(15)	2231(15)	2542(11)	262(12)
O(16W)	7884(10)	3436(9)	4133(7)	160(6)
O(17W)	5790(20)	2480(20)	1588(18)	430(20)
O(18W)	9447(11)	-2358(11)	3377(8)	186(8)
O(19W)	5446(14)	12465(13)	-1309(10)	239(11)
O(20W)	1493(8)	-1790(8)	2307(6)	126(5)
O(21W)	1152(9)	-395(9)	2301(7)	156(6)
O(22W)	869(18)	4027(18)	2267(13)	324(16)
O(23W)	10353(14)	-1267(14)	-1799(10)	245(11)
O(24W)	7424(12)	4693(12)	4304(9)	207(9)
O(25W)	2374(16)	1375(16)	2853(11)	275(13)
O(27W)	5240(20)	3280(20)	5555(16)	378(19)
O(26W)	4860(20)	460(30)	2814(18)	440(20)
O(28W)	6094(16)	2255(16)	5690(12)	284(13)
O(29W)	6940(20)	840(20)	2590(16)	390(20)
O(30W)	9929(13)	-858(13)	3612(9)	229(10)
O(31W)	11754(19)	-3188(19)	3909(13)	327(16)
O(11S)	-2340(11)	6132(11)	1883(8)	175(7)
C(10S)	-2180(20)	6760(20)	1582(16)	240(17)
C(11S)	-1550(13)	6871(13)	1679(9)	142(9)
O(21S)	5910(14)	-2915(13)	3881(10)	229(10)
C(21S)	6270(20)	-2680(20)	4174(17)	236(16)
C(22S)	6222(15)	-2765(16)	4695(11)	175(11)
O(31S)	4216(14)	5719(14)	3549(10)	237(10)
C(31S)	4865(16)	5834(15)	3184(11)	158(10)
C(32S)	4929(19)	6619(19)	3138(14)	235(16)

Table 3. Bond lengths [Å and angles [°] for $3^{12+}\bullet(NO_3^-)_{12}$.

Pd(1)-N(1A)	1.997(9)
Pd(1)-N(2A)	2.001(9)
Pd(1)-N(12A)	2.013(8)
Pd(1)-N(12B)	2.015(9)
Pd(2)-N(1B)	2.020(9)
Pd(2)-N(42B)	2.043(8)
Pd(2)-N(42A)	2.043(8)
Pd(2)-N(2B)	2.061(9)
Pd(3)-N(22A)	2.010(9)
Pd(3)-N(1C)	2.013(11)
Pd(3)-N(22C)	2.019(10)
Pd(3)-N(2C)	2.029(10)
Pd(4)-N(2D)	2.012(11)
Pd(4)-N(32A)	2.023(9)
Pd(4)-N(1D)	2.021(10)
Pd(4)-N(32C)	2.038(10)
Pd(5)-N(22B)	2.012(10)
Pd(5)-N(1E)	2.014(12)
Pd(5)-N(2E)	2.027(12)
Pd(5)-N(12C)	2.049(10)
Pd(6)-N(42C)	2.023(10)
Pd(6)-N(32B)	2.025(9)
Pd(6)-N(2F)	2.031(11)
Pd(6)-N(1F)	2.033(10)
Zn(1)-N(41C)	2.042(10)
Zn(1)-N(11C)	2.058(9)
Zn(1)-N(31C)	2.067(9)
Zn(1)-O(1A)	2.088(10)
Zn(1)-N(21C)	2.101(9)
Zn(2)-N(31A)	2.052(7)
Zn(2)-N(11A)	2.060(8)
Zn(2)-N(21A)	2.076(8)
Zn(2)-N(41A)	2.086(8)
Zn(2)-O(2A)	2.100(8)
Zn(3)-N(21B)	2.037(9)
Zn(3)-N(31B)	2.040(9)
Zn(3)-N(11B)	2.041(9)
Zn(3)-N(41B)	2.056(8)
Zn(3)-O(4A)	2.414(15)
Zn(3)-O(3A)	2.430(18)
N(11A)-C(13A)	1.350(12)
N(11A)-C(10A)	1.389(12)
N(12A)-C(19A)	1.310(13)
N(12A)-C(16A)	1.357(11)
C(10A)-C(24A)	1.400(14)
C(10A)-C(11A)	1.414(13)
C(11A)-C(12A)	1.351(14)
C(12A)-C(13A)	1.453(14)
C(13A)-C(14A)	1.384(14)
C(14A)-C(40A)	1.433(14)
C(14A)-C(15A)	1.498(13)
C(15A)-C(17A)	1.354(14)
C(15A)-C(16A)	1.400(13)
C(17A)-C(18A)	1.418(14)
C(18A)-C(19A)	1.381(14)
N(21A)-C(20A)	1.357(12)
N(21A)-C(23A)	1.367(13)
N(22A)-C(29A)	1.336(14)
N(22A)-C(26A)	1.362(13)
C(20A)-C(34A)	1.418(14)
C(20A)-C(21A)	1.464(15)
C(21A)-C(22A)	1.372(15)
C(22A)-C(23A)	1.461(15)
C(23A)-C(24A)	1.405(14)
C(24A)-C(25A)	1.515(14)
C(25A)-C(26A)	1.375(14)
C(25A)-C(27A)	1.412(16)
C(27A)-C(28A)	1.329(17)
C(28A)-C(29A)	1.409(17)
N(31A)-C(30A)	1.362(13)
N(31A)-C(33A)	1.397(12)
N(32A)-C(39A)	1.333(15)
N(32A)-C(36A)	1.337(12)
C(30A)-C(44A)	1.426(14)
C(30A)-C(31A)	1.452(13)
C(31A)-C(32A)	1.353(15)
C(32A)-C(33A)	1.414(14)
C(33A)-C(34A)	1.369(14)
C(34A)-C(35A)	1.487(13)
C(35A)-C(37A)	1.381(17)
C(35A)-C(36A)	1.392(14)
C(37A)-C(38A)	1.422(17)
C(38A)-C(39A)	1.368(17)
N(41A)-C(43A)	1.361(12)
N(41A)-C(40A)	1.366(11)
N(42A)-C(49A)	1.349(13)
N(42A)-C(46A)	1.352(12)
C(40A)-C(41A)	1.424(14)
C(41A)-C(42A)	1.356(14)
C(42A)-C(43A)	1.431(14)
C(43A)-C(44A)	1.415(13)
C(44A)-C(45A)	1.457(13)
C(45A)-C(46A)	1.354(13)
C(45A)-C(47A)	1.387(14)
C(47A)-C(48A)	1.394(14)
C(48A)-C(49A)	1.394(14)
N(11B)-C(10B)	1.349(14)
N(11B)-C(13B)	1.370(13)
N(12B)-C(19B)	1.329(14)
N(12B)-C(16B)	1.368(12)
C(10B)-C(44B)	1.423(15)
C(10B)-C(11B)	1.464(15)
C(11B)-C(12B)	1.332(15)
C(12B)-C(13B)	1.455(15)

C(13B)-C(14B)	1.412(15)	C(12C)-C(13C)	1.471(17)
C(14B)-C(20B)	1.389(15)	C(13C)-C(14C)	1.409(17)
C(14B)-C(15B)	1.476(14)	C(14C)-C(40C)	1.326(17)
C(15B)-C(16B)	1.370(15)	C(14C)-C(15C)	1.502(16)
C(15B)-C(17B)	1.382(16)	C(15C)-C(16C)	1.362(15)
C(17B)-C(18B)	1.360(15)	C(15C)-C(17C)	1.454(18)
C(18B)-C(19B)	1.409(16)	C(17C)-C(18C)	1.294(19)
N(21B)-C(23B)	1.367(13)	C(18C)-C(19C)	1.46(2)
N(21B)-C(20B)	1.386(13)	N(21C)-C(23C)	1.329(14)
N(22B)-C(26B)	1.350(14)	N(21C)-C(20C)	1.337(14)
N(22B)-C(29B)	1.349(15)	N(22C)-C(26C)	1.333(15)
C(20B)-C(21B)	1.451(14)	N(22C)-C(29C)	1.346(15)
C(21B)-C(22B)	1.365(15)	C(20C)-C(34C)	1.413(16)
C(22B)-C(23B)	1.435(14)	C(20C)-C(21C)	1.463(17)
C(23B)-C(24B)	1.414(14)	C(21C)-C(22C)	1.340(17)
C(24B)-C(30B)	1.396(15)	C(22C)-C(23C)	1.451(17)
C(24B)-C(25B)	1.490(15)	C(23C)-C(24C)	1.400(15)
C(25B)-C(26B)	1.361(16)	C(24C)-C(25C)	1.478(17)
C(25B)-C(27B)	1.375(16)	C(25C)-C(27C)	1.368(17)
C(27B)-C(28B)	1.367(17)	C(25C)-C(26C)	1.401(16)
C(28B)-C(29B)	1.361(18)	C(27C)-C(28C)	1.414(18)
N(31B)-C(30B)	1.362(13)	C(28C)-C(29C)	1.391(18)
N(31B)-C(33B)	1.381(13)	N(31C)-C(33C)	1.381(14)
N(32B)-C(39B)	1.330(14)	N(31C)-C(30C)	1.382(14)
N(32B)-C(36B)	1.347(13)	N(32C)-C(39C)	1.349(16)
C(30B)-C(31B)	1.503(15)	N(32C)-C(36C)	1.348(14)
C(31B)-C(32B)	1.370(17)	C(30C)-C(44C)	1.399(17)
C(32B)-C(33B)	1.445(16)	C(30C)-C(31C)	1.441(16)
C(33B)-C(34B)	1.371(15)	C(31C)-C(32C)	1.334(17)
C(34B)-C(35B)	1.430(13)	C(32C)-C(33C)	1.434(16)
C(34B)-C(40B)	1.432(15)	C(33C)-C(34C)	1.370(16)
C(35B)-C(37B)	1.421(15)	C(34C)-C(35C)	1.498(15)
C(35B)-C(36B)	1.424(15)	C(35C)-C(36C)	1.379(16)
C(37B)-C(38B)	1.420(16)	C(35C)-C(37C)	1.384(17)
C(38B)-C(39B)	1.391(17)	C(37C)-C(38C)	1.392(17)
N(41B)-C(43B)	1.344(13)	C(38C)-C(39C)	1.370(19)
N(41B)-C(40B)	1.384(12)	N(41C)-C(40C)	1.407(15)
N(42B)-C(49B)	1.327(13)	N(41C)-C(43C)	1.408(15)
N(42B)-C(46B)	1.328(12)	N(42C)-C(46C)	1.330(14)
C(40B)-C(41B)	1.420(14)	N(42C)-C(49C)	1.359(16)
C(41B)-C(42B)	1.374(14)	C(40C)-C(41C)	1.537(19)
C(42B)-C(43B)	1.417(14)	C(41C)-C(42C)	1.271(19)
C(43B)-C(44B)	1.415(14)	C(42C)-C(43C)	1.473(19)
C(44B)-C(45B)	1.489(15)	C(43C)-C(44C)	1.397(17)
C(45B)-C(46B)	1.372(14)	C(44C)-C(45C)	1.500(16)
C(45B)-C(47B)	1.413(16)	C(45C)-C(46C)	1.395(16)
C(47B)-C(48B)	1.361(16)	C(45C)-C(47C)	1.430(17)
C(48B)-C(49B)	1.322(15)	C(47C)-C(48C)	1.379(18)
N(11C)-C(13C)	1.351(15)	C(48C)-C(49C)	1.352(19)
N(11C)-C(10C)	1.389(15)	N(1A)-C(1A)	1.528(15)
N(12C)-C(19C)	1.311(16)	N(2A)-C(2A)	1.498(16)
N(12C)-C(16C)	1.343(14)	C(1A)-C(2A)	1.493(18)
C(10C)-C(24C)	1.404(17)	N(1B)-C(1B)	1.502(15)
C(10C)-C(11C)	1.458(16)	N(2B)-C(2B)	1.476(15)
C(11C)-C(12C)	1.376(18)	C(2B)-C(1B)	1.549(18)

N(1C)-C(1C)	1.510(19)
N(2C)-C(2C)	1.486(16)
C(2C)-C(1C)	1.50(2)
N(2D)-C(2D)	1.478(17)
N(1D)-C(1D)	1.491(18)
C(1D)-C(2D)	1.43(2)
N(1E)-C(1E)	1.486(18)
N(2E)-C(2E)	1.43(2)
C(1E)-C(2E)	1.32(3)
N(1F)-C(1F)	1.431(17)
N(2F)-C(2F)	1.45(2)
C(1F)-C(2F)	1.52(2)
N(100)-O(101)	1.228(11)
N(100)-O(102)	1.235(10)
N(100)-O(103)	1.258(11)
N(200)-O(202)	1.219(16)
N(200)-O(201)	1.253(16)
N(200)-O(203)	1.276(15)
O(203)-O(203)#1	1.54(4)
N(300)-O(302)	1.202(12)
N(300)-O(303)	1.214(11)
N(300)-O(301)	1.242(13)
N(400)-O(401)	1.214(11)
N(400)-O(403)	1.228(10)
N(400)-O(402)	1.225(12)
N(500)-O(502)	1.205(12)
N(500)-O(501)	1.213(11)
N(500)-O(503)	1.248(11)
N(600)-O(602)	1.221(10)
N(600)-O(601)	1.241(10)
N(600)-O(603)	1.257(10)
N(800)-O(801)	1.210(15)
N(800)-O(802)	1.214(15)
N(800)-O(803)	1.276(14)
N(900)-O(902)	1.236(15)
N(900)-O(901)	1.259(14)
N(900)-O(903)	1.275(14)
N(110)-O(112)	1.201(14)
N(110)-O(111)	1.236(14)
N(110)-O(113)	1.245(13)
N(120)-O(122)	1.191(11)
N(120)-O(123)	1.237(10)
N(120)-O(121)	1.239(10)
N(130)-O(132)	1.150(11)
N(130)-O(133)	1.264(10)
N(130)-O(131)	1.330(13)
O(11S)-C(10S)	1.43(4)
C(10S)-C(11S)	1.51(4)
O(21S)-C(21S)	1.52(4)
C(21S)-C(22S)	1.41(4)
O(31S)-C(31S)	1.51(3)
C(31S)-C(32S)	1.65(4)
N(1A)-Pd(1)-N(2A)	85.2(4)
N(1A)-Pd(1)-N(12A)	178.9(4)
N(2A)-Pd(1)-N(12A)	93.9(3)
N(1A)-Pd(1)-N(12B)	92.3(4)
N(2A)-Pd(1)-N(12B)	175.7(3)
N(12A)-Pd(1)-N(12B)	88.7(3)
N(1B)-Pd(2)-N(42B)	92.7(3)
N(1B)-Pd(2)-N(42A)	178.5(4)
N(42B)-Pd(2)-N(42A)	87.0(3)
N(1B)-Pd(2)-N(2B)	84.0(4)
N(42B)-Pd(2)-N(2B)	176.8(3)
N(42A)-Pd(2)-N(2B)	96.3(3)
N(22A)-Pd(3)-N(1C)	175.9(5)
N(22A)-Pd(3)-N(22C)	87.1(4)
N(1C)-Pd(3)-N(22C)	96.1(4)
N(22A)-Pd(3)-N(2C)	93.5(4)
N(1C)-Pd(3)-N(2C)	83.3(4)
N(22C)-Pd(3)-N(2C)	179.2(4)
N(2D)-Pd(4)-N(32A)	93.2(4)
N(2D)-Pd(4)-N(1D)	84.9(4)
N(32A)-Pd(4)-N(1D)	175.7(4)
N(2D)-Pd(4)-N(32C)	176.2(4)
N(32A)-Pd(4)-N(32C)	90.4(4)
N(1D)-Pd(4)-N(32C)	91.5(4)
N(22B)-Pd(5)-N(1E)	176.8(4)
N(22B)-Pd(5)-N(2E)	93.1(4)
N(1E)-Pd(5)-N(2E)	83.8(5)
N(22B)-Pd(5)-N(12C)	89.5(4)
N(1E)-Pd(5)-N(12C)	93.7(4)
N(2E)-Pd(5)-N(12C)	177.1(4)
N(42C)-Pd(6)-N(32B)	88.1(4)
N(42C)-Pd(6)-N(2F)	96.0(5)
N(32B)-Pd(6)-N(2F)	175.9(4)
N(42C)-Pd(6)-N(1F)	177.0(4)
N(32B)-Pd(6)-N(1F)	94.1(4)
N(2F)-Pd(6)-N(1F)	81.8(5)
N(41C)-Zn(1)-N(11C)	87.2(4)
N(41C)-Zn(1)-N(31C)	89.2(4)
N(11C)-Zn(1)-N(31C)	161.9(4)
N(41C)-Zn(1)-O(1A)	102.2(4)
N(11C)-Zn(1)-O(1A)	99.1(4)
N(31C)-Zn(1)-O(1A)	99.0(4)
N(41C)-Zn(1)-N(21C)	159.9(4)
N(11C)-Zn(1)-N(21C)	89.6(4)
N(31C)-Zn(1)-N(21C)	87.8(4)
O(1A)-Zn(1)-N(21C)	97.8(4)
N(31A)-Zn(2)-N(11A)	160.5(3)
N(31A)-Zn(2)-N(21A)	88.7(3)
N(11A)-Zn(2)-N(21A)	89.1(3)
N(31A)-Zn(2)-N(41A)	87.7(3)
N(11A)-Zn(2)-N(41A)	89.1(3)
N(21A)-Zn(2)-N(41A)	164.1(3)
N(31A)-Zn(2)-O(2A)	99.9(4)
N(11A)-Zn(2)-O(2A)	99.6(4)
N(21A)-Zn(2)-O(2A)	97.9(4)
N(41A)-Zn(2)-O(2A)	98.0(3)
N(21B)-Zn(3)-N(31B)	90.8(3)

N(21B)-Zn(3)-N(11B)	89.6(3)	C(26A)-C(25A)-C(27A)	118.8(10)
N(31B)-Zn(3)-N(11B)	177.7(4)	C(26A)-C(25A)-C(24A)	119.3(10)
N(21B)-Zn(3)-N(41B)	178.7(4)	C(27A)-C(25A)-C(24A)	121.9(10)
N(31B)-Zn(3)-N(41B)	90.4(3)	N(22A)-C(26A)-C(25A)	121.2(10)
N(11B)-Zn(3)-N(41B)	89.2(3)	C(28A)-C(27A)-C(25A)	120.4(12)
N(21B)-Zn(3)-O(4A)	87.6(5)	C(27A)-C(28A)-C(29A)	118.5(13)
N(31B)-Zn(3)-O(4A)	85.6(6)	N(22A)-C(29A)-C(28A)	122.3(11)
N(11B)-Zn(3)-O(4A)	92.2(6)	C(30A)-N(31A)-C(33A)	105.2(7)
N(41B)-Zn(3)-O(4A)	93.1(5)	C(30A)-N(31A)-Zn(2)	127.9(6)
N(21B)-Zn(3)-O(3A)	91.4(5)	C(33A)-N(31A)-Zn(2)	126.9(7)
N(31B)-Zn(3)-O(3A)	91.0(5)	C(39A)-N(32A)-C(36A)	118.4(9)
N(11B)-Zn(3)-O(3A)	91.3(5)	C(39A)-N(32A)-Pd(4)	117.3(7)
N(41B)-Zn(3)-O(3A)	88.0(5)	C(36A)-N(32A)-Pd(4)	124.2(7)
O(4A)-Zn(3)-O(3A)	176.4(7)	N(31A)-C(30A)-C(44A)	125.4(8)
C(13A)-N(11A)-C(10A)	106.3(8)	N(31A)-C(30A)-C(31A)	111.2(9)
C(13A)-N(11A)-Zn(2)	126.4(7)	C(44A)-C(30A)-C(31A)	123.4(9)
C(10A)-N(11A)-Zn(2)	127.3(6)	C(32A)-C(31A)-C(30A)	104.9(9)
C(19A)-N(12A)-C(16A)	118.6(9)	C(31A)-C(32A)-C(33A)	109.1(9)
C(19A)-N(12A)-Pd(1)	121.9(6)	C(34A)-C(33A)-N(31A)	125.4(9)
C(16A)-N(12A)-Pd(1)	119.0(7)	C(34A)-C(33A)-C(32A)	125.1(9)
N(11A)-C(10A)-C(24A)	124.1(8)	N(31A)-C(33A)-C(32A)	109.5(9)
N(11A)-C(10A)-C(11A)	109.8(9)	C(33A)-C(34A)-C(20A)	126.0(9)
C(24A)-C(10A)-C(11A)	126.1(10)	C(33A)-C(34A)-C(35A)	117.0(9)
C(12A)-C(11A)-C(10A)	107.6(9)	C(20A)-C(34A)-C(35A)	116.8(9)
C(11A)-C(12A)-C(13A)	106.5(9)	C(37A)-C(35A)-C(36A)	118.2(10)
N(11A)-C(13A)-C(14A)	126.3(9)	C(37A)-C(35A)-C(34A)	119.7(10)
N(11A)-C(13A)-C(12A)	109.8(9)	C(36A)-C(35A)-C(34A)	121.9(10)
C(14A)-C(13A)-C(12A)	123.9(9)	N(32A)-C(36A)-C(35A)	123.0(10)
C(13A)-C(14A)-C(40A)	125.8(9)	C(35A)-C(37A)-C(38A)	118.8(11)
C(13A)-C(14A)-C(15A)	118.8(9)	C(39A)-C(38A)-C(37A)	118.1(12)
C(40A)-C(14A)-C(15A)	115.5(9)	N(32A)-C(39A)-C(38A)	123.4(11)
C(17A)-C(15A)-C(16A)	118.7(9)	C(43A)-N(41A)-C(40A)	106.6(8)
C(17A)-C(15A)-C(14A)	123.3(9)	C(43A)-N(41A)-Zn(2)	125.5(6)
C(16A)-C(15A)-C(14A)	117.9(9)	C(40A)-N(41A)-Zn(2)	124.4(6)
N(12A)-C(16A)-C(15A)	121.5(9)	C(49A)-N(42A)-C(46A)	118.6(8)
C(15A)-C(17A)-C(18A)	120.3(10)	C(49A)-N(42A)-Pd(2)	119.5(7)
C(19A)-C(18A)-C(17A)	116.4(9)	C(46A)-N(42A)-Pd(2)	121.0(7)
N(12A)-C(19A)-C(18A)	124.4(9)	N(41A)-C(40A)-C(41A)	110.2(8)
C(20A)-N(21A)-C(23A)	107.6(8)	N(41A)-C(40A)-C(14A)	124.0(9)
C(20A)-N(21A)-Zn(2)	126.5(7)	C(41A)-C(40A)-C(14A)	125.9(8)
C(23A)-N(21A)-Zn(2)	125.6(6)	C(42A)-C(41A)-C(40A)	106.4(9)
C(29A)-N(22A)-C(26A)	118.8(10)	C(41A)-C(42A)-C(43A)	107.4(9)
C(29A)-N(22A)-Pd(3)	119.7(7)	N(41A)-C(43A)-C(44A)	125.3(9)
C(26A)-N(22A)-Pd(3)	121.6(8)	N(41A)-C(43A)-C(42A)	109.4(8)
N(21A)-C(20A)-C(34A)	125.2(9)	C(44A)-C(43A)-C(42A)	125.4(9)
N(21A)-C(20A)-C(21A)	110.2(9)	C(43A)-C(44A)-C(30A)	123.7(9)
C(34A)-C(20A)-C(21A)	124.6(9)	C(43A)-C(44A)-C(45A)	119.7(9)
C(22A)-C(21A)-C(20A)	105.8(9)	C(30A)-C(44A)-C(45A)	116.7(8)
C(21A)-C(22A)-C(23A)	107.0(10)	C(46A)-C(45A)-C(47A)	116.2(9)
N(21A)-C(23A)-C(24A)	125.5(9)	C(46A)-C(45A)-C(44A)	122.0(9)
N(21A)-C(23A)-C(22A)	109.3(9)	C(47A)-C(45A)-C(44A)	121.7(9)
C(24A)-C(23A)-C(22A)	124.9(10)	C(45A)-C(46A)-N(42A)	125.0(9)
C(10A)-C(24A)-C(23A)	126.4(10)	C(45A)-C(47A)-C(48A)	121.0(9)
C(10A)-C(24A)-C(25A)	116.5(9)	C(47A)-C(48A)-C(49A)	118.5(9)
C(23A)-C(24A)-C(25A)	117.0(9)	N(42A)-C(49A)-C(48A)	120.6(9)

C(10B)-N(11B)-C(13B)	106.7(9)	N(31B)-C(30B)-C(31B)	108.5(10)
C(10B)-N(11B)-Zn(3)	126.4(7)	C(24B)-C(30B)-C(31B)	122.8(10)
C(13B)-N(11B)-Zn(3)	126.1(7)	C(32B)-C(31B)-C(30B)	105.4(11)
C(19B)-N(12B)-C(16B)	119.3(10)	C(31B)-C(32B)-C(33B)	108.4(10)
C(19B)-N(12B)-Pd(1)	117.6(7)	C(34B)-C(33B)-N(31B)	126.5(9)
C(16B)-N(12B)-Pd(1)	123.0(7)	C(34B)-C(33B)-C(32B)	124.5(10)
N(11B)-C(10B)-C(44B)	126.4(10)	N(31B)-C(33B)-C(32B)	109.0(10)
N(11B)-C(10B)-C(11B)	109.5(10)	C(33B)-C(34B)-C(35B)	117.3(9)
C(44B)-C(10B)-C(11B)	124.0(11)	C(33B)-C(34B)-C(40B)	124.5(9)
C(12B)-C(11B)-C(10B)	107.3(10)	C(35B)-C(34B)-C(40B)	118.1(9)
C(11B)-C(12B)-C(13B)	106.5(10)	C(37B)-C(35B)-C(34B)	122.9(11)
N(11B)-C(13B)-C(14B)	126.4(10)	C(37B)-C(35B)-C(36B)	116.5(10)
N(11B)-C(13B)-C(12B)	109.8(9)	C(34B)-C(35B)-C(36B)	120.4(10)
C(14B)-C(13B)-C(12B)	123.8(9)	N(32B)-C(36B)-C(35B)	123.9(10)
C(20B)-C(14B)-C(13B)	124.6(9)	C(35B)-C(37B)-C(38B)	117.6(11)
C(20B)-C(14B)-C(15B)	118.1(9)	C(39B)-C(38B)-C(37B)	121.0(11)
C(13B)-C(14B)-C(15B)	117.3(9)	N(32B)-C(39B)-C(38B)	121.4(10)
C(16B)-C(15B)-C(17B)	117.6(10)	C(43B)-N(41B)-C(40B)	106.5(8)
C(16B)-C(15B)-C(14B)	121.2(11)	C(43B)-N(41B)-Zn(3)	128.3(7)
C(17B)-C(15B)-C(14B)	121.1(11)	C(40B)-N(41B)-Zn(3)	125.1(7)
C(15B)-C(16B)-N(12B)	122.6(10)	C(49B)-N(42B)-C(46B)	119.1(9)
C(18B)-C(17B)-C(15B)	120.5(11)	C(49B)-N(42B)-Pd(2)	121.3(7)
C(17B)-C(18B)-C(19B)	119.6(11)	C(46B)-N(42B)-Pd(2)	119.5(7)
N(12B)-C(19B)-C(18B)	120.2(10)	N(41B)-C(40B)-C(41B)	108.2(9)
C(23B)-N(21B)-C(20B)	105.7(8)	N(41B)-C(40B)-C(34B)	126.3(9)
C(23B)-N(21B)-Zn(3)	126.7(7)	C(41B)-C(40B)-C(34B)	125.5(9)
C(20B)-N(21B)-Zn(3)	127.5(7)	C(42B)-C(41B)-C(40B)	108.7(9)
C(26B)-N(22B)-C(29B)	117.1(11)	C(41B)-C(42B)-C(43B)	104.6(10)
C(26B)-N(22B)-Pd(5)	120.7(7)	N(41B)-C(43B)-C(44B)	124.5(9)
C(29B)-N(22B)-Pd(5)	122.2(9)	N(41B)-C(43B)-C(42B)	112.1(9)
N(21B)-C(20B)-C(14B)	125.1(9)	C(44B)-C(43B)-C(42B)	123.3(10)
N(21B)-C(20B)-C(21B)	109.9(9)	C(43B)-C(44B)-C(10B)	124.2(10)
C(14B)-C(20B)-C(21B)	124.9(9)	C(43B)-C(44B)-C(45B)	118.5(9)
C(22B)-C(21B)-C(20B)	106.4(9)	C(10B)-C(44B)-C(45B)	117.3(9)
C(21B)-C(22B)-C(23B)	106.9(9)	C(46B)-C(45B)-C(47B)	116.1(10)
N(21B)-C(23B)-C(24B)	125.5(9)	C(46B)-C(45B)-C(44B)	122.0(10)
N(21B)-C(23B)-C(22B)	111.0(9)	C(47B)-C(45B)-C(44B)	121.8(10)
C(24B)-C(23B)-C(22B)	123.4(10)	N(42B)-C(46B)-C(45B)	122.7(10)
C(30B)-C(24B)-C(23B)	123.7(10)	C(48B)-C(47B)-C(45B)	119.6(11)
C(30B)-C(24B)-C(25B)	118.4(9)	C(49B)-C(48B)-C(47B)	119.6(11)
C(23B)-C(24B)-C(25B)	117.9(10)	C(48B)-C(49B)-N(42B)	122.8(11)
C(26B)-C(25B)-C(27B)	117.5(11)	C(13C)-N(11C)-C(10C)	106.6(10)
C(26B)-C(25B)-C(24B)	119.8(10)	C(13C)-N(11C)-Zn(1)	128.5(9)
C(27B)-C(25B)-C(24B)	122.7(11)	C(10C)-N(11C)-Zn(1)	124.9(8)
N(22B)-C(26B)-C(25B)	123.7(10)	C(19C)-N(12C)-C(16C)	122.1(11)
C(28B)-C(27B)-C(25B)	120.4(12)	C(19C)-N(12C)-Pd(5)	116.8(9)
C(29B)-C(28B)-C(27B)	118.9(12)	C(16C)-N(12C)-Pd(5)	121.0(8)
N(22B)-C(29B)-C(28B)	122.5(12)	N(11C)-C(10C)-C(24C)	126.6(10)
C(30B)-N(31B)-C(33B)	108.6(9)	N(11C)-C(10C)-C(11C)	109.4(11)
C(30B)-N(31B)-Zn(3)	124.4(7)	C(24C)-C(10C)-C(11C)	124.0(12)
C(33B)-N(31B)-Zn(3)	126.5(7)	C(12C)-C(11C)-C(10C)	107.5(12)
C(39B)-N(32B)-C(36B)	119.4(10)	C(11C)-C(12C)-C(13C)	105.1(11)
C(39B)-N(32B)-Pd(6)	120.4(7)	N(11C)-C(13C)-C(14C)	124.4(11)
C(36B)-N(32B)-Pd(6)	120.2(7)	N(11C)-C(13C)-C(12C)	111.4(11)
N(31B)-C(30B)-C(24B)	128.7(10)	C(14C)-C(13C)-C(12C)	124.1(11)

C(40C)-C(14C)-C(13C)	125.2(11)	C(38C)-C(37C)-C(35C)	119.6(12)
C(40C)-C(14C)-C(15C)	119.8(11)	C(39C)-C(38C)-C(37C)	119.0(13)
C(13C)-C(14C)-C(15C)	114.9(11)	N(32C)-C(39C)-C(38C)	121.7(12)
C(16C)-C(15C)-C(17C)	116.7(11)	C(40C)-N(41C)-C(43C)	107.2(10)
C(16C)-C(15C)-C(14C)	122.0(11)	C(40C)-N(41C)-Zn(1)	125.8(8)
C(17C)-C(15C)-C(14C)	121.1(11)	C(43C)-N(41C)-Zn(1)	125.9(8)
N(12C)-C(16C)-C(15C)	122.6(11)	C(46C)-N(42C)-C(49C)	119.3(11)
C(18C)-C(17C)-C(15C)	119.3(13)	C(46C)-N(42C)-Pd(6)	120.4(8)
C(17C)-C(18C)-C(19C)	121.8(14)	C(49C)-N(42C)-Pd(6)	119.9(8)
N(12C)-C(19C)-C(18C)	117.4(13)	C(14C)-C(40C)-N(41C)	126.7(11)
C(23C)-N(21C)-C(20C)	109.2(10)	C(14C)-C(40C)-C(41C)	126.7(12)
C(23C)-N(21C)-Zn(1)	123.9(8)	N(41C)-C(40C)-C(41C)	106.6(10)
C(20C)-N(21C)-Zn(1)	124.3(8)	C(42C)-C(41C)-C(40C)	107.5(13)
C(26C)-N(22C)-C(29C)	119.7(11)	C(41C)-C(42C)-C(43C)	111.1(14)
C(26C)-N(22C)-Pd(3)	120.6(9)	C(44C)-C(43C)-N(41C)	125.1(11)
C(29C)-N(22C)-Pd(3)	119.3(8)	C(44C)-C(43C)-C(42C)	127.3(12)
N(21C)-C(20C)-C(34C)	126.4(11)	N(41C)-C(43C)-C(42C)	107.5(12)
N(21C)-C(20C)-C(21C)	108.1(10)	C(30C)-C(44C)-C(43C)	125.9(11)
C(34C)-C(20C)-C(21C)	125.5(11)	C(30C)-C(44C)-C(45C)	115.5(11)
C(22C)-C(21C)-C(20C)	107.2(11)	C(43C)-C(44C)-C(45C)	118.5(11)
C(21C)-C(22C)-C(23C)	106.0(12)	C(46C)-C(45C)-C(47C)	117.9(12)
N(21C)-C(23C)-C(24C)	128.2(11)	C(46C)-C(45C)-C(44C)	120.9(11)
N(21C)-C(23C)-C(22C)	109.6(10)	C(47C)-C(45C)-C(44C)	121.2(12)
C(24C)-C(23C)-C(22C)	122.2(11)	N(42C)-C(46C)-C(45C)	122.2(12)
C(23C)-C(24C)-C(10C)	124.1(11)	C(48C)-C(47C)-C(45C)	118.0(13)
C(23C)-C(24C)-C(25C)	119.8(11)	C(49C)-C(48C)-C(47C)	120.4(14)
C(10C)-C(24C)-C(25C)	115.9(10)	N(42C)-C(49C)-C(48C)	122.2(13)
C(27C)-C(25C)-C(26C)	117.8(12)	C(1A)-N(1A)-Pd(1)	108.6(7)
C(27C)-C(25C)-C(24C)	121.9(11)	C(2A)-N(2A)-Pd(1)	108.0(7)
C(26C)-C(25C)-C(24C)	120.2(11)	C(2A)-C(1A)-N(1A)	105.1(9)
N(22C)-C(26C)-C(25C)	123.2(12)	C(1A)-C(2A)-N(2A)	108.3(11)
C(25C)-C(27C)-C(28C)	119.2(12)	C(1B)-N(1B)-Pd(2)	110.5(7)
C(29C)-C(28C)-C(27C)	119.6(13)	C(2B)-N(2B)-Pd(2)	109.1(8)
N(22C)-C(29C)-C(28C)	120.5(12)	N(2B)-C(2B)-C(1B)	107.5(10)
C(33C)-N(31C)-C(30C)	105.9(9)	N(1B)-C(1B)-C(2B)	107.8(10)
C(33C)-N(31C)-Zn(1)	127.4(8)	C(1C)-N(1C)-Pd(3)	107.7(9)
C(30C)-N(31C)-Zn(1)	126.3(8)	C(2C)-N(2C)-Pd(3)	108.1(8)
C(39C)-N(32C)-C(36C)	119.2(10)	N(2C)-C(2C)-C(1C)	105.1(12)
C(39C)-N(32C)-Pd(4)	120.5(8)	C(2C)-C(1C)-N(1C)	104.3(13)
C(36C)-N(32C)-Pd(4)	120.2(8)	C(2D)-N(2D)-Pd(4)	108.8(9)
N(31C)-C(30C)-C(44C)	125.2(11)	C(1D)-N(1D)-Pd(4)	108.8(8)
N(31C)-C(30C)-C(31C)	109.6(11)	C(2D)-C(1D)-N(1D)	110.8(12)
C(44C)-C(30C)-C(31C)	125.1(11)	C(1D)-C(2D)-N(2D)	112.8(14)
C(32C)-C(31C)-C(30C)	107.1(11)	C(1E)-N(1E)-Pd(5)	108.9(9)
C(31C)-C(32C)-C(33C)	108.2(11)	C(2E)-N(2E)-Pd(5)	109.2(11)
C(34C)-C(33C)-N(31C)	124.2(10)	C(2E)-C(1E)-N(1E)	115.8(15)
C(34C)-C(33C)-C(32C)	126.5(11)	C(1E)-C(2E)-N(2E)	118(2)
N(31C)-C(33C)-C(32C)	109.2(10)	C(1F)-N(1F)-Pd(6)	111.1(9)
C(33C)-C(34C)-C(20C)	126.2(11)	C(2F)-N(2F)-Pd(6)	110.5(10)
C(33C)-C(34C)-C(35C)	115.7(10)	N(1F)-C(1F)-C(2F)	108.2(12)
C(20C)-C(34C)-C(35C)	118.1(11)	N(2F)-C(2F)-C(1F)	107.2(14)
C(36C)-C(35C)-C(37C)	118.3(11)	O(101)-N(100)-O(102)	118.8(11)
C(36C)-C(35C)-C(34C)	119.6(11)	O(101)-N(100)-O(103)	116.6(11)
C(37C)-C(35C)-C(34C)	122.1(11)	O(102)-N(100)-O(103)	124.6(11)
N(32C)-C(36C)-C(35C)	122.1(11)	O(202)-N(200)-O(201)	114(3)

O(202)-N(200)-O(203)	122(3)
O(201)-N(200)-O(203)	115(2)
N(200)-O(203)-O(203)#1	171(4)
O(302)-N(300)-O(303)	126.1(15)
O(302)-N(300)-O(301)	115.6(15)
O(303)-N(300)-O(301)	117.7(15)
O(401)-N(400)-O(403)	127.1(13)
O(401)-N(400)-O(402)	113.8(13)
O(403)-N(400)-O(402)	118.3(13)
O(502)-N(500)-O(501)	114.8(13)
O(502)-N(500)-O(503)	124.5(14)
O(501)-N(500)-O(503)	120.7(12)
O(602)-N(600)-O(601)	120.1(10)
O(602)-N(600)-O(603)	120.3(11)
O(601)-N(600)-O(603)	119.6(11)
O(801)-N(800)-O(802)	112(2)
O(801)-N(800)-O(803)	121(2)
O(802)-N(800)-O(803)	122(2)
O(902)-N(900)-O(901)	112(2)
O(902)-N(900)-O(903)	117(2)
O(901)-N(900)-O(903)	125(2)
O(112)-N(110)-O(111)	114.3(19)
O(112)-N(110)-O(113)	120(2)
O(111)-N(110)-O(113)	120(2)
O(122)-N(120)-O(123)	117.7(11)
O(122)-N(120)-O(121)	119.9(12)
O(123)-N(120)-O(121)	122.3(11)
O(132)-N(130)-O(133)	131.5(12)
O(132)-N(130)-O(131)	125.3(14)
O(133)-N(130)-O(131)	103.2(12)
O(11S)-C(10S)-C(11S)	117(3)
C(22S)-C(21S)-O(21S)	132(4)
O(31S)-C(31S)-C(32S)	114(3)

Symmetry transformations used to generate equivalent atoms:
#1 -x,-y,-z+1

Table 4. Anisotropic displacement parameters ($Å^2 x\ 10^3$) for $3^{12+}\cdot(NO_3^-)_{12}$. The anisotropic displacement factor exponent takes the form: $-2\pi^2[\ h^2\ a^{*2}U^{11} + \ldots + 2\ h\ k\ a^*\ b^*\ U^{12}\ ]$

	U^{11}	U^{22}	U^{33}	U^{23}	U^{13}	U^{12}
Pd(1)	28(1)	35(1)	46(1)	-4(1)	-13(1)	-18(1)
Pd(2)	21(1)	31(1)	44(1)	-7(1)	-7(1)	-5(1)
Pd(3)	29(1)	61(1)	48(1)	-6(1)	-1(1)	-21(1)
Pd(4)	31(1)	55(1)	49(1)	3(1)	-18(1)	-20(1)
Pd(5)	36(1)	69(1)	71(1)	-33(1)	2(1)	-27(1)
Pd(6)	34(1)	67(1)	55(1)	-28(1)	-6(1)	-9(1)
Zn(1)	37(1)	61(1)	37(1)	-14(1)	-4(1)	-22(1)
Zn(2)	18(1)	31(1)	35(1)	-5(1)	-6(1)	-11(1)
Zn(3)	27(1)	99(1)	50(1)	32(1)	-11(1)	-21(1)
N(11A)	23(4)	40(5)	42(5)	-9(4)	-5(4)	-19(4)
N(12A)	26(4)	29(4)	41(5)	-10(4)	-13(4)	-12(4)
C(10A)	16(5)	39(6)	37(6)	-6(5)	-3(4)	-9(4)
C(11A)	22(5)	34(6)	54(7)	-14(5)	-2(5)	-11(5)
C(12A)	20(5)	42(6)	49(7)	-11(5)	-9(5)	-16(5)
C(13A)	28(5)	31(5)	39(6)	-9(4)	-4(4)	-18(5)
C(14A)	29(5)	25(5)	42(6)	-5(4)	-11(5)	-12(4)
C(15A)	16(5)	25(5)	49(6)	-13(5)	-3(4)	-9(4)
C(16A)	26(5)	36(6)	40(6)	-8(5)	-10(4)	-14(5)
C(17A)	33(6)	39(6)	39(6)	5(5)	-13(5)	-16(5)
C(18A)	44(6)	43(6)	31(6)	0(5)	-8(5)	-27(5)
C(19A)	31(6)	38(6)	54(7)	-10(5)	-20(5)	-13(5)
N(21A)	17(4)	42(5)	33(5)	-13(4)	-2(3)	-13(4)
N(22A)	26(5)	57(6)	48(6)	-11(5)	0(4)	-19(5)
C(20A)	35(6)	47(7)	36(6)	-8(5)	-10(5)	-16(5)
C(21A)	33(6)	72(8)	42(7)	-20(6)	-8(5)	-18(6)
C(22A)	40(7)	75(9)	37(6)	-23(6)	-8(5)	-14(6)
C(23A)	25(5)	46(6)	42(6)	-9(5)	-6(5)	-16(5)
C(24A)	25(5)	42(6)	42(6)	-10(5)	6(5)	-16(5)
C(25A)	24(5)	57(7)	31(6)	-6(5)	-5(4)	-20(5)
C(26A)	26(5)	49(7)	32(6)	-8(5)	-3(4)	-15(5)
C(27A)	45(7)	60(8)	51(7)	-24(6)	5(6)	-29(6)
C(28A)	61(9)	98(11)	75(10)	-48(9)	15(7)	-50(9)
C(29A)	32(6)	71(9)	63(8)	-35(7)	11(6)	-25(6)
N(31A)	16(4)	30(4)	32(4)	4(4)	-10(3)	-6(3)
N(32A)	33(5)	50(6)	50(6)	-12(5)	-16(4)	-20(4)
C(30A)	24(5)	24(5)	45(6)	1(4)	-14(5)	-11(4)
C(31A)	12(5)	35(6)	47(6)	-3(5)	-6(4)	-6(4)
C(32A)	35(6)	23(5)	54(7)	2(5)	-22(5)	-13(5)
C(33A)	20(5)	29(5)	43(6)	-10(4)	-11(4)	-8(4)
C(34A)	22(5)	40(6)	42(6)	1(5)	-15(5)	-16(5)
C(35A)	30(6)	58(7)	48(7)	-14(6)	-17(5)	-14(5)
C(36A)	34(6)	39(6)	43(6)	-5(5)	-12(5)	-17(5)
C(37A)	115(13)	36(7)	127(14)	1(8)	-96(12)	-25(8)
C(38A)	111(13)	57(9)	154(17)	15(10)	-94(13)	-46(9)
C(39A)	85(11)	46(8)	107(12)	-8(7)	-77(10)	-11(7)
N(41A)	20(4)	30(4)	33(5)	-7(4)	-4(3)	-10(4)
N(42A)	21(4)	30(4)	39(5)	-5(4)	-2(4)	-12(4)
C(40A)	24(5)	33(5)	37(6)	-1(4)	-15(4)	-15(4)
C(41A)	29(6)	40(6)	42(6)	-10(5)	-15(5)	-12(5)
C(42A)	30(6)	43(6)	46(7)	-18(5)	-3(5)	-9(5)

C(43A)	21(5)	27(5)	45(6)	-6(4)	-9(4)	-10(4)
C(44A)	18(5)	24(5)	36(6)	0(4)	-4(4)	-6(4)
C(45A)	24(5)	21(5)	40(6)	-8(4)	-1(4)	-8(4)
C(46A)	28(5)	35(6)	35(6)	-9(4)	-6(4)	-16(5)
C(47A)	27(5)	32(6)	46(6)	8(5)	-14(5)	-9(5)
C(48A)	33(6)	41(6)	25(5)	0(4)	-2(4)	-10(5)
C(49A)	27(5)	34(6)	39(6)	-3(5)	4(5)	-6(5)
N(11B)	25(5)	46(5)	51(6)	6(4)	-6(4)	-15(4)
N(12B)	33(5)	32(5)	50(6)	1(4)	-16(4)	-19(4)
C(10B)	47(7)	50(7)	51(7)	11(6)	-15(6)	-27(6)
C(11B)	39(7)	63(8)	52(7)	28(6)	-18(6)	-31(6)
C(12B)	32(6)	61(8)	55(8)	21(6)	-21(6)	-21(6)
C(13B)	32(6)	46(7)	46(7)	7(5)	-11(5)	-15(5)
C(14B)	36(6)	32(6)	49(7)	4(5)	-14(5)	-17(5)
C(15B)	37(6)	39(6)	50(7)	10(5)	-10(5)	-26(5)
C(16B)	34(6)	43(6)	46(6)	-1(5)	-15(5)	-24(5)
C(17B)	45(7)	38(6)	48(7)	-1(5)	-14(6)	-11(5)
C(18B)	60(8)	52(7)	34(6)	-5(5)	-6(6)	-20(6)
C(19B)	49(7)	34(6)	47(7)	-6(5)	-16(6)	-17(5)
N(21B)	34(5)	36(5)	43(5)	1(4)	-13(4)	-18(4)
N(22B)	58(6)	42(6)	49(6)	-12(4)	-2(5)	-34(5)
C(20B)	34(6)	36(6)	47(7)	-1(5)	-13(5)	-17(5)
C(21B)	35(6)	39(6)	58(7)	-1(5)	-14(5)	-20(5)
C(22B)	26(5)	39(6)	50(7)	-4(5)	-5(5)	-17(5)
C(23B)	34(6)	33(6)	49(7)	-4(5)	-16(5)	-17(5)
C(24B)	47(7)	33(6)	31(6)	2(4)	-7(5)	-21(5)
C(25B)	39(6)	40(7)	51(7)	-2(5)	-11(5)	-19(5)
C(26B)	38(6)	38(6)	46(7)	1(5)	-6(5)	-21(5)
C(27B)	57(8)	39(7)	57(8)	-4(6)	5(6)	-18(6)
C(28B)	65(9)	38(7)	70(9)	-10(6)	10(7)	-26(7)
C(29B)	79(10)	71(9)	54(8)	-5(7)	0(7)	-55(8)
N(31B)	37(5)	34(5)	47(6)	7(4)	-6(4)	-17(4)
N(32B)	27(5)	44(5)	41(5)	-5(4)	-12(4)	-3(4)
C(30B)	34(6)	36(6)	48(7)	7(5)	-4(5)	-9(5)
C(31B)	57(8)	51(8)	46(7)	18(6)	-6(6)	-19(6)
C(32B)	40(7)	65(8)	58(8)	11(6)	-19(6)	-18(6)
C(33B)	39(6)	36(6)	38(6)	8(5)	-15(5)	-9(5)
C(34B)	34(6)	34(6)	36(6)	0(5)	-14(5)	-4(5)
C(35B)	32(6)	45(7)	32(6)	-1(5)	-5(5)	-9(5)
C(36B)	33(6)	35(6)	39(6)	-6(5)	-5(5)	-5(5)
C(37B)	51(7)	48(7)	56(8)	5(6)	-17(6)	-27(6)
C(38B)	39(7)	34(7)	62(8)	10(6)	-9(6)	2(6)
C(39B)	34(6)	42(7)	50(7)	-5(6)	-10(5)	-4(5)
N(41B)	32(5)	37(5)	37(5)	-3(4)	-8(4)	-12(4)
N(42B)	22(4)	30(4)	34(5)	-5(4)	-4(4)	-10(4)
C(40B)	31(6)	32(6)	40(6)	-1(5)	-13(5)	-4(5)
C(41B)	33(6)	32(6)	45(6)	-1(5)	-12(5)	-11(5)
C(42B)	31(6)	38(6)	43(6)	-4(5)	-7(5)	-12(5)
C(43B)	33(6)	37(6)	39(6)	0(5)	-8(5)	-17(5)
C(44B)	32(6)	37(6)	46(6)	-1(5)	-11(5)	-14(5)
C(45B)	33(6)	29(6)	36(6)	0(4)	-5(5)	-11(5)
C(46B)	21(5)	29(5)	37(6)	-1(4)	-11(4)	-1(4)
C(47B)	70(9)	56(8)	55(8)	-7(6)	-13(7)	-40(7)
C(48B)	65(8)	47(7)	33(6)	-13(5)	3(6)	-32(6)
C(49B)	40(6)	42(6)	41(7)	-7(5)	3(5)	-20(5)

N(11C)	30(5)	70(7)	45(6)	-9(5)	-6(4)	-29(5)
N(12C)	40(6)	62(7)	43(6)	-8(5)	4(4)	-30(5)
C(10C)	31(6)	71(9)	37(6)	-10(6)	-7(5)	-20(6)
C(11C)	38(7)	79(10)	57(8)	-13(7)	3(6)	-21(7)
C(12C)	44(7)	60(8)	50(7)	-16(6)	-4(6)	-22(6)
C(13C)	58(8)	59(8)	41(7)	-15(6)	-8(6)	-24(7)
C(14C)	46(7)	54(8)	53(7)	-10(6)	-15(6)	-29(6)
C(15C)	51(7)	57(8)	42(7)	-17(6)	-10(6)	-19(6)
C(16C)	35(6)	49(7)	48(7)	-16(5)	5(5)	-23(6)
C(17C)	92(11)	76(10)	65(9)	-11(8)	-20(8)	-50(9)
C(18C)	108(13)	64(9)	52(8)	-5(7)	-9(9)	-44(9)
C(19C)	53(8)	63(9)	68(9)	-13(7)	-2(7)	-22(7)
N(21C)	43(6)	48(6)	44(5)	-7(4)	-13(4)	-23(5)
N(22C)	29(5)	73(7)	48(6)	-7(5)	0(4)	-19(5)
C(20C)	40(7)	52(8)	48(7)	-3(6)	-10(6)	-17(6)
C(21C)	54(8)	63(8)	55(8)	-18(6)	-6(6)	-34(7)
C(22C)	45(7)	75(9)	51(8)	-13(7)	-2(6)	-27(7)
C(23C)	34(6)	58(7)	29(6)	-13(5)	2(5)	-17(6)
C(24C)	36(6)	59(8)	37(6)	-9(5)	-3(5)	-21(6)
C(25C)	49(7)	60(8)	39(7)	-6(6)	-3(6)	-32(6)
C(26C)	49(7)	58(8)	32(6)	-3(5)	3(5)	-30(7)
C(27C)	43(7)	75(9)	36(7)	-6(6)	3(5)	-20(7)
C(28C)	58(9)	79(10)	53(8)	-16(7)	2(7)	-29(8)
C(29C)	37(7)	58(8)	46(7)	-7(6)	0(6)	-14(6)
N(31C)	43(5)	50(6)	30(5)	-13(4)	-1(4)	-15(5)
N(32C)	36(5)	48(6)	44(5)	-3(5)	-12(4)	-22(5)
C(30C)	40(7)	62(8)	41(7)	-9(6)	-13(5)	-17(6)
C(31C)	37(7)	77(10)	40(7)	-12(6)	-7(5)	-24(7)
C(32C)	44(7)	54(8)	45(7)	-18(6)	-11(5)	-18(6)
C(33C)	42(7)	58(8)	40(6)	-12(6)	-8(5)	-26(6)
C(34C)	38(6)	53(7)	44(7)	-9(5)	-14(5)	-18(6)
C(35C)	33(6)	46(7)	50(7)	-2(5)	-14(5)	-19(5)
C(36C)	34(6)	46(7)	45(7)	-7(5)	-19(5)	-11(5)
C(37C)	51(8)	71(9)	48(7)	-8(7)	-7(6)	-31(7)
C(38C)	78(10)	74(10)	65(9)	-24(8)	-10(8)	-41(8)
C(39C)	55(8)	69(9)	66(9)	-7(7)	-23(7)	-32(7)
N(41C)	48(6)	57(6)	53(6)	-24(5)	-9(5)	-24(5)
N(42C)	42(6)	63(7)	41(6)	-19(5)	-7(5)	-3(5)
C(40C)	53(8)	49(8)	63(8)	-25(6)	-1(6)	-22(6)
C(41C)	51(9)	86(11)	105(13)	-34(9)	-19(8)	-35(8)
C(42C)	74(11)	61(10)	110(13)	-40(9)	-25(10)	-9(8)
C(43C)	60(8)	47(7)	47(7)	-19(6)	-2(6)	-21(6)
C(44C)	33(6)	59(8)	53(7)	-26(6)	-5(5)	-11(6)
C(45C)	52(7)	50(7)	56(8)	-17(6)	-18(6)	-20(6)
C(46C)	36(6)	66(8)	40(7)	-15(6)	-9(5)	-16(6)
C(47C)	60(9)	64(9)	53(8)	-22(7)	-8(7)	-24(7)
C(48C)	76(10)	65(9)	70(10)	-9(8)	-31(9)	-16(8)
C(49C)	58(8)	67(9)	43(7)	-16(7)	-8(6)	-10(7)
N(1A)	41(6)	38(5)	72(7)	-7(5)	-12(5)	-20(5)
N(2A)	35(5)	42(5)	74(7)	-18(5)	-10(5)	-19(5)
C(1A)	31(6)	36(7)	127(13)	-9(7)	-11(7)	-20(6)
C(2A)	32(7)	59(9)	99(11)	-18(8)	13(7)	-22(6)
N(1B)	40(5)	32(5)	66(7)	-7(5)	-19(5)	-6(4)
N(2B)	42(6)	40(5)	71(7)	-21(5)	-24(5)	-6(5)
C(2B)	46(8)	64(9)	84(10)	-24(8)	-32(7)	-3(7)

C(1B)	40(7)	39(7)	108(11)	-5(7)	-43(8)	-4(6)
N(1C)	58(7)	137(12)	67(8)	26(8)	-12(6)	-67(8)
N(2C)	48(6)	76(8)	57(7)	-2(6)	-12(5)	-37(6)
C(2C)	50(8)	105(12)	67(10)	3(9)	-17(7)	-36(8)
C(1C)	75(11)	130(15)	91(12)	-13(11)	-20(9)	-68(11)
N(2D)	37(6)	72(7)	68(7)	12(6)	-14(5)	-21(5)
N(1D)	43(6)	73(7)	70(7)	4(6)	-22(6)	-23(6)
C(1D)	37(8)	140(15)	68(10)	11(10)	-29(7)	-23(9)
C(2D)	43(9)	111(14)	99(13)	10(11)	-24(9)	0(9)
N(1E)	36(6)	146(13)	116(11)	-89(10)	-10(7)	-12(8)
N(2E)	31(6)	115(11)	114(11)	-55(9)	-10(6)	-13(7)
C(1E)	57(9)	101(13)	114(14)	-58(11)	-34(9)	2(9)
C(2E)	65(13)	340(40)	240(30)	-240(30)	-51(16)	30(18)
N(1F)	44(6)	74(8)	57(7)	-28(6)	-2(5)	-16(6)
N(2F)	52(7)	145(13)	100(10)	-78(10)	12(7)	-50(8)
C(1F)	69(10)	107(13)	82(11)	-50(10)	16(8)	-47(10)
C(2F)	92(13)	111(14)	81(12)	-48(11)	22(10)	-53(11)
O(1A)	115(9)	130(10)	49(6)	-19(6)	-11(6)	-67(8)
O(2A)	91(7)	44(5)	69(6)	1(4)	3(5)	-30(5)
O(3A)	184(17)	142(14)	181(18)	-31(13)	-34(14)	-49(13)
O(4A)	211(19)	170(16)	199(19)	-90(15)	3(15)	-100(15)

Table 5. Hydrogen coordinates (x 10^4) and isotropic displacement parameters ($Å^2$x 10^3) for 3^{12+}•$(NO_3^-)_{12}$.

	x	y	z	U(eq)
H(11A)	8715	4442	-1568	43
H(12A)	8565	4802	-777	42
H(16A)	8042	6246	-675	39
H(17A)	7385	4983	572	45
H(18A)	8114	5173	999	44
H(19A)	8847	5816	527	45
H(21A)	5617	4932	-2575	56
H(22A)	6937	4655	-2714	60
H(26A)	8466	5244	-2505	43
H(27A)	7877	3519	-2190	58
H(28A)	8852	3005	-2744	84
H(29A)	9583	3665	-3228	63
H(31A)	3336	5916	-235	39
H(32A)	3502	5555	-1029	42
H(36A)	3889	6163	-2220	44
H(37A)	4693	4094	-1543	98
H(38A)	3895	3861	-1882	114
H(39A)	3102	4809	-2334	87
H(41A)	6319	6325	411	42
H(42A)	5008	6620	541	48
H(46A)	3313	7148	-223	36
H(47A)	4291	5815	899	45
H(48A)	3301	6351	1471	44
H(49A)	2283	7225	1166	45
H(11B)	4565	8419	318	65
H(12B)	5866	8108	180	63
H(16B)	7649	7896	-824	46
H(17B)	6493	9000	249	54
H(18B)	7348	8305	743	60
H(19B)	8405	7450	418	50
H(21B)	7759	9174	-1173	51
H(22B)	7695	10046	-1992	46
H(26B)	7519	9958	-2877	49
H(27B)	6467	11936	-2640	67
H(28B)	7321	12312	-3245	72
H(29B)	8238	11505	-3672	76
H(31B)	5712	11530	-3160	70
H(32B)	4424	11708	-3062	69
H(36B)	2935	10658	-2392	46
H(37B)	3328	12483	-2567	61
H(38B)	2465	13051	-3103	66
H(39B)	1861	12421	-3243	55
H(41B)	2465	11009	-1557	45
H(42B)	2471	10266	-685	46
H(46B)	2923	8919	-396	38
H(47B)	3467	9648	547	66
H(48B)	2678	9226	1186	55
H(49B)	2027	8706	1020	50
H(11C)	8693	7211	-4436	73

H(12C)	8398	8519	-4501	60
H(16C)	7749	9351	-3793	51
H(17C)	7119	10379	-5134	84
H(18C)	7829	11005	-5271	87
H(19C)	8539	10816	-4665	76
H(21C)	5925	5655	-3836	62
H(22C)	7202	5486	-3955	68
H(26C)	8493	6162	-3597	56
H(27C)	8132	5903	-4839	66
H(28C)	9224	4919	-4861	76
H(29C)	9910	4592	-4242	61
H(31C)	3201	9250	-4084	60
H(32C)	3512	7966	-4012	54
H(36C)	3941	6905	-3229	49
H(37C)	5023	6213	-4501	66
H(38C)	4306	5521	-4349	79
H(39C)	3383	5599	-3667	71
H(41C)	5906	10795	-4351	87
H(42C)	4689	10934	-4231	95
H(46C)	3246	9969	-3388	56
H(47C)	3816	10866	-4849	68
H(48C)	2721	11806	-4768	85
H(49C)	1927	11792	-4032	71
H(1A1)	9390	7723	-1121	58
H(1A2)	9441	7811	-638	58
H(2A1)	10169	5788	-399	57
H(2A2)	9867	5727	-789	57
H(1A3)	10598	7338	-1181	77
H(1A4)	10540	6933	-609	77
H(2A3)	10913	6076	-1098	80
H(2A4)	10264	6528	-1388	80
H(1B1)	940	9376	164	56
H(1B2)	1260	9317	-358	56
H(2B1)	1627	7294	-104	58
H(2B2)	1090	7477	342	58
H(2B3)	429	7999	-255	77
H(2B4)	1048	8250	-628	77
H(1B3)	200	9276	-333	75
H(1B4)	172	8847	231	75
H(1C1)	10894	5169	-3885	105
H(1C2)	10370	5884	-3836	105
H(2C1)	10153	4896	-2488	69
H(2C2)	10440	4172	-2589	69
H(2C3)	11403	4348	-3142	89
H(2C4)	11343	4665	-2681	89
H(1C1)	11384	5547	-3435	107
H(1C2)	10630	5814	-3082	107
H(2D1)	1796	6039	-2103	76
H(2D2)	1995	6548	-1962	76
H(1D1)	2101	7444	-3331	76
H(1D2)	2100	6847	-3504	76
H(1D3)	965	7581	-3067	105
H(1D4)	1137	6749	-2972	105
H(2D3)	834	6968	-2217	118
H(2D4)	1265	7493	-2362	118

H(1E1)	9565	8799	-3973	111
H(1E2)	9770	9380	-4336	111
H(2E1)	9558	10159	-3241	101
H(2E2)	9253	9642	-2880	101
H(1E3)	10544	8493	-3717	105
H(1E4)	10609	9246	-3982	105
H(2E3)	10517	9300	-3281	243
H(2E4)	10114	8751	-3056	243
H(1F1)	1384	10659	-2055	70
H(1F2)	962	11407	-2242	70
H(2F1)	957	10684	-3287	104
H(2F2)	1566	10014	-3207	104
H(1F3)	188	11153	-2456	96
H(1F4)	353	10576	-1956	96
H(2F3)	1166	9713	-2406	108
H(2F4)	465	10047	-2645	108
H(10A)	-2603	7178	1632	288
H(10B)	-2084	6731	1230	288
H(11D)	-1516	7321	1475	212
H(11E)	-1113	6485	1595	212
H(11F)	-1623	6879	2029	212
H(21D)	6777	-2884	4047	283
H(21E)	6136	-2163	4046	283
H(22D)	6514	-2540	4747	263
H(22E)	6390	-3269	4846	263
H(22F)	5730	-2546	4847	263
H(31D)	4846	5797	2853	190
H(31E)	5295	5453	3289	190
H(32D)	5340	6666	2888	352
H(32E)	4983	6647	3458	352
H(32F)	4501	7000	3040	352

NMR spectra
Chapter 5

^{1}H NMR of ligand **1** (free base) in $CDCl_3$

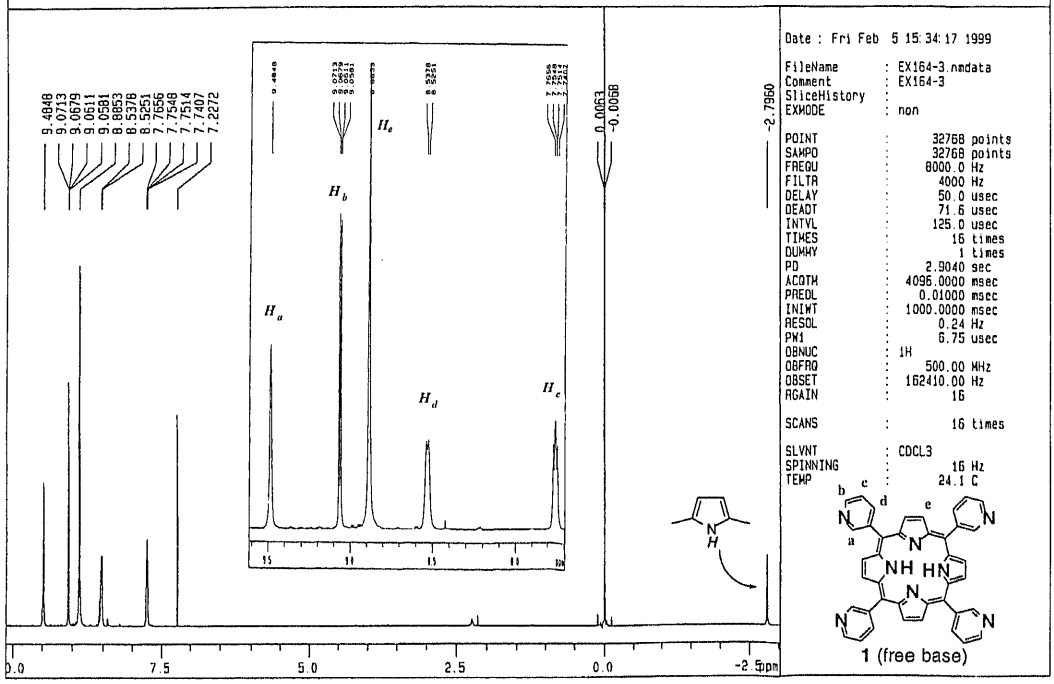

^{13}C NMR of ligand **1** (free base) at 323 K in $CDCl_3$

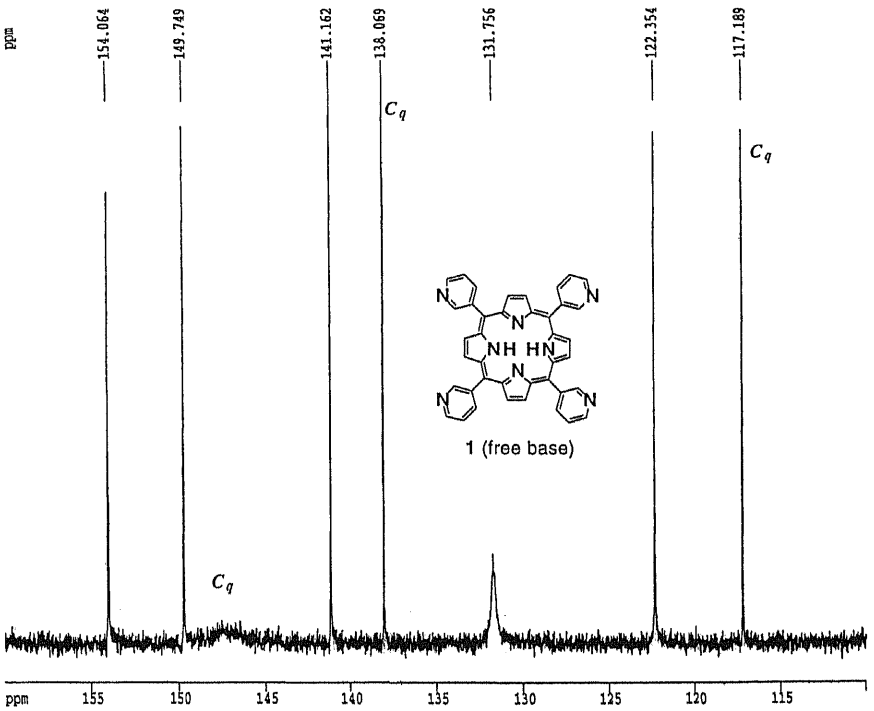


```
Current Data Parameters
NAME              ligand
EXPNO                  8
PROCNO                 1

F2 - Acquisition Parameters
Date_           20000822
Time               10.46
INSTRUM           drx500
PROBHD   5 mm BBO BB-1
PULPROG          zgpg30
TD                65536
SOLVENT             D2O
NS                  1540
DS                     2
SWH           39682.539 Hz
FIDRES        0.605507 Hz
AQ            0.8258036 sec
RG                 13004
DW               12.600 usec
DE                6.00 usec
TE               300.0 K
d11           0.03000000 sec
d12           0.00002000 sec
PL13             120.00 dB
D1            2.00000000 sec
CPDPRG2          waltz16
PCPD2             81.00 usec
SFO2          500.1320005 MHz
NUC2                 1H
PL2               -4.00 dB
PL12              16.00 dB
P1                 6.40 usec
SFO1          125.7736214 MHz
NUC1                13C
PL1               2.00 dB

F2 - Processing parameters
SI                 32768
SF          125.7577390 MHz
WDW                   EM
SSB                    0
LB                1.00 Hz
GB                     0
PC                 1.40

1D NMR plot parameters
CX                20.00 cm
F1P              160.000 ppm
F1               20121.24 Hz
F2P              110.000 ppm
F2               13833.35 Hz
PPMCM             2.50000 ppm/cm
HZCM            314.39435 Hz/cm
```

^{13}C NMR of ligand **1** (free base) at 334 K in $CDCl_3$

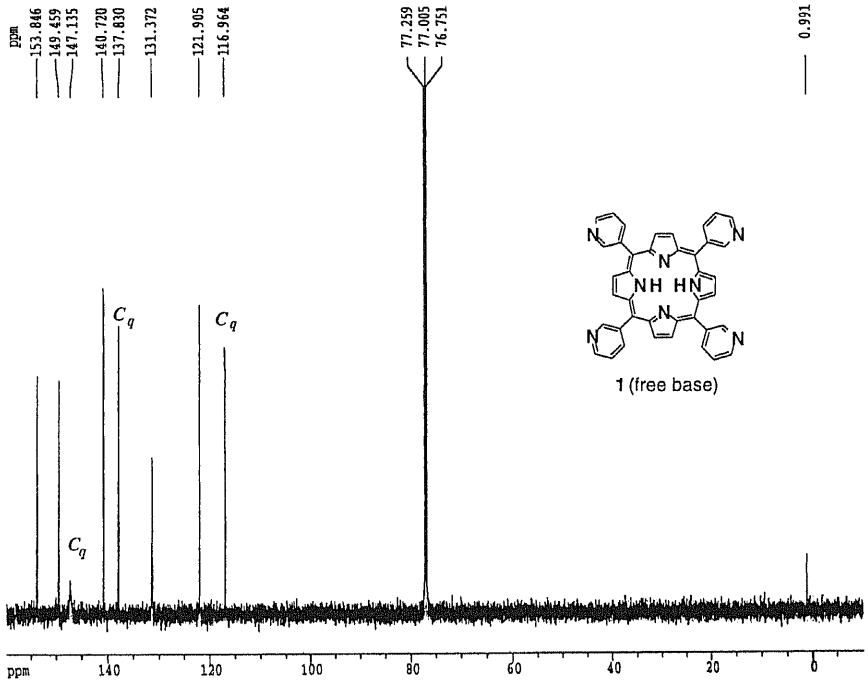


```
Current Data Parameters
NAME                  ligand
EXPNO                      5
PROCNO                     1

F2 - Acquisition Parameters
Date_              20000821
Time                  19.43
INSTRUM              drx500
PROBHD     5 mm BBO BB-1
PULPROG            zgpg30
TD                  65536
SOLVENT               D2O
NS                    515
DS                      2
SWH              39682.539 Hz
FIDRES           0.605507 Hz
AQ               0.8258036 sec
RG                 14596.5
DW                12.600 usec
DE                 6.00 usec
TE                 300.0 K
d11              0.03000000 sec
d12              0.00002000 sec
PL13              120.00 dB
D1               2.00000000 sec
CPDPRG2            waltz16
PCPD2              81.00 usec
SFO2           500.1320005 MHz
NUC2                   1H
PL2                4.00 dB
PL12              16.00 dB
P1                 6.40 usec
SFO1           125.7736214 MHz
NUC1                  13C
PL1                2.00 dB

F2 - Processing parameters
SI                    32768
SF             125.7577676 MHz
WDW                      EM
SSB                       0
LB                 1.00 Hz
GB                        0
PC                     1.40

1D NMR plot parameters
CX                   20.00 cm
F1P                160.000 ppm
F1               20121.24 Hz
F2P                -10.000 ppm
F2               -1257.58 Hz
PPMCM              8.50000 ppm/cm
HZCM            1068.94104 Hz/cm
```

DEPT of ligand **1** (free base) at 323 K in $CDCl_3$

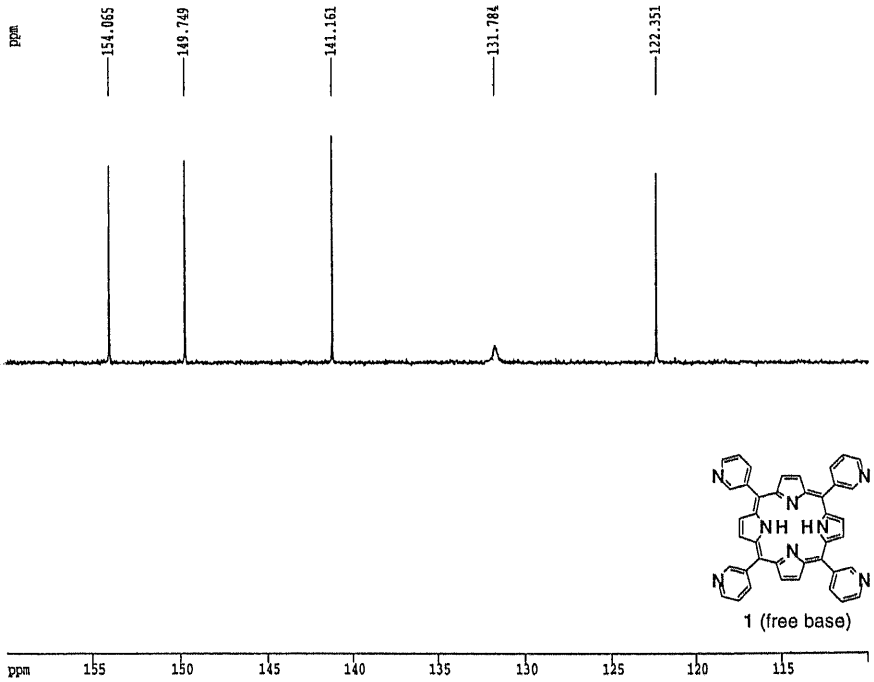


```
Current Data Parameters
NAME                  ligand
EXPNO                     10
PROCNO                     1

F2 - Acquisition Parameters
Date_              20000822
Time                  23.31
INSTRUM              drx500
PROBHD     5 mm BBO BB-1
PULPROG           dept135
TD                  65536
SOLVENT               CDCl3
NS                     1358
DS                        4
SWH              39682.539 Hz
FIDRES           0.605507 Hz
AQ               0.8258036 sec
RG                   16384
DW                12.600 usec
DE                 6.00 usec
TE                 300.0 K
P1                 6.40 usec
p2                12.80 usec
P3                 8.40 usec
p4                16.80 usec
CNST2             145.0000000
d2               0.00344828 sec
d12              0.00002000 sec
DELTA            0.00000815 sec
D1               2.00000000 sec
PL2                -4.00 dB
SFO2           500.1320005 MHz
NUC2                   1H
SFO1           125.7736214 MHz
NUC1                  13C
PL1                2.00 dB
PL12              16.00 dB
CPDPRG2            waltz16
PCPD2              81.00 usec

F2 - Processing parameters
SI                    32768
SF             125.7577390 MHz
WDW                      EM
SSB                       0
LB                 1.00 Hz
GB                        0
PC                     1.40

1D NMR plot parameters
CX                   20.00 cm
F1P                160.000 ppm
F1               20121.24 Hz
F2P                110.000 ppm
F2               13833.35 Hz
PPMCM              2.50000 ppm/cm
HZCM            314.39435 Hz/cm
```

^{1}H NMR of $3^{12+}(NO_3^-)_{12}$ in CD_3CN-D_2O=1:1

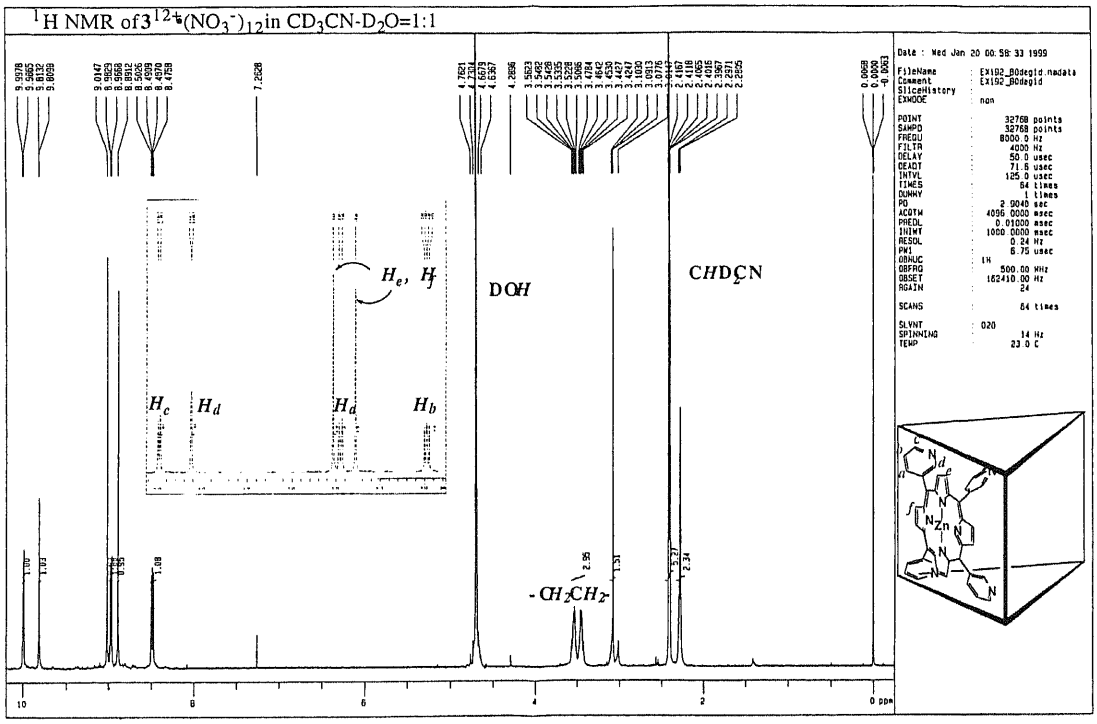

^{13}C NMR of $3^{12+}(NO_3^-)_{12}$ in CD_3CN-D_2O=1:1

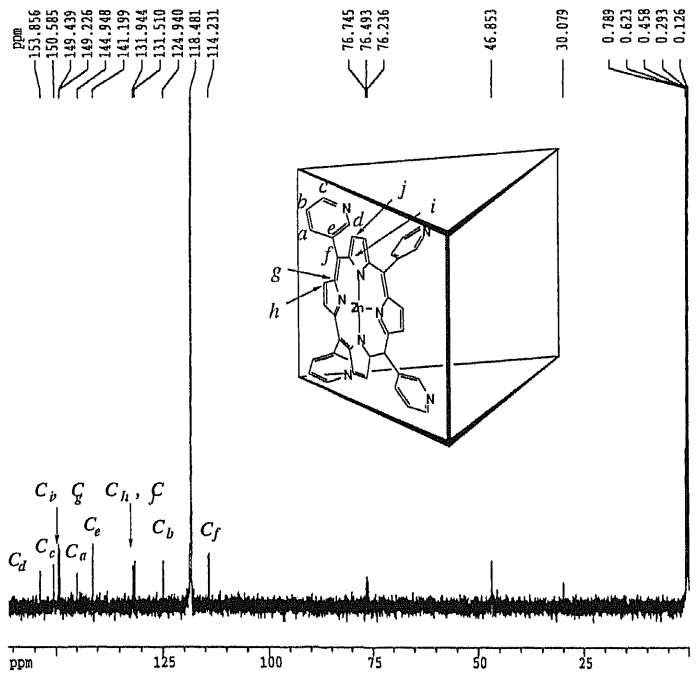

Current Data Parameters

NAME	prism
EXPNO	6
PROCNO	1

F2 - Acquisition Parameters

Date_	20001002
Time	12.02
INSTRUM	drx500
PROBHD	5 mm BBO BB-1
PULPROG	zgpg30
TD	65536
SOLVENT	D2O
NS	1024
DS	2
SWH	39682.539 Hz
FIDRES	0.605507 Hz
AQ	0.8258036 sec
RG	1625.5
DW	12.600 usec
DE	6.00 usec
TE	300.0 K
d11	0.03000000 sec
d12	0.00002000 sec
PL13	120.00 dB
D1	1.00000000 sec
CPDPRG2	waltz16
PCPD2	81.00 usec
SFO2	500.1320005 MHz
NUC2	1H
PL2	-4.00 dB
PL12	16.00 dB
P1	6.40 usec
SFO1	125.7736214 MHz
NUC1	13C
PL1	2.00 dB

F2 - Processing parameters

SI	32768
SF	125.7578606 MHz
WDW	EM
SSB	0
LB	1.00 Hz
GB	0
PC	1.40

1D NMR plot parameters

CX	15.49 cm
F1P	161.300 ppm
F1	20272.20 Hz
F2P	0.000 ppm
F2	0.00 Hz
PPMCM	10.40640 ppm/cm
HZCM	1308.68640 Hz/cm

^{13}C NMR of $\mathbf{3}^{12+}(NO_3^-)_{12}$ in CD_3CN-D_2O=1:1

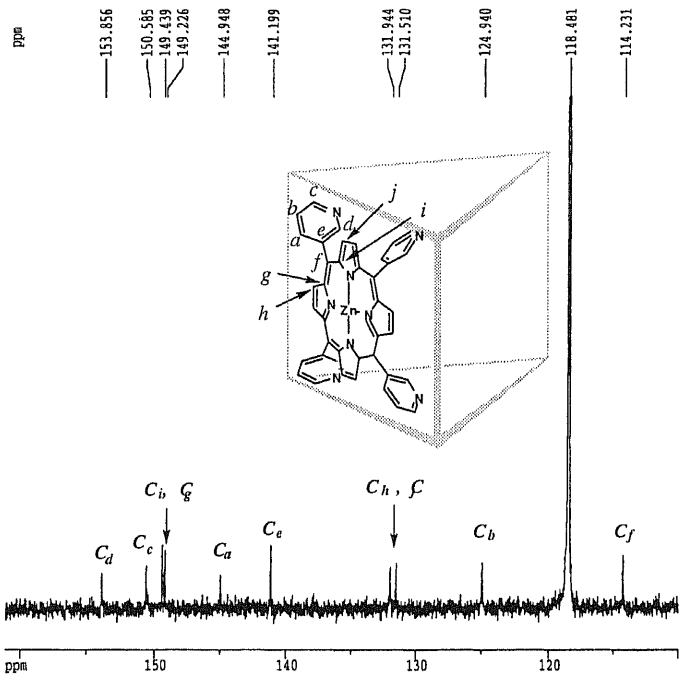

Current Data Parameters
NAME prism
EXPNO 6
PROCNO 1

F2 - Acquisition Parameters
Date_ 20001002
Time 12.02
INSTRUM drx500
PROBHD 5 mm BBO BB-1
PULPROG zgpg30
TD 65536
SOLVENT D2O
NS 1024
DS 2
SWH 39682.539 Hz
FIDRES 0.605507 Hz
AQ 0.8258036 sec
RG 1625.5
DW 12.600 usec
DE 6.00 usec
TE 300.0 K
d11 0.03000000 sec
d12 0.00002000 sec
PL13 120.00 dB
D1 2.00000000 sec
CPDPRG2 waltz16
PCPD2 81.00 usec
SFO2 500.1320005 MHz
NUC2 1H
PL2 -4.00 dB
PL12 16.00 dB
P1 6.40 usec
SFO1 125.7736214 MHz
NUC1 13C
PL1 2.00 dB

F2 - Processing parameters
SI 32768
SF 125.7578606 MHz
WDW EM
SSB 0
LB 1.00 Hz
GB 0
PC 1.40

1D NMR plot parameters
CX 15.49 cm
F1P 161.200 ppm
F1 20272.20 Hz
F2P 110.000 ppm
F2 13833.36 Hz
PPMCM 3.30527 ppm/cm
HZCM 415.66370 Hz/cm

HH COSY of $\mathbf{3}^{12+}(NO_3^-)_{12}$ in CD_3CN-D_2O=1:1

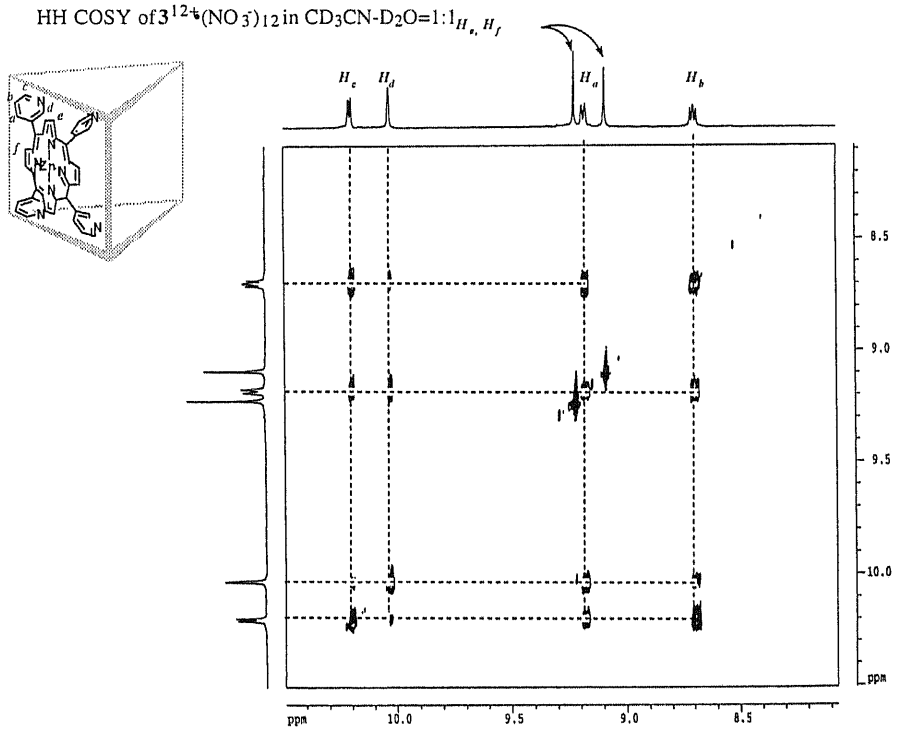

COSYGS

Current Data Parameters
NAME prism
EXPNO 6
PROCNO 1

F2 - Acquisition Parameters
Date_ 20001002
Time 12.02
INSTRUM drx500
PROBHD 5 mm BBO BB-1
PULPROG zgpg30
TD 65536
SOLVENT D2O
NS 1024
DS 2
SWH 39682.539 Hz
FIDRES 0.605507 Hz
AQ 0.8258036 sec
RG 1625.5
DW 12.600 usec
DE 6.00 usec
TE 300.0 K
d11 0.03000000 sec
d12 0.00002000 sec
PL13 120.00 dB
D1 2.00000000 sec
CPDPRG2 waltz16
PCPD2 81.00 usec
SFO2 500.1320005 MHz
NUC2 1H
PL2 -4.00 dB
PL12 16.00 dB
P1 6.40 usec
SFO1 125.7736214 MHz
NUC1 13C
PL1 2.00 dB

F2 - Processing parameters
SI 32768
SF 125.7578606 MHz
WDW EM
SSB 0
LB 1.00 Hz
GB 0
PC 1.40

1D NMR plot parameters
CX 15.49 cm
F1P 161.200 ppm
F1 20272.20 Hz
F2P 110.000 ppm
F2 13833.36 Hz
PPMCM 3.30527 ppm/cm
HZCM 415.66370 Hz/cm

HMQC of $3^{12+}(NO_3^-)_{12}$ in CD_3CN-D_2O=1:1

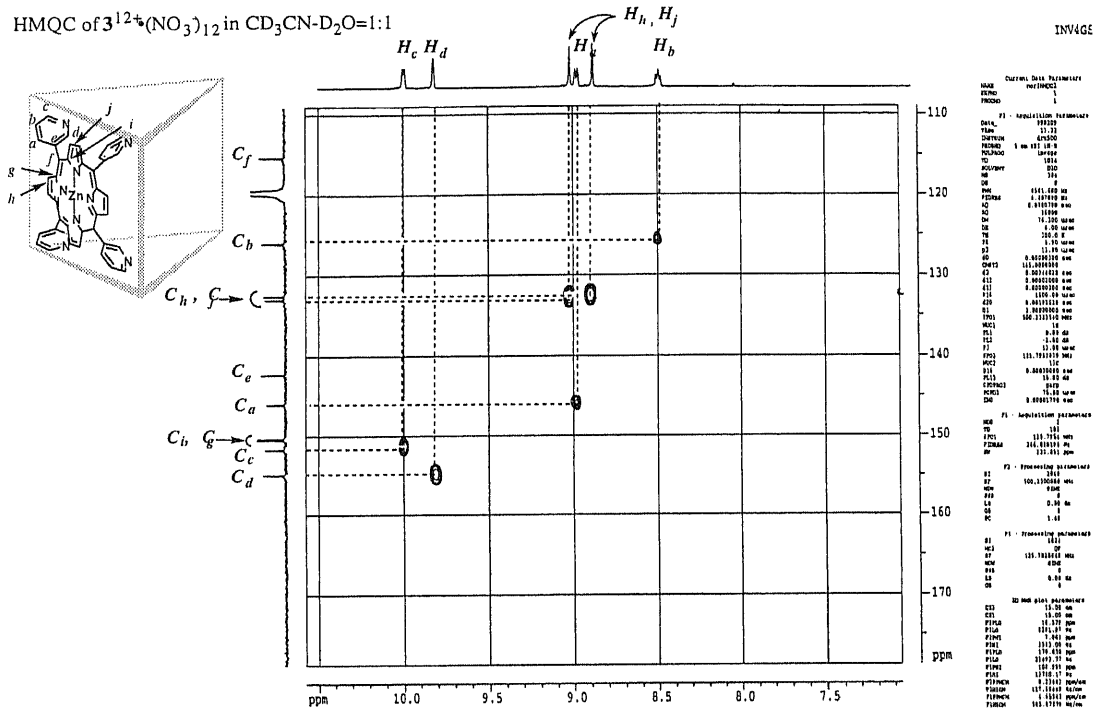

HMBC of $3^{12+}(NO_3^-)_{12}$ in CD_3CN-D_2O=1:1

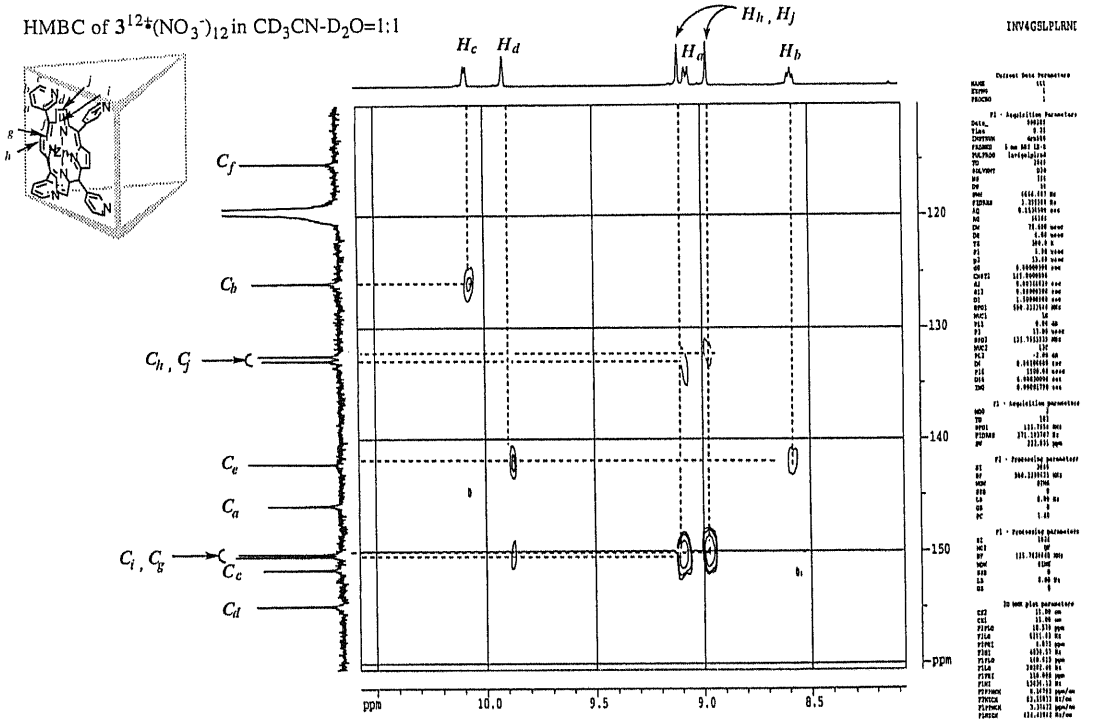

^{1}H NMR of $\mathbf{3}^{12+}(NO_3^-)_{12}$•pyrene and $\mathbf{3}^{12+}(NO_3^-)_{12}$•pyrene d_{-10} in CD_3OD-D_2O=1:1 at 323 K

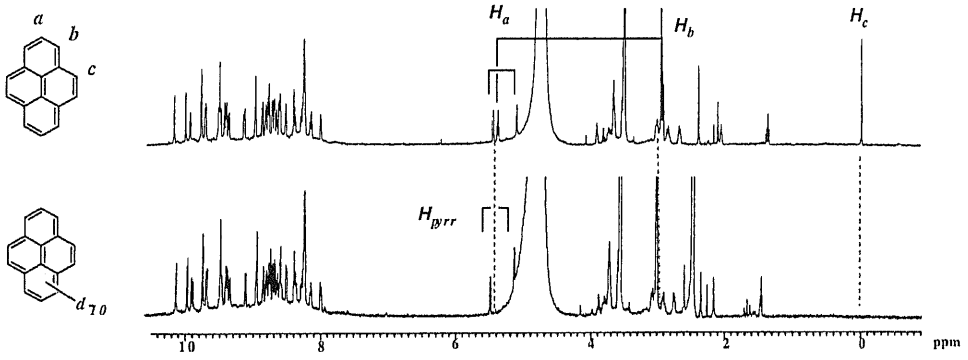

CH COSY of $\mathbf{3}^{12+}(NO_3^-)_{12}$•pyrene in CD_3OD-D_2O=1:1

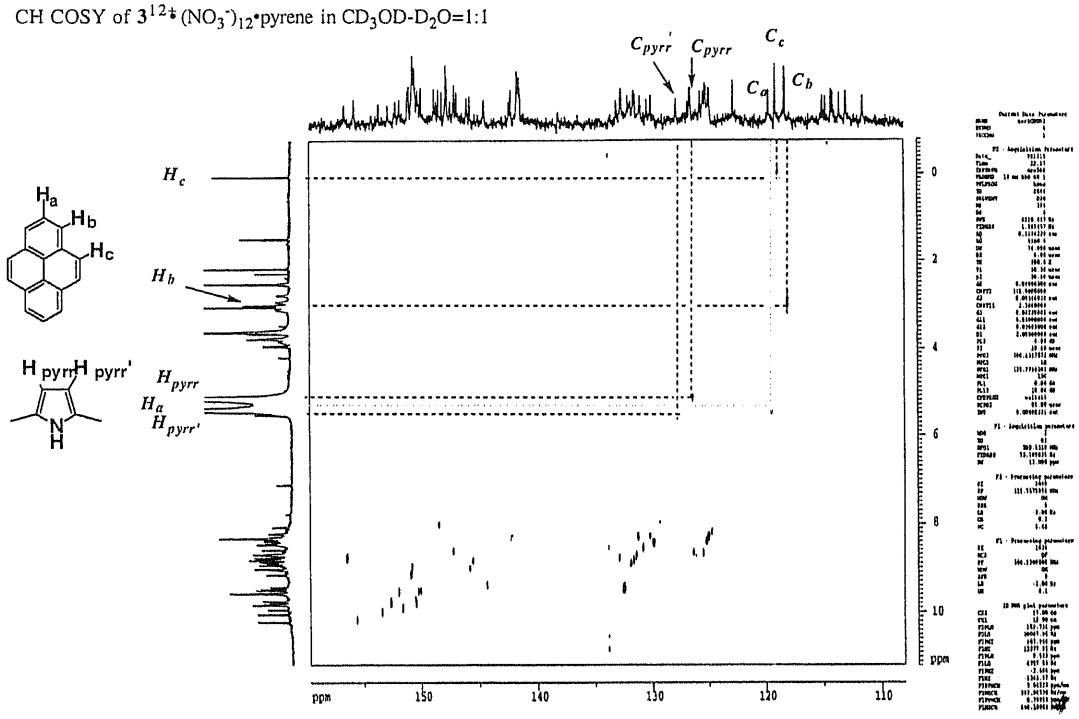

DQF COSY of $3^{12+}(NO_3^-)_{12}$•pyrene in CD_3OD-D_2O=1:1

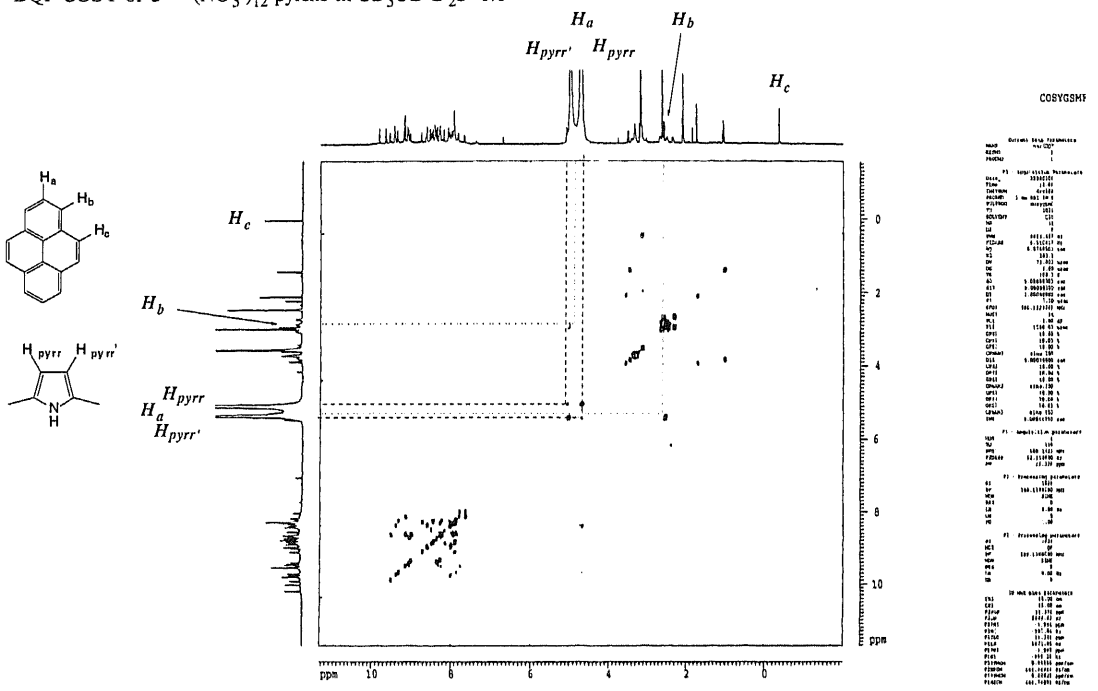

HH COSY (800 MHz) of $3^{12+}(NO_3^-)_{12}$•pyrene in CD_3OD-D_2O=1:1

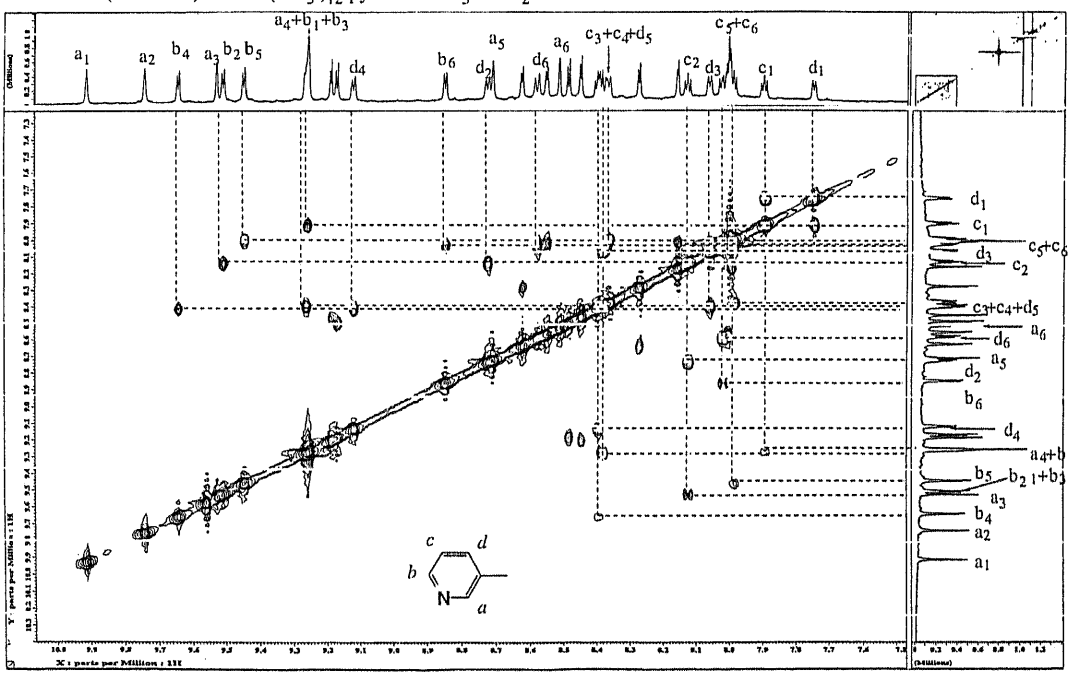

HH COSY (800 MHz) of 3^{12+}•$(NO_3^-)_{12}$•pyrene in CD_3OD-D_2O=1:1

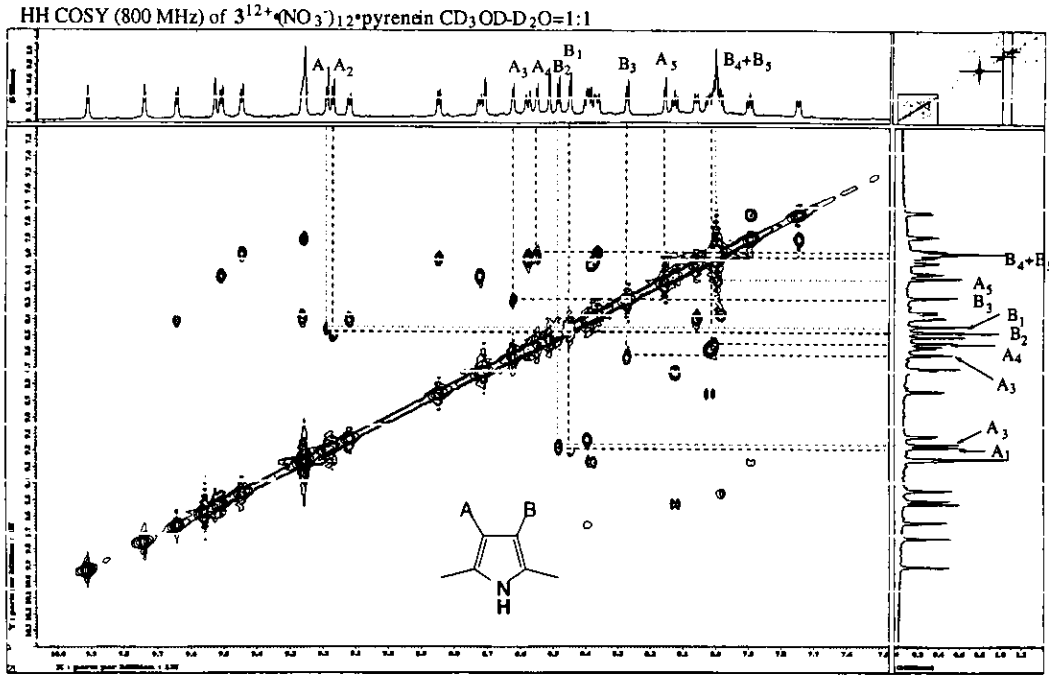

CSI-MS of 3^{12+}•$(PF_6^-)_{11}$•NO_3^- in CH_3CN

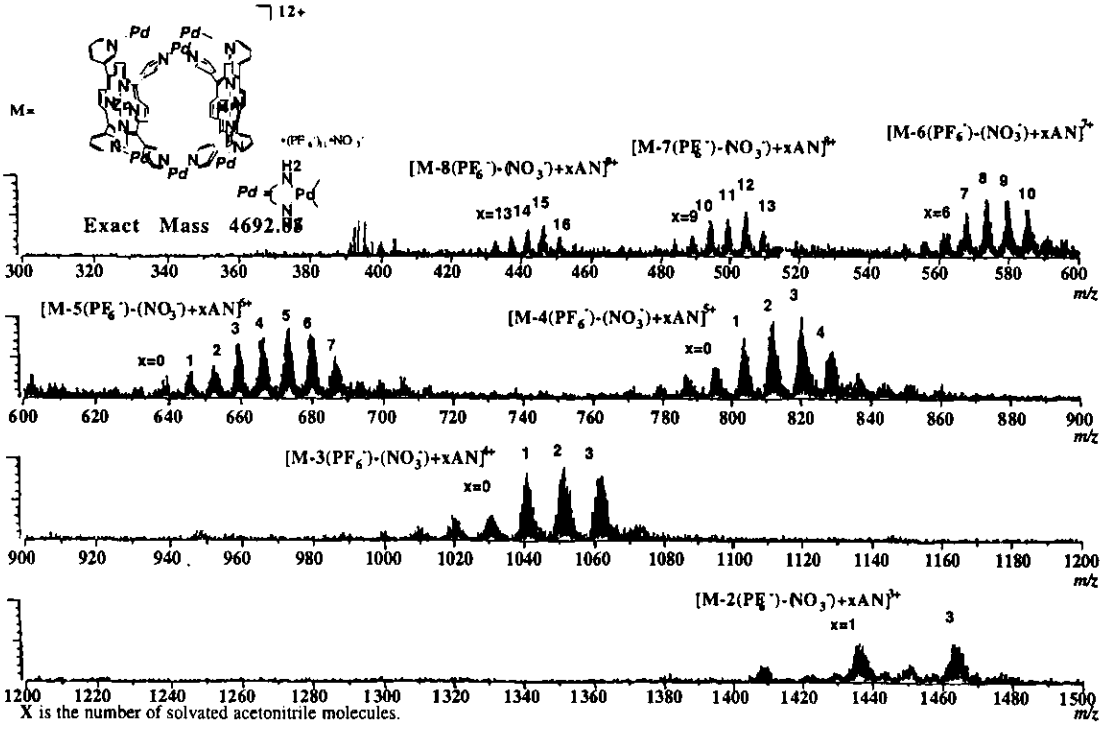

X is the number of solvated acetonitrile molecules.

HR CSI-MS of $3^{12+}(PF_6^-)_{11}.NO_3^-$ in CH_3CN

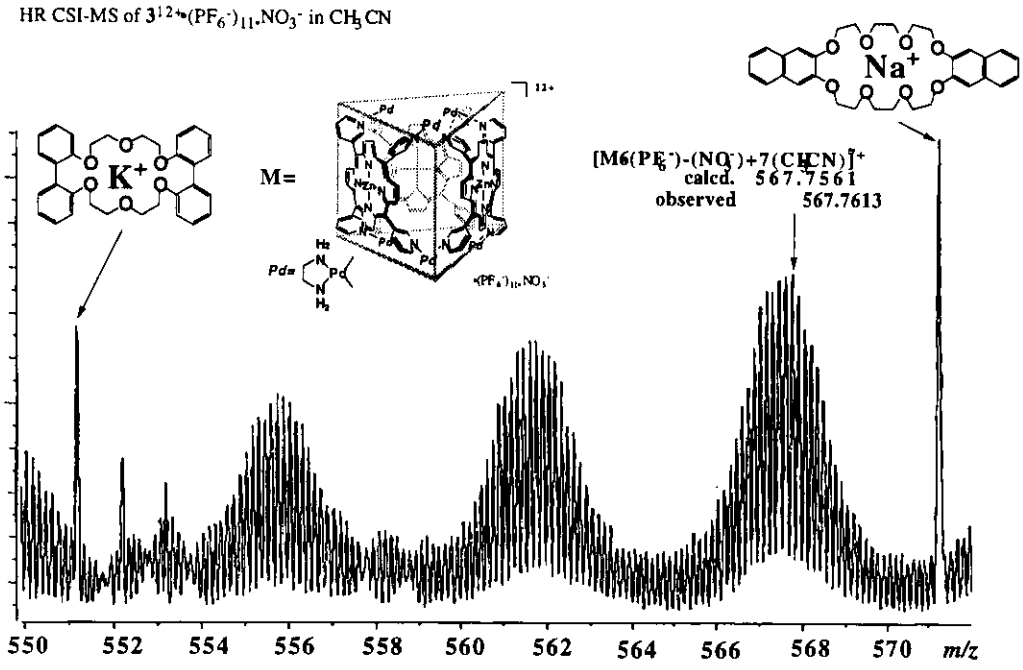

CSI-MS of $3^{12+}(PF_6^-)_{11}.NO_3^-$ in CH_3CN

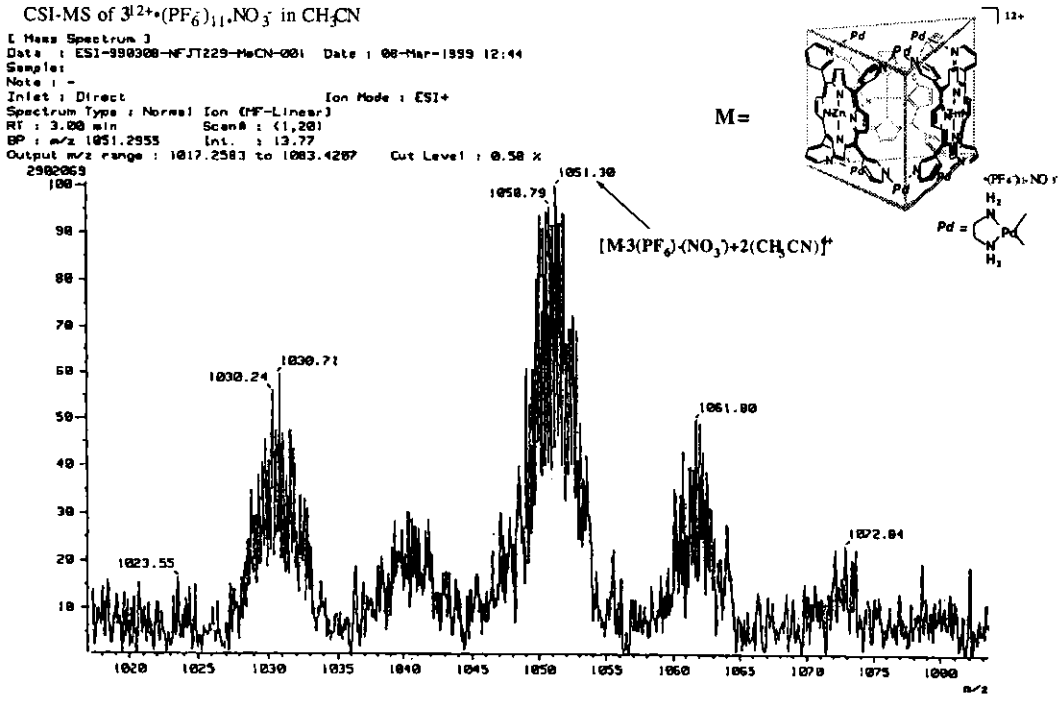

CSI-MS of 3^{12+}•$(PF_6^-)_{11}$•NO_3^- in CD_3CN

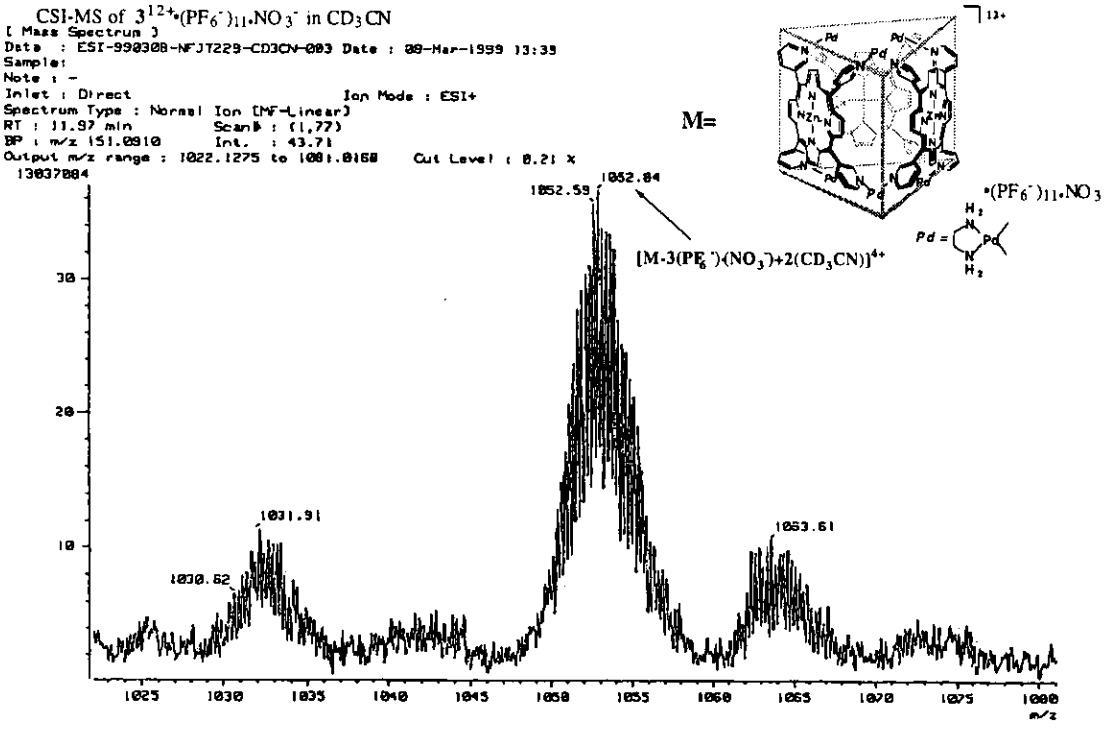

CSI-MS of 3^{12+}•$(NO_3^-)_{12}$•pyrenein CH_3CN-H_2O=1:1

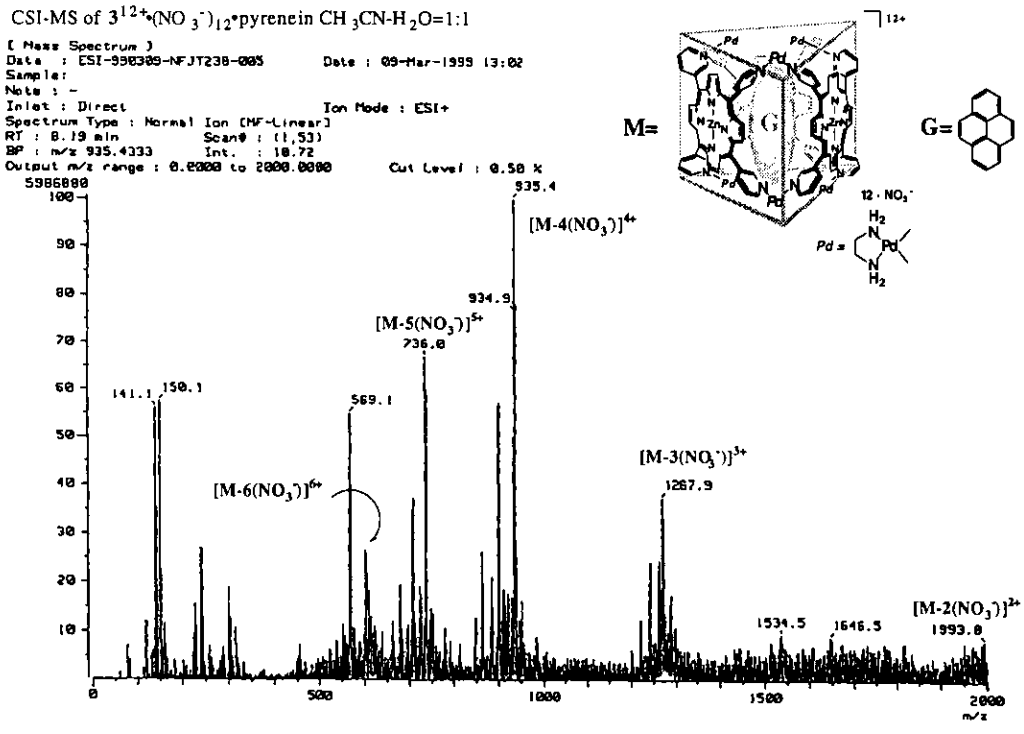

Development chart of D_{3h} and C_2 prism complex

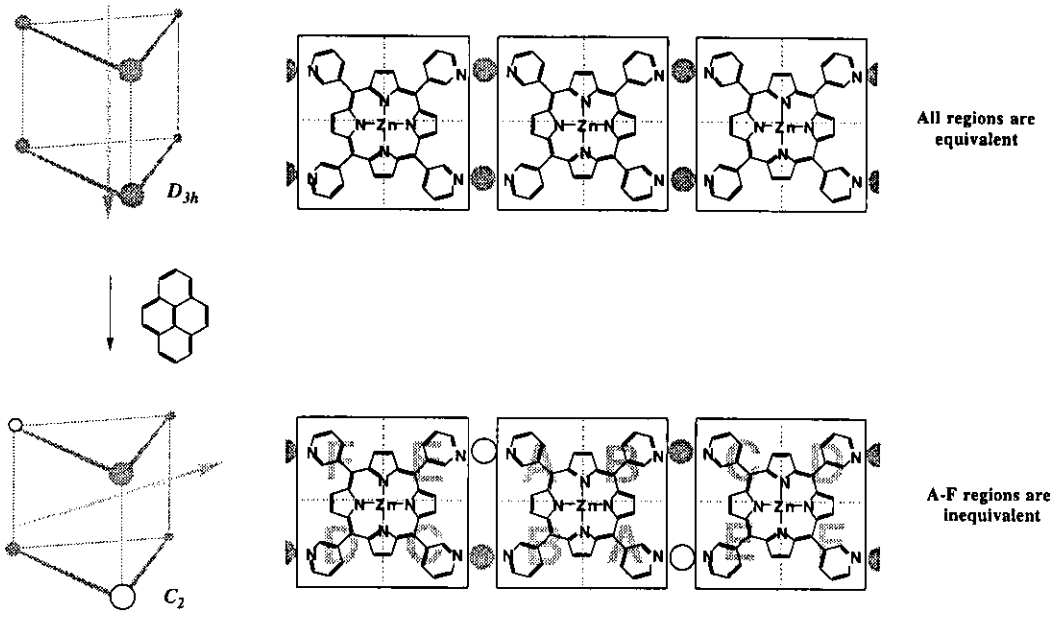

List of Publications

Fujita, M.; Fujita, N.; Ogura, K.; Yamaguchi, K. Spontaneous assembly of ten components into two interlocked, identical coordination cages *Nature* **1999**, *400*, 52-55.

Fujita, N.; Biradha, K.; Fujita, M.; Sakamoto, S.; Yamaguchi, K. A Porphyrin Prism: Structural Switching Triggered by Guest-Inclusion *Angew. Chem. Int. Ed.* **2001**, *40*, 1718-1721.

Fujita, M.; Umemoto, K.; Yoshizawa, M.; Fujita, N.; Kusukawa, T.; Biradha, K. Molecular paneling *via* coordination *Chem. Commun.* **2001**, 509-518.

Linke, M.; Fujita, N.; Chambron, J.-C.; Heitz, V.; Sauvage, J.-P. A [2]–Catenane Whose Rings Incorporate Two Differently Metallated Porphyrins *New J. Chem.* **2001**, *25*, 790-796.

Acknowledgement

The author wishes to express his grateful acknowledgement to Professor Makoto Fujita of Nagoya University for his continued encouragement, kind direction, and helpful discussion throughout this work. His thanks are due to Professor Katsuyuki Ogura of Chiba university for giving him valuable advice. He wishes to acknowledge to Dr. Jean-Pierre Sauvage of Louis Pasteur University who introduce the author to topological chemistry. He also thanks to Dr. Takahiro Kusukawa and Dr. Takashi Okano of Nagoya University, Dr. Jean-Claude Chambron and Dr. Valérie Heitz and Dr. Myriam Linke of Louis Pasteur University for useful suggestion. He is indebted to Professor Koji Tanaka of Institute for Molecular Science for his continuous encouragement. Thanks are due to Dr. Kumar Biradha of Nagoya University, Professor Kentaro Yamaguchi, Mr. Shigeru Sakamoto and Dr. Hiroko Seki of Chemical analysis center of Chiba University for X-ray, ESI-MS and NMR measurement. He thanks all the members of Fujita group of Chiba University, Institute for Molecular Science, and Nagoya University for their continuous encouragement and helpful suggestion during his study. He thanks JSPS for a Research Fellowship for Young Scientists.